NASA Contractor Report 3475

Radiation Testing of Composite Materials, In Situ Versus Ex Situ Effects

Richard M. Kurland, James F. Thomasson, and William C. Beggs

NASA

NASA Contractor Report 3475

Radiation Testing of Composite Materials, In Situ Versus Ex Situ Effects

Richard M. Kurland, James F. Thomasson,
and William C. Beggs
TRW Defense and Space Systems Group
Redondo Beach, California

NASA

National Aeronautics
and Space Administration

Scientific and Technical
Information Branch

1981

FOREWORD

The work reported herein was performed by TRW Defense and Space Systems Group (DSSG), Redondo Beach, California, under NAS1-15848 and was sponsored by the National Aeronautics and Space Administration, Langley Research Center (NASA/LaRC), Hampton, Virginia. Mr. W.S. Slemp, Environmental Effects Branch, Materials Division, served as the NASA/LaRC technical representative.

The program at TRW DSSG was performed under the auspices of the Mechanical Engineering Laboratory (MEL) of the Space Systems Division, Mr. M.E. White, MEL Manager. TRW Program Manager was Mr. R.M. Kurland. Principal Investigator was Mr. J.F. Thomasson. Responsible engineer for High Energy Radiation Test Operations was Mr. W.C. Beggs. Several other engineers and laboratory support personnel contributed to the success of this program. Their contributions are acknowledged below:

M.D. Cawley	Vacuum Chamber Design and Tensile Property Measurements
G.I. Fukumoto	Tensile Property Measurements
N. Harvey, Jr.	Van de Graaff Calibration and Operation
P. Guilfoyle	Van de Graaff Operation
J.C. McKeegan	Van de Graaff Operation

Certain commercial materials and products are identified herein in order to specify adequately which materials and products were investigated in the research effort. In no case does such identification imply recommendation or endorsement of the product by NASA, nor does it imply that the materials and products are necessarily the only ones or the best ones available for the purposes. In many cases equivalent materials and products are available and could produce equivalent results.

TABLE OF CONTENTS

TABLE OF CONTENTS (Continued)

LIST OF ILLUSTRATIONS

LIST OF ILLUSTRATIONS (Continued)

LIST OF TABLES

NOMENCLATURE

Below is a list of the most frequently used symbols and acronyms in the report. Except for radiation flux and fluence notations, all analysis and test data were developed using the English system of units and later converted into SI units for reporting purposes (with English units in parentheses).

A	cross-sectional area of test specimen; ampere
A_s	frontal area of electron scatterer
AMFL	Air Force Materials Laboratory
C	coulomb
C6000/P1700	graphite/polysulfone composite material
D	dose
D_B	dose, fully backed specimen
D_o	dose, unbacked specimen
DVM	digital voltmeter
E	modulus of elasticity; electron energy level
$\overline{E}$	on-target average electron energy level
E_o	VDG emerging electron energy level
E_p	most probable emerging electron energy level
EA	exit aperture
F_{TU}	ultimate tensile strength
F_{TY}	yield tensile strength
FUV	far ultraviolet
ISTTC	in situ tensile test chamber
L	gage length
LaRC	Langley Research Center
LN_2	liquid nitrogen
LVDT	linear variable differential transducer

MeV	million electron volts
NASA	National Aeronautics and Space Administration
NUV	Near ultraviolet
P	applied tensile load
P_Y	yield tensile load (at 0.01 strain)
P_U	ultimate tensile load
Q_{FC}	Faraday cup charge (current)
Q_{EA}	exit aperture charge (current)
S	standard deviation (small population)
SESL	Space Environmental Simulation Laboratory
TIGER	Monte Carlo electron transport computer code
TLD	thermoluminescent dosimeter
T300/934	graphite/epoxy composite material
T300/5208	graphite/epoxy composite material
VDG	Van de Graaff generator
WPAFB	Wright Patterson Air Force Base
$\overline{X}$	average value of population of X_i's
d	distance
e	electron
keV	thousand electron volts
$\Delta\Omega$	solid angle
δ	deflection; change-in-length
ε	strain or elongation
ε_u	ultimate strain or elongation
σ	stress

1.0 SUMMARY

Three [±45/∓45] laminate composite material systems, T300/5208, T300/934, and C6000/P1700, were irradiated up to a bulk dose of 1×10^{10} rads using a mono-energetic fluence of 700 keV electrons from a Van de Graaff accelerator. Irradiations were performed in vacuum at 20°C (68°F) and 120°C (248°F). Post-irradiation tensile testing was conducted in situ (while being irradiated), in vacuo, and ex situ in air.

Because of the exploratory nature of the study, only a limited number of specimens per material and test condition were evaluated; thus, engineering design data was not generated. Nevertheless, the data were representative of material behavior. The results were useful in establishing trends and in developing general conclusions about the significance of post-irradiation test environments and the suitability of the materials to withstand long-term space radiation.

The radiation-induced changes to the tensile properties (modulus of elasticity, ultimate strength, yield strength, ultimate elongation) for all materials were small. There was indication that radiation improved some tensile properties in that there was a slight increase in modulus and strength. There was, however, a decrease in ultimate elongation.

Because radiation damage thresholds may not have been reached during the study or because radiation-induced changes were small for these materials, the ability to realistically evaluate the importance of post-irradiation test environments was compromised. The differences among in situ, in vacuo, and ex situ test results were small.

2.0 INTRODUCTION

2.1 BACKGROUND

Future space systems will use increasing amounts of composite
materials in the primary structural system. Composites are a natural
candidate material due to their unique combination of good strength, high
stiffness, low density, high dimensional stability, and because their
properties can be tailored for specific applications. However, the reli-
able performance of composites in the long-term space radiation environment
is presently unknown. Since advanced composite materials may be suscepti-
ble to radiation-induced changes in their mechanical properties, it is
important that the radiation effects on critical properties be well
characterized to ensure that only relatively stable materials are used.

The significant space radiation environment components which may cause
changes in both surface and/or bulk properties are solar ultraviolet radia-
tion and charged particles (electrons and protons). The other environ-
mental components such as cosmic rays, neutrons, alpha particles and X-rays
are considered to have negligible probability for creating measurable
effects in the materials because of the relatively less severe energy
levels or fluences. The charged particle radiation is of special impor-
tance because of its ability to penetrate deep into the bulk of the
material and thus affect an appreciable percentage of the material cross-
section.

Organic materials, like polymer films, adhesives and resin systems,
because of the dependence of their bulk physical properties on molecular
weight and the integrity of their carbon-to-carbon and other covalent
linkages, are more susceptible to radiation-induced changes than metals and
inorganic materials. For organic materials, changes in material properties
due to ionization of atoms dominates those changes that may result from
displacement of atoms. Thus, for most composite material systems, the
resin and resin/fiber interface will be more vulnerable than the
reinforcement fibers.

The types of reactions that take place in organic materials exposed to
space radiation are chain scission and cross-linking. Both processes are
induced by free radical formation and interaction which result in changes

within or between adjacent molecular chains. Typical manifestations of this energy interaction and deposition within the material can include outgassing, shrinkage, cracking, crazing, pitting, embrittlement and discoloration. These, in turn, can cause changes in strength, stiffness, thermal expansion, and thermophysical and optical characteristics.

Unlike conventional material property testing under ambient conditions or at temperature, space radiation effects testing is complex and expensive. Conducting real-time tests in space is not practical for obvious reasons. Performing simulation tests in earth-based laboratories with total fidelity to the natural space environment is neither possible, necessary nor economically feasible. Compromises in testing scenarios/techniques are necessary to obtain reliable material properties data in a reasonable time period for a reasonable cost. The question is to determine which compromises are acceptable.

To date there is little hard data to provide guidance in the selection of acceptable/required simulation techniques. The issues of accelerated testing effects, post-radiation test environments, ionization equivalence of different ionizing sources, synergistic effects of combined radiation, and serial versus simultaneous radiation, to name a few, have yet to be fully investigated. Unfortunately, the resolution of many of these issues may be a function of the material system and the material property in question and may not be possible without the development of better test facilities.

2.2 OBJECTIVE

NASA/LaRC and WPAFB/AFML (Reference 1) have recently completed studies for the evaluation of radiation effects on composite materials. All of the post-irradiation testing, however, on these programs was done ex situ; that is, the material specimens were tested in air following irradiation because of the limitations of the testing equipment. One of the major uncertainties about the above approach was whether the post-irradiation exposure to air could mask or alter important radiation effects.

4

The objective of this program was to investigate the effect of the post-irradiation test environment on the tensile properties of representative advanced composite material systems. It was not the purpose of the tests to obtain engineering design data because only a limited number of specimens per material and test condition could be evaluated under this exploratory program. However, the data would be useful: (1) to draw initial conclusions about the importance of the test conditions, and (2) to provide some indications about the radiation hardness of the materials tested.

2.3 TECHNICAL APPROACH

Test specimens were fabricated by NASA/LaRC and supplied to TRW for preconditioning prior to testing. The radiation test facility had a vacuum chamber in which a miniature tensile testing apparatus was incorporated. This permitted undersize specimens - 2.54 cm (1 in.) gage length by 0.95 cm (0.375 in.) wide by 0.635 mm (0.025 in.) thick - to be irradiated and evaluated under different post-irradiation test environments without removing them from the chamber.

Tensile stress-strain tests were performed on control specimens under ambient conditions using a regular testing machine and in the chamber in air and in vacuum to obtain reference-level material properties. Test specimens were then exposed in vacuum to a radiation environment up to 1 x 10^{10} rads consisting of a mono-energetic fluence of 700 keV electrons from a Van de Graaff accelerator. The bulk dose was nearly uniform throughout the material. The dose levels were selected to represent that expected from long-term exposure to critical trapped radiation belt environments.

In present conventional testing techniques, (1) interruptions in irradiation are permitted, (2) time delays between cessation of irradiation and post-irradiation testing are allowed, and (3) post-irradiation testing is performed in air or an inert environment. These compromises are accepted because of the complexity, expense and constraints associated with alternative test methods which attempt to replicate the natural environment more realistically. Under this study, test programs were designed to compare more exact techniques with the more conventional techniques.

Post-irradiation testing was performed while the specimens were being irradiated (termed in situ testing), in vacuum immediately after cessation of irradition (termed in vacuo testing), and after varying periods of air exposure (termed ex situ testing). Room temperature and elevated temperature effects were evaluated. Effects of intermittent versus continuous irradiation were also investigated to evaluate the presence of vacuum annealing of the radiation-induced changes to the tensile properties.

3.0 TEST SPECIMENS

3.1 MATERIAL DESCRIPTION

Three composite material systems were evaluated during the course of the study. Table 3-1 lists the materials and associated identification symbols. During the Phase I Test Series, a laminate of Union Carbide Thornel 300 PAN fiber impregnated with Narmco 5208 epoxy resin (T300/5208) was tested. In Phase II, two materials were tested: a laminate of Union Carbide Thornel 300 PAN fiber impregnated with Fiberite 934 epoxy resin (T300/934); and Celanese Celion 6000 fiber impregnated with Union Carbide Udel P1700 polysulfone thermoplastic resin (C6000/P1700).

The chemistry of two of the composites was determined to assist in the calculation of absorbed dose-depth profiles. Analysis of the polysulfone laminate was provided by NASA/LaRC. The T300/934 analysis was performed at TRW. It was assumed that the T300/5208 chemistry was similar to the T300/934 material for absorbed dose-depth profile calculations. Table 3-2 summarizes the chemical analysis.

3.2 CONFIGURATION

Figure 3-1 shows a typical test specimen. An undersize specimen was selected to maximize the number of specimens that could be accommodated at one time within the target plane radiation zone, and to be compatible with the stiffness of the tensile testing apparatus/support structure within the vacuum chamber. Figure 3-2 presents the critical dimensions. The specimen consisted of the composite gage length section with oversized fiberglass reinforcement tapered tabs bonded on each end. Overall specimen length was 50.8 mm (2.0 in.). Gage length was 25.4 mm (1.0 in.). Specimen width was 9.53 mm (0.375 in.). Nominal thickness for the specimens was 0.635 mm (0.025 in.). A 2.54 mm (0.10 in.) diameter hole was located in each end to accommodate small pins in the target plane fixturing for positive grip control.

All of the composites tested consisted of a 4-ply balanced layup [+45, -45, -45, +45 degrees]. The balanced layup provided a flat laminate, resulting in more precise tensile strain measurements. The 45-degree orientation allowed modulus measurements to be obtained at relatively low

Table 3-1. Test Materials

No.	Symbol	Fiber/Resin	Source
1	T300/5208	Union Carbide Thornel 300 PAN Fiber/Narmco 5208 Epoxy Resin	NASA/LaRC
2	T300/934	Union Carbide Thornel 300 PAN Fiber/Fiberite 934 Epoxy Resin	NASA/LaRC
3	C6000/P1700	Celanese Celium 6000 Fiber/ Union Carbide Udel P1700 Polysulphone Resin	NASA/LaRC

Table 3-2. Test Material Chemistry

Element	Percent by Weight		
	T300/5208*	T300/934	C6000/P1700
Carbon	85.7	85.7	81.6
Hydrogen	1.7	1.7	2.1
Nitrogen	5.0	5.0	3.6
Sulphur	0.1	0.1	2.8
Phosphorus	-	-	1.3
Oxygen	7.5	7.5	8.6
Density (gm/cm^3)	1.58	1.58	1.51

*Assumed similar to T300/934

loadings, reducing the effect of support and specimen holder structural deflections on measured strain values. In addition, the 45-degree layup would be more sensitive than a unidirectional layup to changes in resin or resin-fiber interface properties resulting from irradiation.

Each specimen was numbered with a scribe on the fiberglass tabs on each end of the specimen. The numbers identified the location of each specimen on the target plane. In addition, the outer end load fittings were also stamped with similar numbers.
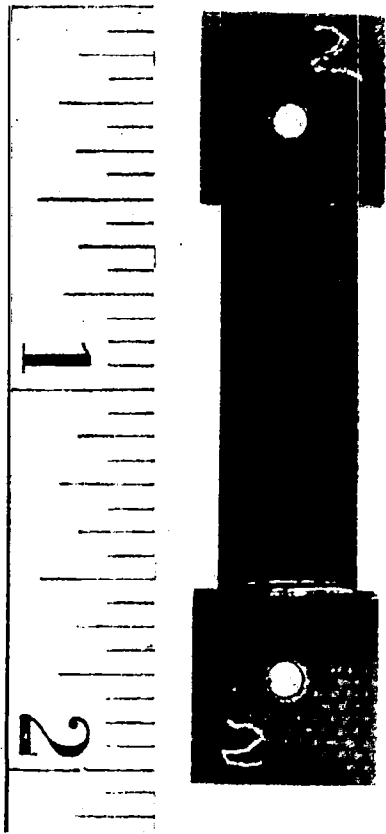
(a) Front View   (b) Side View

Figure 3-1. Typical Test Specimen (2x).

1.168 (0.046) TABS
FIBERGLASS LAMINATE
MIL-P-18177, TYPE GEB

12.70
(0.50)

9.53
(0.375)

2.54
(0.100) DIA
(2 REQD)

12.70
(0.50)

50.80
(2.00)

GAGE LENGTH

25.40
(1.00)

4.32
(0.17)

7.11 (0.28)

12.70
(0.50)

TAPERED EDGE
FOR TABS

≈ 0.635
(0.025)

1.59
(0.062)

6.35
(0.25)

BOND AND FILL EDGE GAP
WITH RIGID EPOXY ADHESIVE

NOTE: ALL DIMENSIONS IN
MM (INCHES)
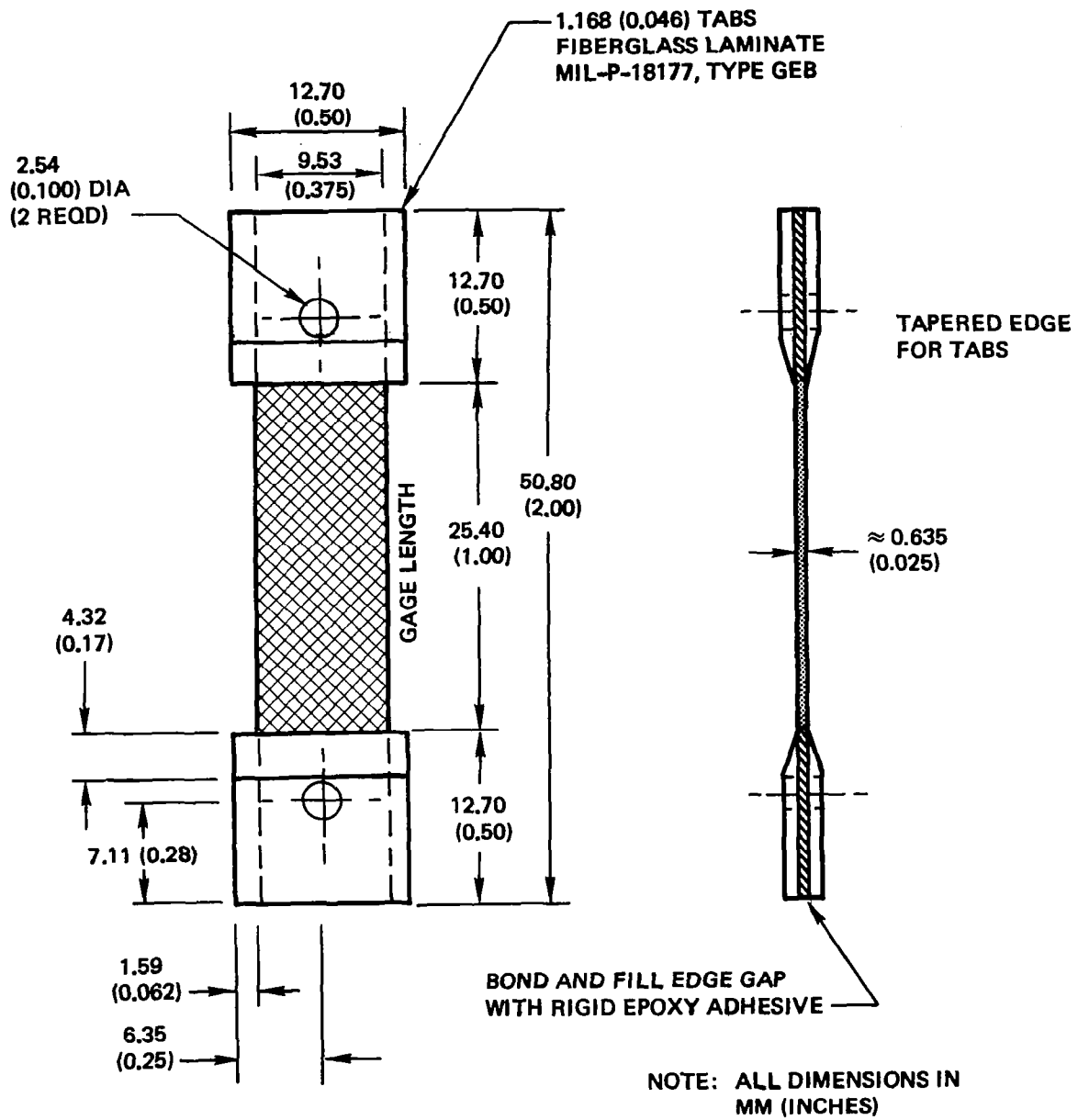
Figure 3-2. Test Specimen Dimensions.

3.3 ENVIRONMENTAL PRECONDITIONING

All specimens were preconditioned prior to radiation or baseline tensile testing by exposure to a temperature of 65°C ±5°C (150°F ±9°F) for 72 hours in a vacuum. Heating was accomplished in a Brew vacuum furnace which utilizes a diffusion pumping system. Vacuum was maintained below 5×10^{-5} torr.

Upon removal from the preconditioning environment, the specimens were immediately mounted on the target plane and installed in the vacuum chamber. Preconditioned specimens were under vacuum or tested to failure (in the case of control specimens) within 3 hours of exposure to ambient conditions. Ambient conditions did not exceed 60 percent relative humidity or a temperature of 20°C ±5°C (68°F ±9°F).

4.0 TEST ENVIRONMENT DEFINITION

No attempt was made to accurately represent natural space radiation conditions. Radiation was limited to a mono-energetic dose of high-energy electrons at an energy level and fluence sufficient to provide a bulk dose in the material representative of that to be experienced under long-term geosynchronous orbit conditions. No other type of radiation (i.e., ultraviolet, protons) were provided. Irradiation was performed in vacuum at room and elevated temperatures.

4.1 HIGH ENERGY ELECTRON RADIATION

The specific radiation environment required that the mono-energetic electrons be of sufficient energy level to keep the dose through the material uniform within a factor of two. For Phase I tests, specimens were irradiated to an average bulk dose of 1×10^9 rads and 2×10^9 rads. This was increased to 1×10^{10} rads for Phase II tests.

A preliminary estimate of the required electron energy was made by comparing the range from Berger-Seltzer tables (Reference 2) to obtain the energy required to get a range 2.5 to 3 times the average specimen thickness of 0.635 mm (25 mils) and density of 1.55 gm/cm^3. From this comparison, 700 keV was determined to be an appropriate energy. Initial calculations of 500 keV, 600 keV, 700 keV and 1 MeV were then made using TIGER (Reference 3), a one-dimensional Monte Carlo electron transport computer code. For these calculations, 2000 history calculations were made, since the statistics (-10 percent batch) were adequate for scoping purposes. Figures 4-1 and 4-2 present the results of these initial calculations for two of the three materials. From these calculations, 700 keV was determined to adequately meet the criteria previously stated for the energy.

To better define the dose profiles and energy deposited, 8000 history calculations (-5 percent batch statistics) were then made for the two materials. The results (dose profiles and average dose) are presented in Figures 4-3 and 4-4. The average dose is the total energy deposited in the material divided by the material mass per square centimeter (or thickness). Table 4-1 presents these average doses and their associated fluence levels for a dose of 1×10^9 rads. For 2×10^9 rads and 1×10^{10} rads, the levels are 2X and 10X those shown, respectively. As a comparison, the
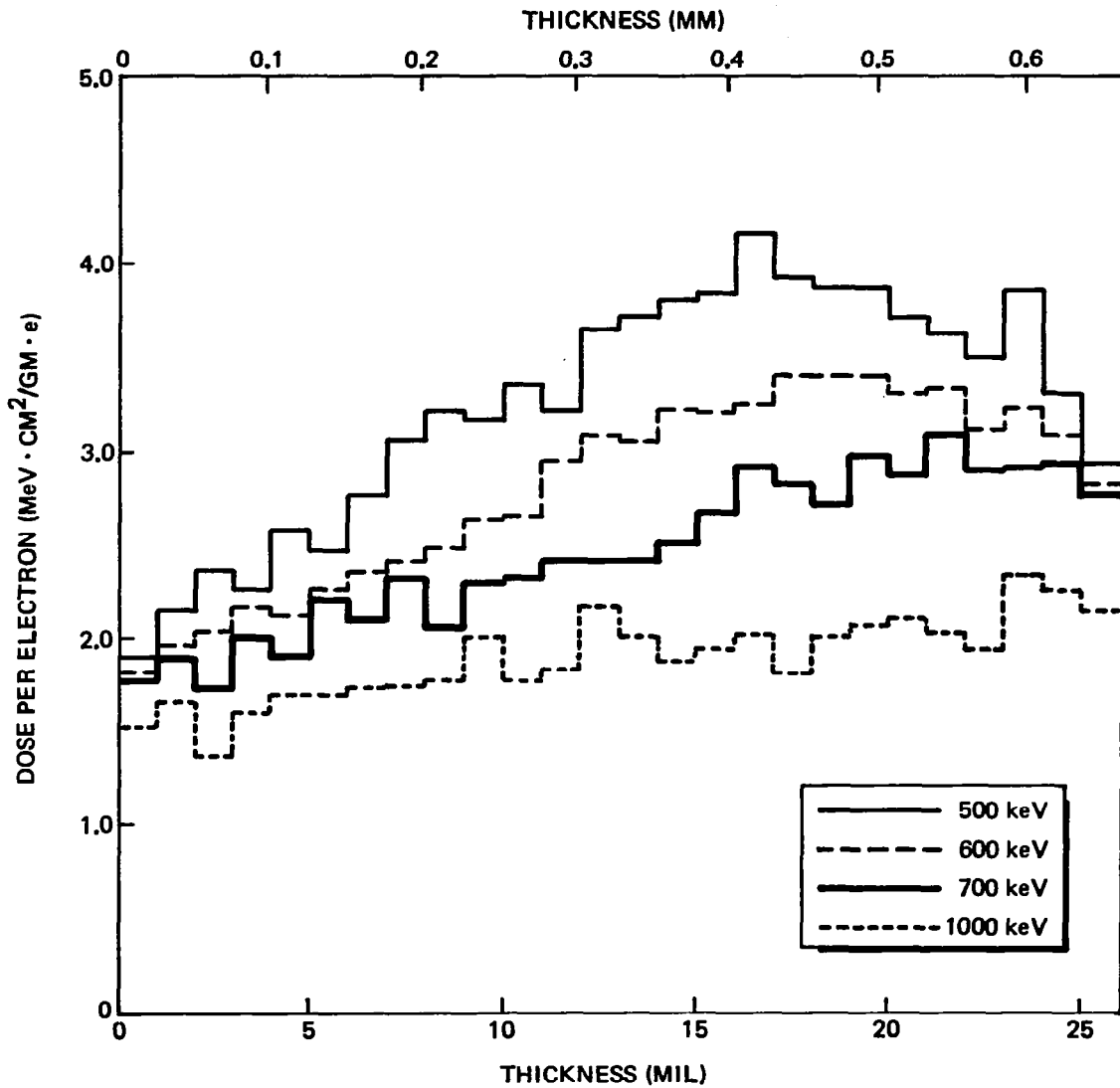
Figure 4-1. Unit Dose as a Function of Thickness for a Unit Electron Fluence Normally Incident on Material C6000/P1700.
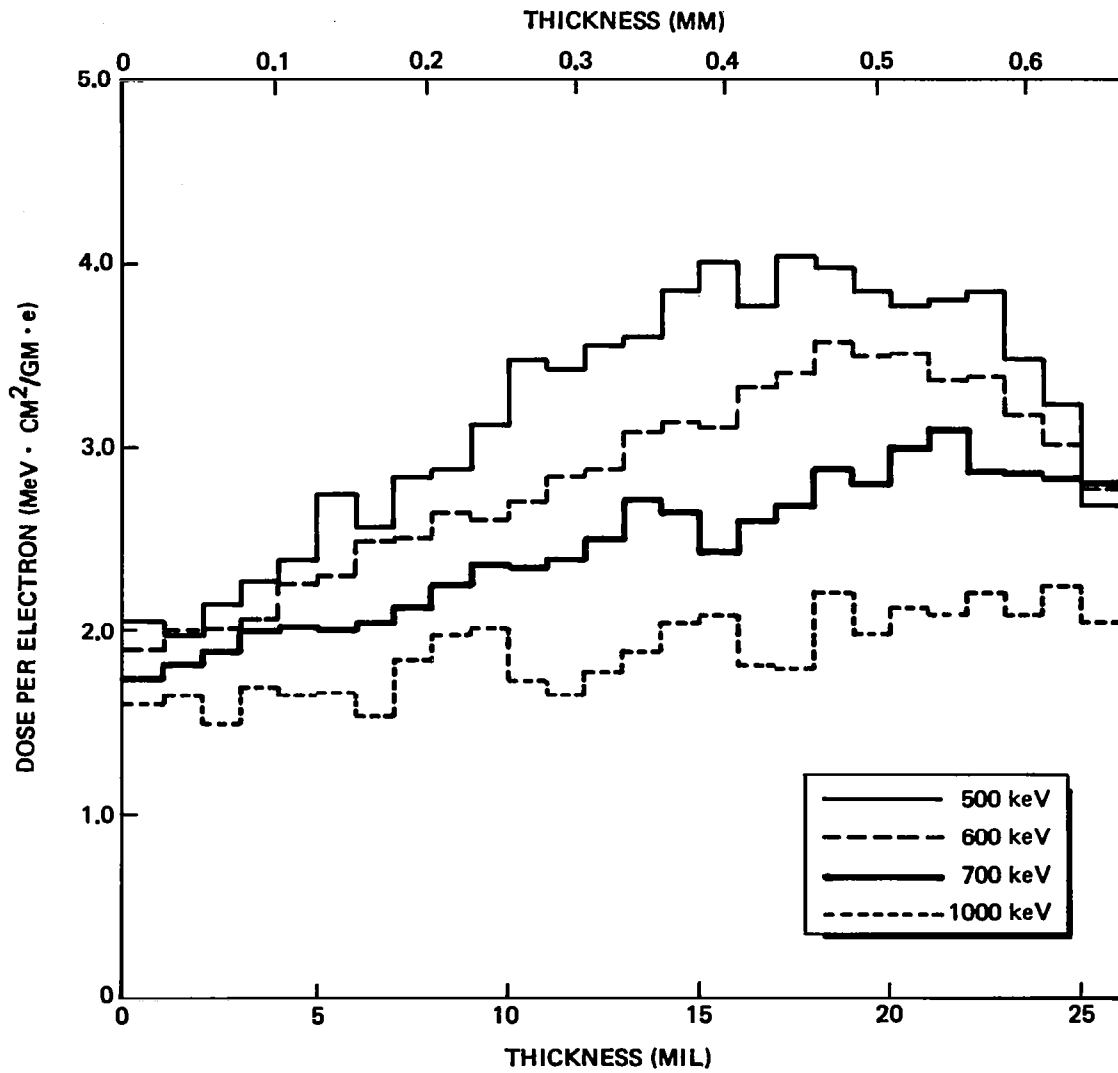
Figure 4-2. Unit Dose as a Function of Thickness for a Unit Electron Fluence Normally Incident on Material T300/934.
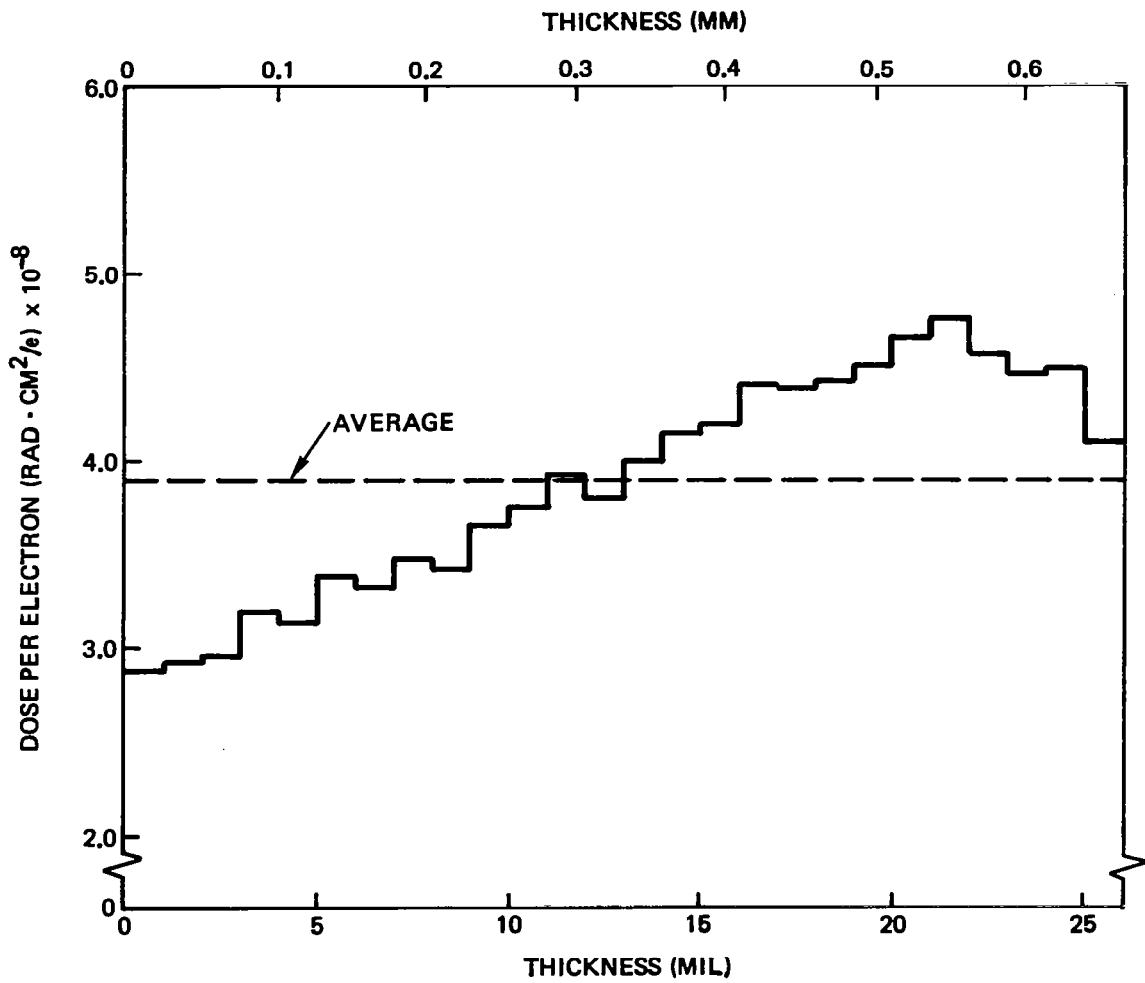
Figure 4-3. Unit Dose as a Function of Thickness for a 700 keV Electron
Fluence Normally Incident on Material C6000/P1700.
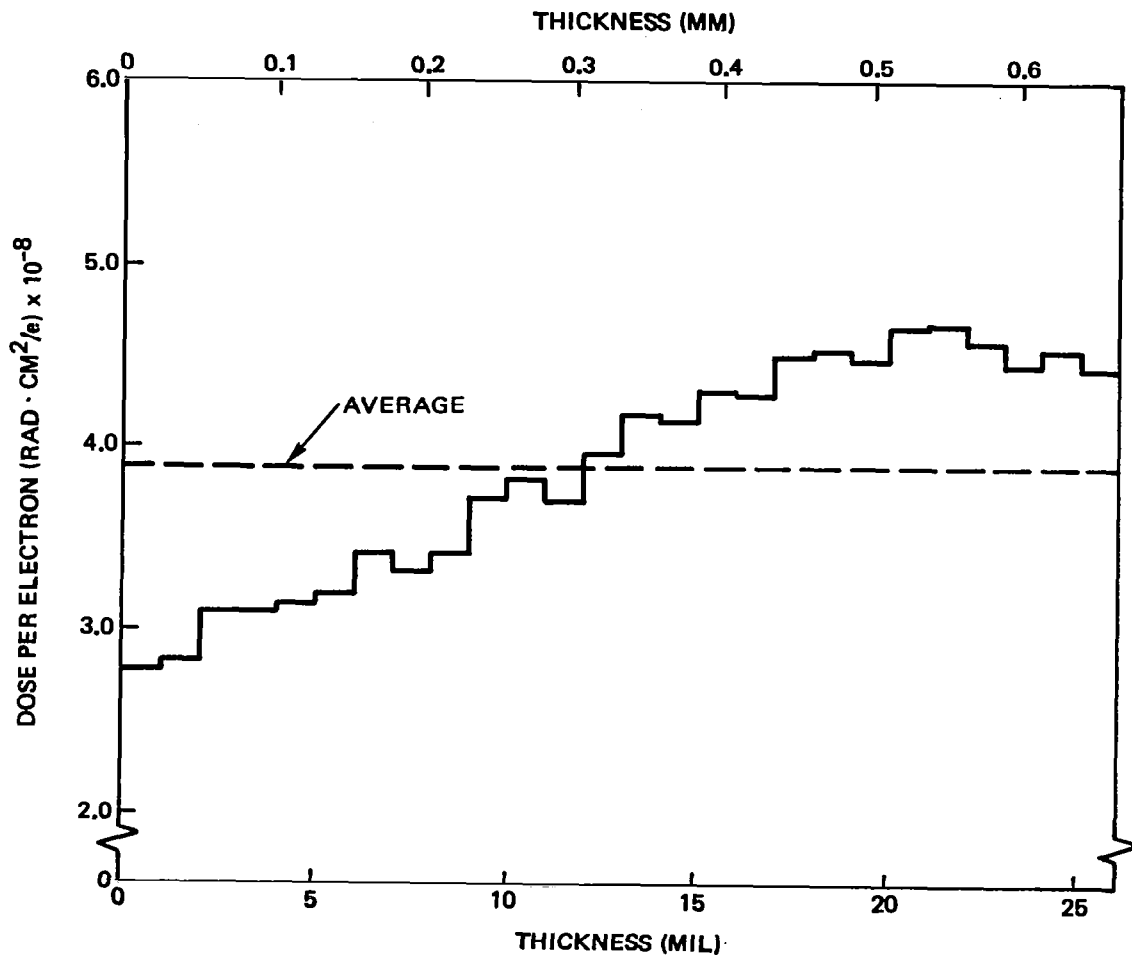
Figure 4-4. Unit Dose as a Function of Thickness for a 700 keV Electron Fluence Normally Incident on Material T300/934.

Table 4-1. Energy and Fluence for 1×10^9 rads Average Dose from a Mono-Energenic Electron Beam Normally Incident on Specimens

Energy (keV)	Material	Average Unit Dose (rad·cm²/e)	Fluence (e/cm²)
700 (b)	C6000/P1700	3.89×10^{-8}	2.57×10^{16}
	T300/934 (a)	3.89×10^{-8}	2.57×10^{16}
500 (c)	C6000/P1700	5.19×10^{-8}	1.93×10^{16}
	T300/934 (a)	5.15×10^{-8}	1.94×10^{16}
600 (c)	C6000/P1700	4.47×10^{-8}	2.24×10^{16}
	T300/934 (a)	4.52×10^{-8}	2.24×10^{16}
1000 (c)	C6000/P1700	3.02×10^{-8}	3.31×10^{16}
	T300/934 (a)	3.00×10^{-8}	3.34×10^{16}

(a) Assume results applicable to T300/5208 material
(b) 8000 History Monte Carlo analysis
(c) 2000 History Monte Carlo analysis

table includes the 500 keV, 600 keV and 1 MeV results from the 2000 history calculations. The absorbed dose-depth profiles for the materials are almost identical because of the similar chemistry and density properties.

The results listed in Table 4-1 were based on one-dimensional analyses and assumed no influence from the surrounding metal structure in the immediate vicinity of the test specimens. For portions of the Phase I testing, only the rear and sides of the stainless steel vacuum chamber were available for backscattering of electrons. For other Phase I tests and all Phase II tests, a resistance wire heating coil and reflector plate were placed in close proximity behind the specimens.

Appendix A presents additional calculations used to quantify any backscattering dose effects from surrounding hardware in the vacuum/irradiation chamber. The results indicate: (1) the backscattering from the chamber walls is negligible; thus, the fluence levels listed in Table 4-1 are acceptable; and (2) the effect of the heating unit behind the specimens

increased the average bulk dose by approximately 18 percent; thus, the 700 keV electron fluence required to produce a given average bulk dose listed in Table 4-1 must be reduced appropriately.

4.2 VACUUM

Irradiation and all in situ and in vacuo post-irradiation tensile testing were performed in a pressure environment below 1×10^{-6} torr. Vacuum was maintained by a 400 ℓ/sec ion pump. No losses in vacuum were incurred during any radiation period or tensile test.

4.3 TEMPERATURE

Control specimens were maintained at a nominal temperature of 20°C ±5°C (68°F ±9°F). For those radiation sequences that required the specimens to be near room temperature, the temperature was held to 25°C ±5°C (77°F ±9°F). For those radiation sequences that required the specimens to be at an elevated temperature, the temperature was held to a nominal level of 120°C ±5°C (248°F ±9°F), using a combination of heating from the electron irradiation and the resistance wire heater located behind the specimens. During periods when the elevated temperature test specimens were receiving no radiation (i.e., overnight shutdowns), a low heater power was maintained to keep the specimen temperatures at approximately 50°C ±5°C (122°F ±9°F). All post-irradiation tensile testing was done at a temperature of 30°C ±5°C (86°F ±9°F).

5.0 TEST FACILITIES

5.1 LABORATORY OVERVIEW

Irradiation of the materials and subsequent tensile testing was performed in TRW's Space Environmental Simulation Laboratory (SESL). SESL is a state-of-the-art facility for exposure of materials and small spacecraft components to a simulated natural space radiation environment. Key features include: (1) combined simulation of critical components of the space environment; (2) simultaneous irradiation of many test specimens; (3) in situ and ex situ evaluation of radiation-induced effects; and (4) evaluation of mechanical, optical, thermophysical, and electrical properties.

Figure 5-1 shows a layout of the overall laboratory. The facility consists of three vacuum/irradiation chambers integrated to a 1 MeV Van de Graaff (VDG) electron accelerator. Additional radiation sources (i.e., ultraviolet, low-energy electrons and protons) are individually connected to the appropriate chambers. Table 5-1 summarizes the capabilities and functions of each chamber. While the chambers have the inherent capabilities shown in Table 5-1, they can be readily adapted to handle other types of specimens and measurements. Each chamber is stainless steel and approximately 46 cm (18 in.) in diameter by 76 cm (30 in.) long. Two of the three chambers have all-metal seals and a full door on each end (except Chamber No. 2), along with various ports extending from the sides and ends to accommodate radiation sources, view windows, vacuum pump, instrumentation leads, and measurement devices.

Table 5-2 indicates how the important natural space radiation environmental components can be simulated and lists the corresponding source characteristics. Radiation from each source covers a 15 cm (6 in.) diameter target plane at an off-normal angle of incidence ranging from 0 to 22 degrees (depending on the specific vacuum chamber, radiation sources and type of test). Flux variation over the target plane is typically ±10 to ±15 percent for the VDG and electron flood gun sources and ±20 to ±25 percent for the proton source and ultraviolet sources.
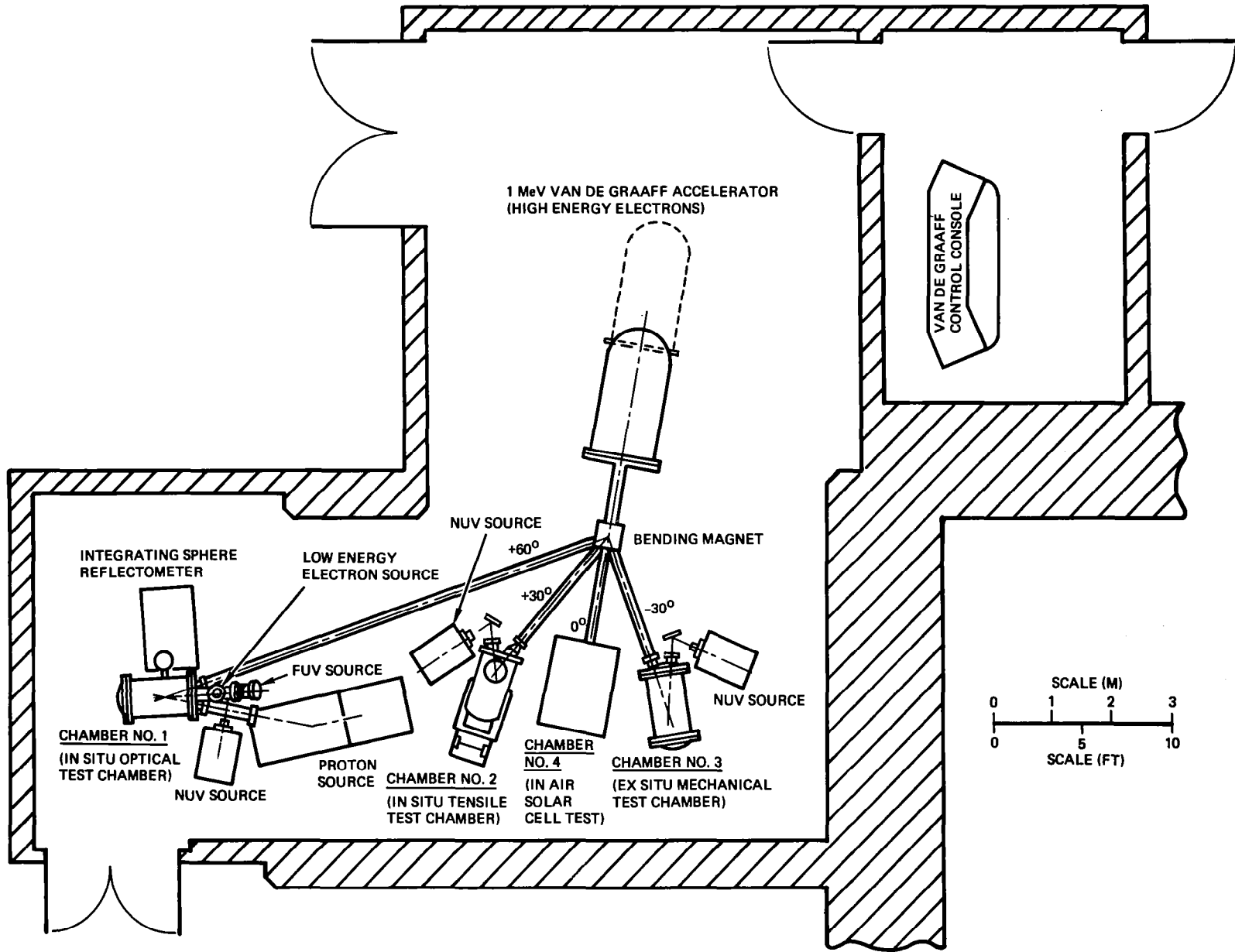
Figure 5-1. Space Environmental Simulation Laboratory (SESL) Layout.

Table 5-1. Vacuum/Irradiation Chamber Functions

Chamber	Number of Samples	Combined Environmental Components	Baseline Measurements*
No. 1 (In Situ Optical)	28 (1 x 2 cm)	Near UV Far UV High Energy Electrons Low Energy Electrons Low Energy Protons High Vacuum	In Situ Spectural Reflectance In Situ Diffuse Reflectance In Situ Bidirectional Reflectance
No. 2 (In Situ Tensile)	18 (2.54 cm Gage Length)	Near UV High Energy Electrons	In Situ Tensile Stress - Strain Properties
No. 3 (Ex Situ Mech)	40 (2.54 cm Gage Length)	Near UV High Energy Electrons High Vacuum	Ex Situ Mechanical Properties

*All chambers can be adapted for ex situ mechanical, electrical or chemical property tests

Table 5-2. Environmental Simulation Description

Radiation Component	Simulation Radiation Source	Simulation Source Characteristics
Near Ultraviolet	3-KW Short Arc Xenon Lamp	0.18 to 0.40 mm Up to 5X Sun Intensity
Far Ultraviolet	Electrodeless Krypton Gas Lamp	0.10 to 0.18 mm Up to 5X Sun Intensity
Radiation Belt Electrons	Van de Graaff Accelerator	70 keV to 1.1 MeV 10^7 to 10^{11} e/cm^{2}sec
Plasma Sheet Electrons	Electron Flood Gun	0.5 to 10 keV Up to 10^{11} e/cm^{2}sec
Radiation Belt Protons	Ionization Equivalent Electrons from Van de Graaff Accelerator	70 keV to 1.1 MeV 10^7 to 10^{11} e/cm^{2}sec
Solar Flare Protons	Ionization Equivalent Electrons from Van de Graaff Accelerator	70 keV to 1.1 MeV 10^7 to 10^{11} e/cm^{2}sec
Plasma Sheet Protons	Hydrogen Ion Plasma Generator	Up to 30 keV Up to 10^{11} p/cm^{2}sec
Vacuum	GN Aspiration, Cryosorption, and 400 P/sec Ion Pumping	10^{-6} to 10^{-8} Torr

23

Specimen temperature control is achieved (1) by conductive and radiative cooling techniques within each chamber using LN_2 or chilled water in shrouds and coldplates, (2) by filtering the infrared energy from the near ultraviolet (NUV) source beams, and/or (3) by heater plates.

5.2 TEST CHAMBER DESCRIPTION

Chamber No. 2 (In Situ Tensile Test Chamber - ISTTC) was used to perform the radiation and tensile testing. The ISTTC is a 46 cm (18 in.) diameter by 76 cm (30 in.) long stainless steel cylindrical chamber with multiple ports (Figure 5-2). All of the ports are metal sealed, except for two ports which house the tensile testing apparatus, the front door, and the manipulator shaft that rotates the carousel target plane. These are sealed with Viton gaskets.

Two ports on the front door are approximately 23 degrees off normal to the specimen carousel target plane. One of these ports is a high purity silica window which allows for viewing or accommodation of the near ultraviolet radiation source. The other port accommodates the high-energy electron beam and incorporates a gate valve for isolation of the chamber from the VDG system. High vacuum is achieved in the chamber through carbon vane pump aspiration, cryosorption and ion pumping with a 400 ℓ/sec pump.

For this test program, since NUV radiation was not being used, the target plane was oriented normal to the incident electron beam. This resulted in a quasi-symmetric electron flux distribution on the target plane, with all specimens receiving about the same fluence.

Figures 5-3 and 5-4 show schematic representations of the components of the chamber that permit in situ, in vacuo or ex situ tensile testing of the specimens. A 2224 N (500 lb) miniature load cell is mounted in the interior of the chamber on top of a rigid support platform which is rigidly attached to the cover of the bottom port. The bottom port incorporates a stainless steel bellows and an aligned feedthrough rod. The internal end of the rod has a clevis-type fitting which is used to grip a compatible fitting on the end of each tensile specimen. The external end of the rod is attached to a ball screw drive through a mechanical coupler structure. The ball screw drive is activated by a variable speed motor. The external mechanism structure acts like the movable head of a tensile testing machine, with a maximum head travel rate of 0.09 cm/min (0.036 in/min).
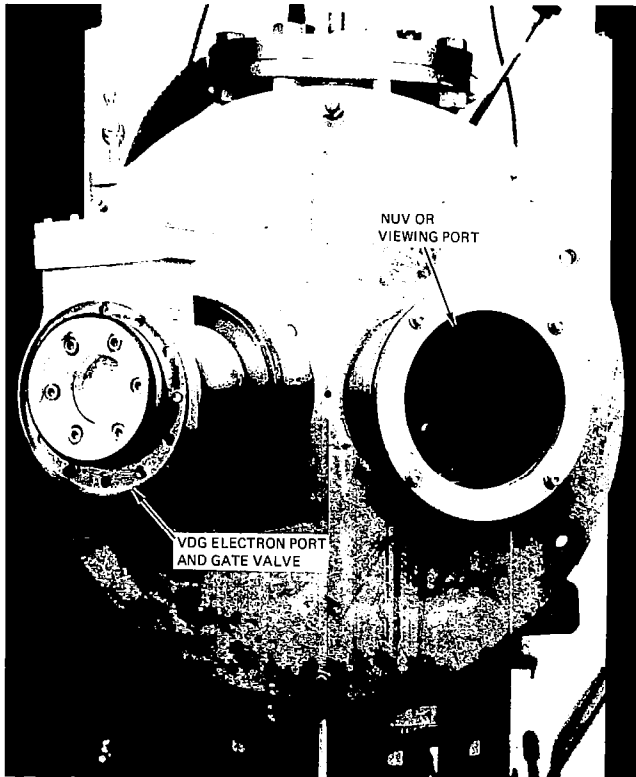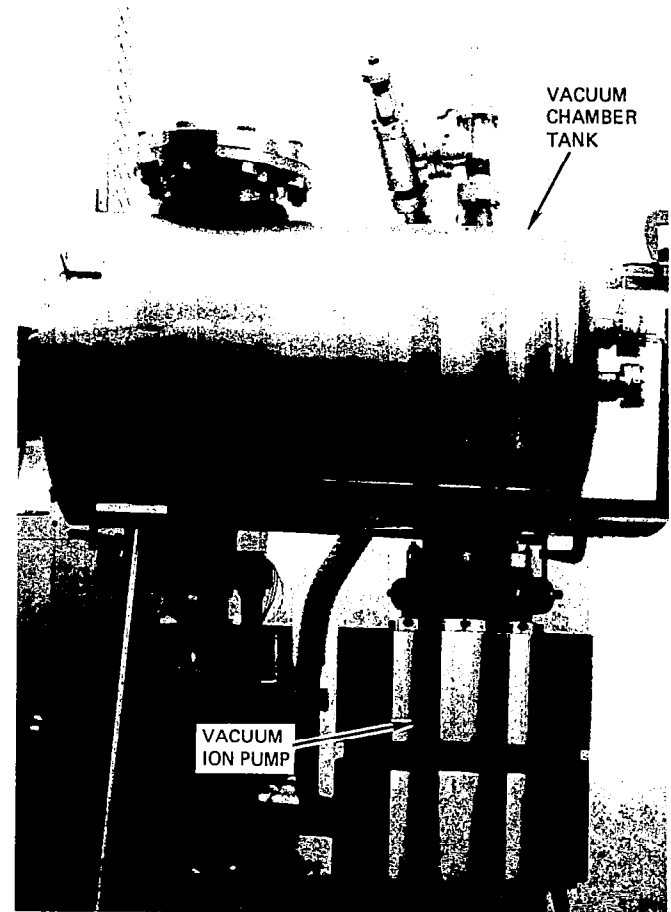
(a) Front view   (b) Side view

Figure 5-2. Vacuum/Irradiation Chamber No. 2.
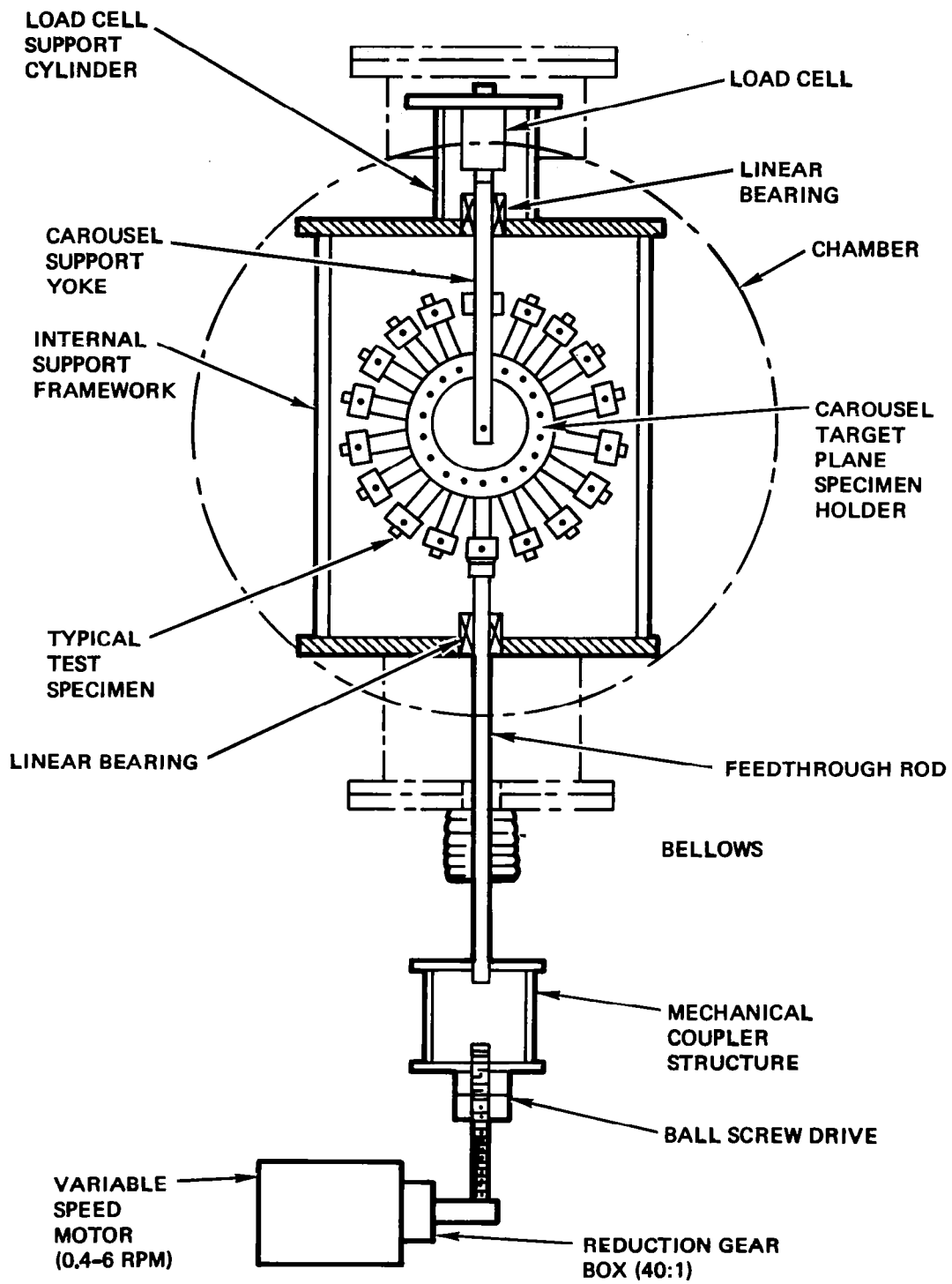
Figure 5-3. Schematic Representation of Tensile Testing Apparatus for the In Situ Tensile Test Chamber.
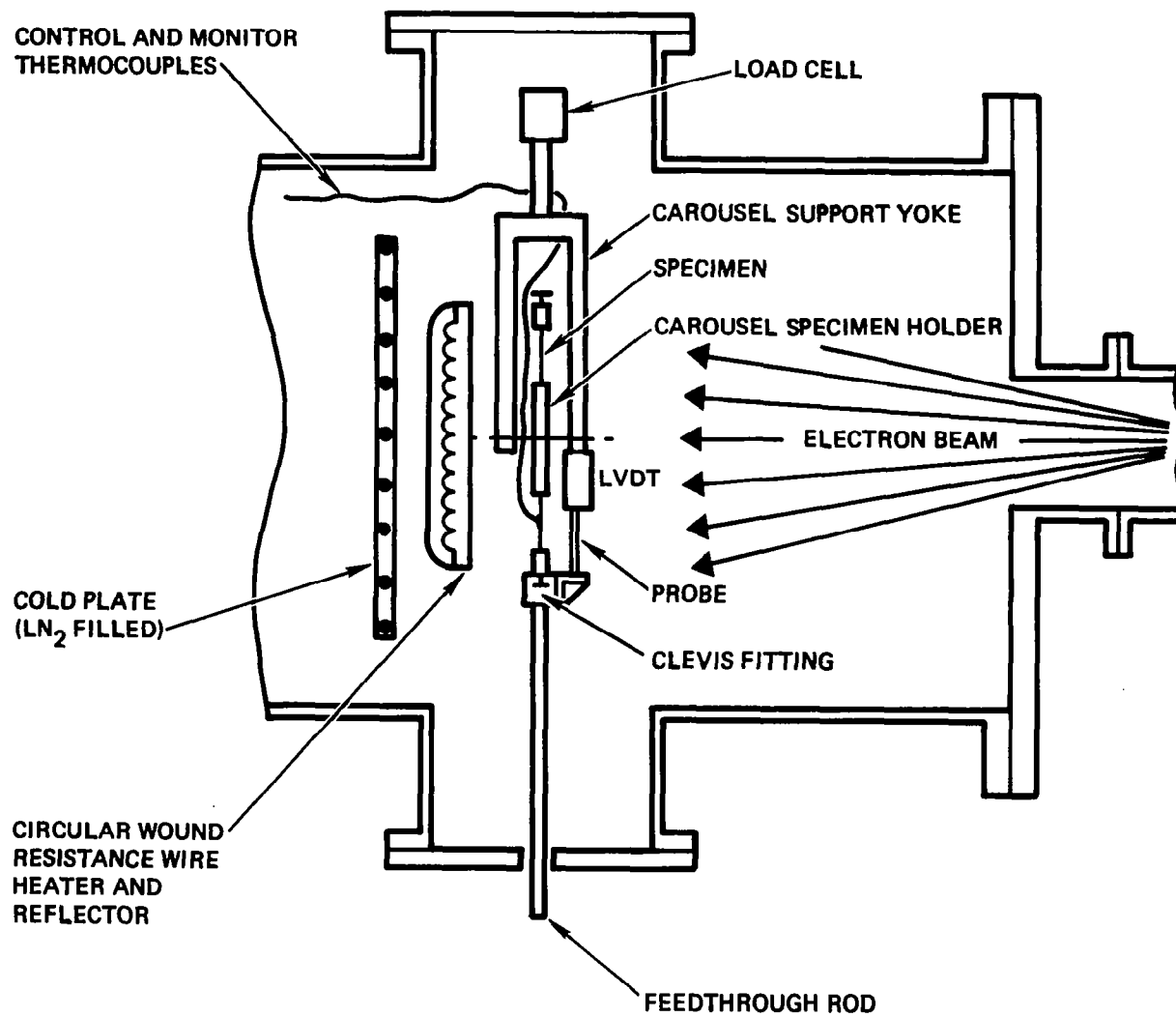
Figure 5-4. Schematic Representation of LVDT Specimen Deflection/
Strain Monitoring Transducer, Heater and Coldplate Units.

The 15 cm (6 in.) diameter target plane (shown in Figure 5-5) is in the form of a carousel which is attached through a yoke directly to the load cell. The carousel is designed to accommodate 18 specimens, 25.4 mm (1 in.) gage length by up to 12.7 mm (0.5 in.) wide, placed in a radial manner. The inward end of the test specimen is firmly clamped in the carousel. The outer end is clamped in a fitting that mates with the clevis fitting on the upper end of the bellows feedthrough rod. The carousel is rotated by means of an external manipulator to index each specimen to the bellows feedthrough rod. It should be noted that the specimens are not directly backed up by any metal plate (like a heat sink plate). Instead they are free standing. Behind the carousel target plane are located heater and coldplate units to maintain proper control over specimen temperature. The heater unit was only installed for elevated temperature irradiation tests.

Axial motion of the feedthrough rod is monitored with a LVDT mounted on the carousel target plane yoke support and indexed to a rigid angle standoff attached to the clevis fitting (shown in Figure 5-6). The LVDT was shielded from direct electron beam exposure by a small lead plate. The LVDT output and load cell output are charted on an X-Y plotter to provide an instantaneous load-deflection (or load-strain) diagram.

Calibration of the chamber load-deflection apparatus with a relatively stiff steel specimen indicated negligible distortion or play in the "load chain" over the load range of interest [0.025 mm (0.001 in.) deflection at 444.8 N (100 lb) load for a 25.4 mm (1 in.) gage length specimen].

5.3 HIGH ENERGY ELECTRON SOURCE

The high energy electrons for the irradiations are produced by a High Voltage Engineering Corporation Model JS 1000 Van de Graaff accelerator (VDG). This generator operates by feeding charge onto a moving belt inside the pressurized VDG tank. This charge is removed from the belt at a terminal in the center of the tank, which then assumes the high voltage required to accelerate electrons from an electron source located in the terminal through an evacuated, many-electrode accelerator tube. The electron beam emerges from the accelerator tube at ground potential with an energy corresponding to the potential on the terminal. The electron beam
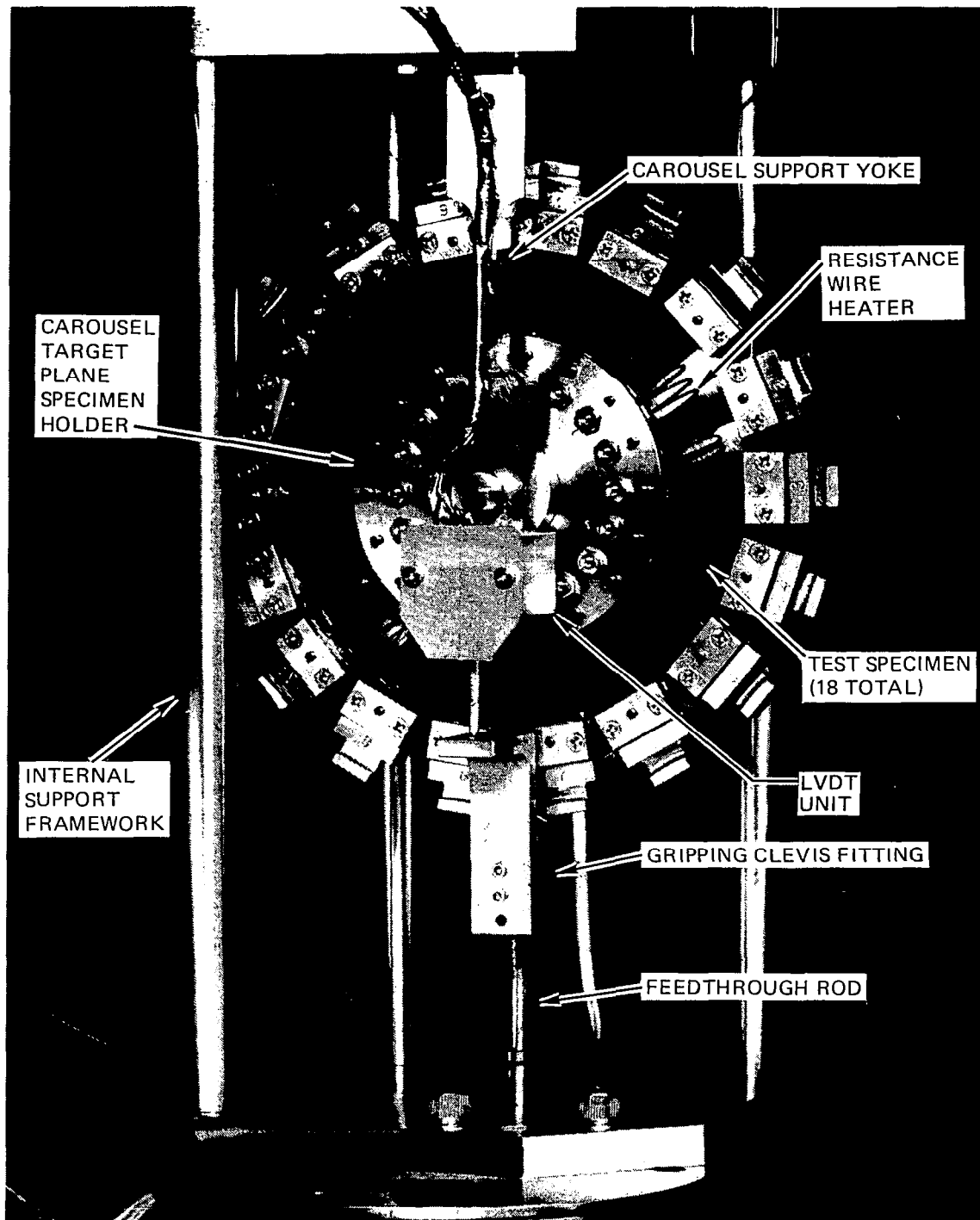
Figure 5-5.   View of Internal Components.
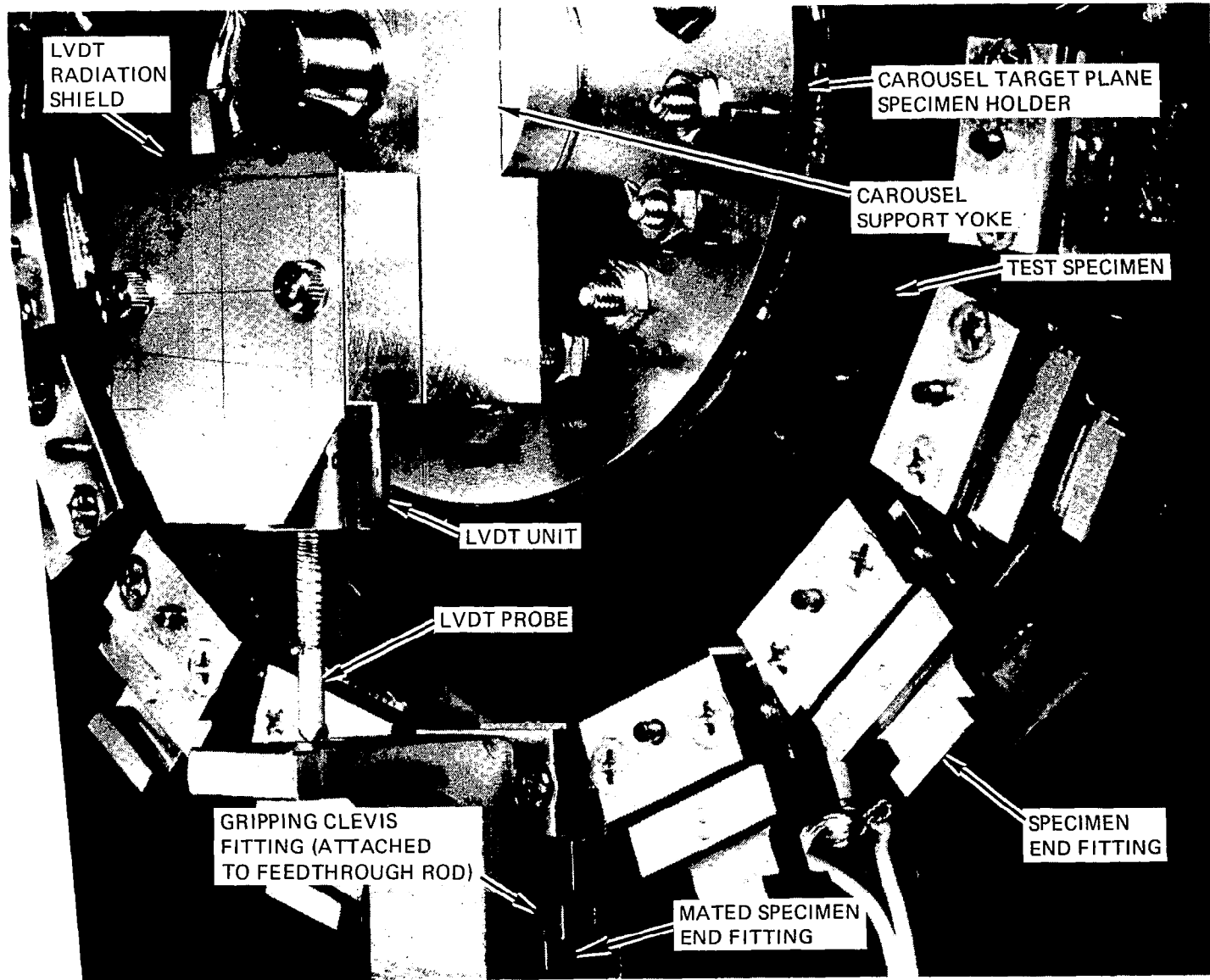
Figure 5-6. Detail of LVDT Installation.

is a dc beam and is controlled in energy and current by electronic stabil-izers. The system is capable of operating continuously with beam currents from 20 nA to 50 μA at electron beam energies from 0.070 to 1.1 MeV.

Figure 5-7 shows the beam line between the VDG and the vacuum/ irradiation chamber used for the subject program. The electron beam pro-duced is initially focused by a solenoidal magnet and then passed through vacuum piping to a switching/bending magnet which can direct the beam into any one of four beam lines. After passing through the switching magnet, the beam passes through a second solenoidal magnet which re-focuses the beam upon scattering foils located in the beam scattering chamber. The beam plumbing is enclosed by Conetic (high permeability nickel steel) shielding to keep the earth's magnetic field and other stray fields from altering the beam path. With the use of the solenoidal magnets and shielding, over 85 percent of the electron beam passes through a 1.27 cm (0.5 in.) diameter aperture at the end of the beam leg into the beam scattering chamber.

This aperture is positioned at the entrance to a scattering chamber (Figure 5-8) where the beam passes through a series of thin aluminum foil diaphragms before passage into the vacuum/irradiation chamber. The last foil acts to isolate the test chamber vacuum from the VDG accelerator vacuum and to disperse the electron beam over the carousel target plane. At the 700 keV energy level, the full dispersion can not be achieved by one foil; hence, additional foils are interposed in the electron beam by means of a remotely controlled rotator. The beam, in passing through the scat-tering foils, loses about 4 percent of its energy. This is compensated for by an appropriate increase in the beam energy level leaving the VDG.

The scattered electron beam is monitored on the downstream annulus/ exit aperture which also defines the extent of the beam that can freely expand into the test chamber. The current impinging on this annulus, biased against externally arriving secondary electrons, is fed to a current integrator to determine accumulated target plane fluence.

Calibration of the VDG system is presented in Appendix B. The appen-dix details the calibration of the annular current against the on-target electron flux (using a Faraday cup), target plane flux mapping (using thermoluminescent dosimeters), and beam energy calculations.
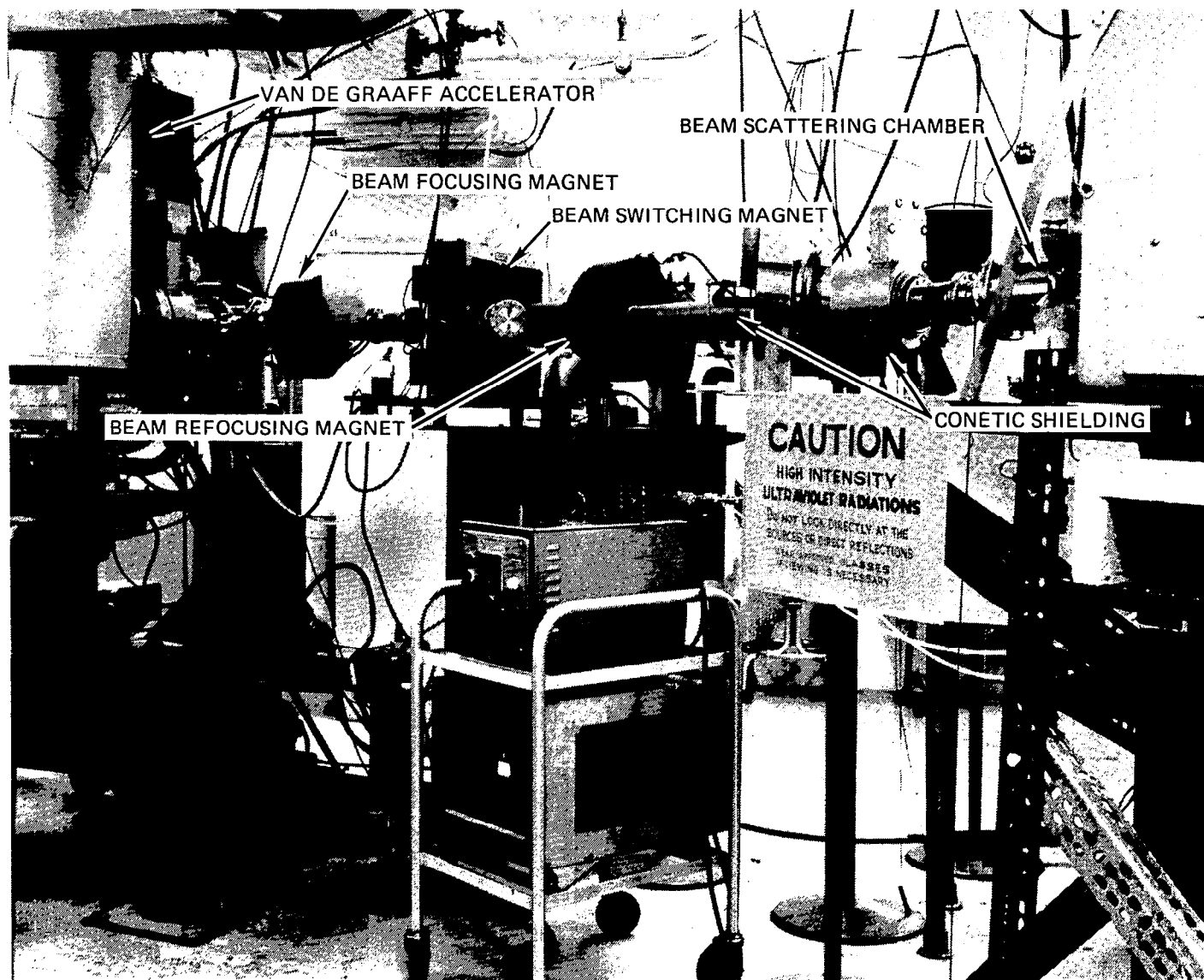
Figure 5-7. High-Energy Electron Beam Distribution System.

REMOTE CONTROL ROTATOR

GRAPHITE STOPPER

EXIT APERTURE

ELECTRON BEAM

ONE 4.6 MG/CM^2 (0.65 MIL) THICK ALUMINUM FOIL

INDIUM SEALS

OPEN APERTURE — LOW ENERGY POSITION

1.27-CM (0.5-INCH) DIAMETER INPUT APERTURE

TWO 7 MG/CM^2 ALUMINUM FOILS (2 MIL TOTAL THICKNESS) FOR 700 keV ELECTRONS
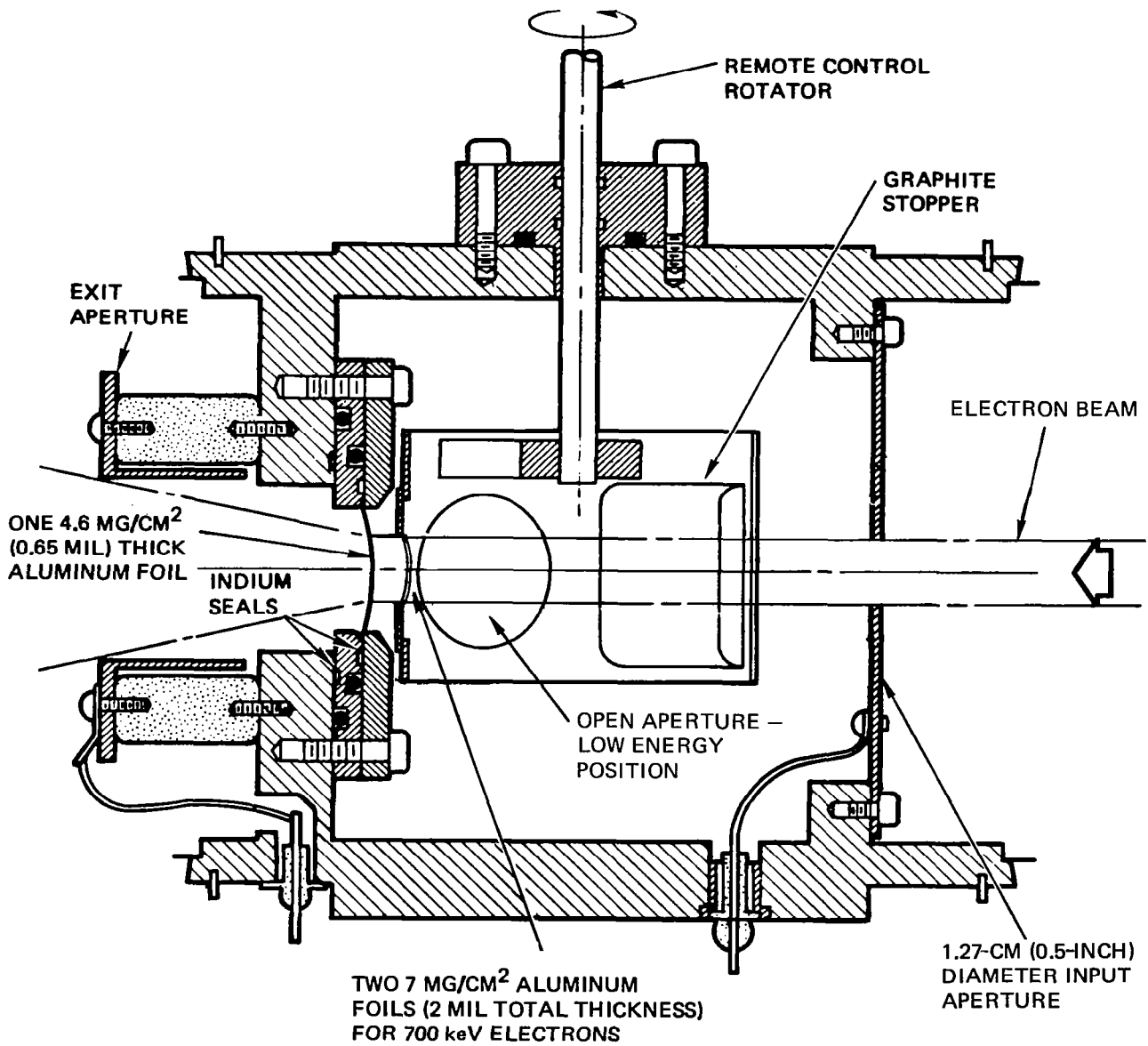
Figure 5-8. VDG Electron Beam Scattering Chamber.

6.0 TEST RESULTS

6.1 TEST OVERVIEW

Tensile testing consisted of baseline measurements on unexposed specimens and measurement of property changes on irradiated specimens. Baseline data were obtained ex situ (in the ambient environment) using an Instron testing machine, and in vacuo and in air in the vacuum/irradiation chamber using the chamber load-deflection testing apparatus.

Testing of irradiated specimens was done exclusively in the vacuum/irradiation chamber using the chamber load-deflection apparatus. Tests were performed on irradiated specimens in situ (while the specimens were being irradiated), in vacuo (in vacuum after cessation of irradiation), and ex situ (in air after cessation of irradiation).

Testing was broken into two phases, with a number of individual test sequences for each phase. Phase I tests evaluated the effects of radiation and post-irradiation test environments on one composite material system (T300/5208). Radiation levels were nominally 1 to 2 x 10^9 rads at room and elevated temperature (120°C). Post-irradiation test environments included in vacuo, in situ, and ex situ.

Based on the negligible changes in material properties obtained during the Phase I tests, the Phase II tests were designed to obtain radiation damage thresholds on the test materials. Two composite material systems (T300/934, C6000/P1700) were subjected up to 1 x 10^{10} rads at elevated temperature (120°C). Post-irradiation test environments included in vacuo and ex situ.

6.2 PHASE I TEST RESULTS

6.2.1 Test Plan

Table 6-1 presents the Phase I Test Series. The series consisted of five test sequences on T300/5208 [±45/∓45] laminate graphite/epoxy material. Control specimens were tested during Sequences 1 and 2 to obtain baseline material properties. Tests on irradiated specimens were conducted during Sequences 3, 4 and 5 to evaluate the differences among in situ, in vacuo, and ex situ effects on tensile properties.

Table 6-1. Phase I Test Series

Test Sequence	Radiation Parameters	Radiation Time (Hrs)	Specimen Temperature °C (°F)	Test Machine	Tensile Test Atmosphere	Material	Number of Specimens Tested	Remarks
1	No radiation	0	20 (68)	Instron	In air	T300/5208 [+45/∓45]	9	Control specimen tests
2a	No radiation	0	20 (68)	Chamber	In vacuo	T300/5208 [+45/∓45]	9	Control specimen tests comparing the effects of air and
2b					In air		9	vacuum on tensile properties and comparing chamber results with Instron results.
3a	1 x 10^9 rads; 700 keV; 2.1 x 10^11 e/cm^2sec; 10^-6 torr	34 hrs total at ≈8 hrs per day for 4.5 days	20 (68)	Chamber	In vacuo	T300/5208 [+45/∓45]	6	18 specimens on target plane. 6 specimens tested to failure in vacuum immediately after termination of radiation.
3b					In air		6	6 specimens tested to failure in air 64 to 72 hours after chamber is backfilled with dry air.
3c					In air		6	
4a	1 x 10^9 rads; 700 keV; 2.1 x 10^11 e/cm^2sec; 10^-6 torr	34 hrs continuous	20 (68)	Chamber	In situ	T300/5208 [+45/∓45]	1	18 specimens on target plane. 1 specimen tested to failure just prior to termination of the initial 34 hours of irradiation. 2 specimens tested to failure in vacuum immediately after termination of the initial 34 hours of irradiation. Remaining specimens are irradiated for another 30 minutes. 1 specimen tested to failure just prior to termination of the 30-minute radiation. 2 specimens tested to failure in vacuum immediately after termination of the 30-minute radiation. This sequence of 30-minute radiations with 1 specimen tested prior to and 2 specimens tested immediately after additional irradiation is repeated.
4b		34			In vacuo		2	
4c		34.5			In situ		1	
4d		34.5			In vacuo		2	
4e		35			In situ		1	
4f		35			In vacuo		2	
4g		35.5			In situ		1	
4h		35.5			In vacuo		2	
4i		36			In situ		1	
4j		36			In vacuo		2	
4k		36.5			In situ		1	
4l		36.5			In vacuo		2	
5a	2 x 10^9 rads; 700 keV; 2.1 x 10^11 e/cm^2sec; 10^-6 torr	68 hrs total at ≈8 hrs per day for 9 days	120 (248) (Irradiated)	Chamber	In vacuo	T300/5208 [+45/∓45]	6	See remarks for test sequence 3.
5b			20 (68) (Tensile		In air		6	
5c			Tested)		In air		6	

The objectives of Sequences 1 and 2 were as follows: (1) to obtain baseline data, (2) to determine any differences in test data caused by differences between the load-deflection apparatus of the Instron and vacuum chamber equipment, and (3) to evaluate whether dry air or vacuum has any effect on the baseline results. For Sequence 1, nine unirradiated control specimens were tensile tested to failure under ambient conditions using a standard Instron testing machine. For Sequence 2, eighteen unirradiated control specimens were tensile tested to failure in the vacuum/irradiation chamber. Nine specimens were tested while under vacuum, and the remaining nine specimens were tested with dry air in the chamber.

The objective of Sequence 3 was to provide data on in vacuo versus ex situ effects. Eighteen specimens were subjected in vacuum to a nominal dose of 1×10^9 rads. Radiation occurred over a 4.5 day period (≈ 8 hours/day), with specimens at a nominal temperature of 20°C (68°F). Six specimens were tensile tested to failure immediately (within 30 minutes) after completion of the full term dose (in vacuo tests). The chamber was then backfilled with dry air and another six specimens were immediately (within 45 minutes) tested to failure (ex situ tests). The remaining six specimens were exposed to dry air for approximately three days in the chamber before being tested to failure (ex situ tests).

Sequence 4 tests explored the differences between in situ and in vacuo effects. Eighteen specimens were subjected in vacuum to a nominal dose of 1×10^9 rads. Full term dose was applied continuously (24 hours/day) over a 34-hour period with specimens at a nominal temperature of 20°C (68°F). One specimen was tensile tested to failure while being irradiated just prior to completion of full term dose (in situ test). Immediately after completing irradiation, two specimens were tensile tested to failure in vacuum (in vacuo tests). The remaining fifteen specimens were irradiated for an additional 30 minutes. One specimen was tested to failure while being irradiated just prior to completion of the 30-minute added radiation, and two specimens were tested to failure immediately after completion of the added radiation. This sequence of 30-minute added radiation periods with tensile testing before and immediately after cessation of irradiation

was repeated with the remaining specimens until all were tested.
This resulted in six specimens being tested in situ and twelve specimens
being tested in vacuo.

Sequence 5 was a repeat of Sequence 3, except that full term dose was
nominally 2×10^9 rads with specimen temperatures at 120°C (248°F). Radiation occurred over a nine-day period ($\approx$8 hours/day). Tensile testing was
performed at near room temperature.

The only major deviations from the plan described above were as follows: (1) temperature of the specimens during irradiation for Sequences 3
and 4 was 7°C (45°F); (2) temperature of the specimens during irradiation
for Sequence 5 was 110 to 118°C (230 to 245°F); (3) the temperature of the
specimens during tensile testing for Sequences 3, 4, and 5 was above and
below the 20°C (68°F) temperature desired; (4) heater malfunction during
Sequence 5 resulted in specimen temperatures of 46°C (115°F) during an
8-hour period at the beginning of irradiation and during a 12-hour period
at the end of irradiation; and (5) due to radiation backscatter from the
heater unit installed for Sequence 5 tests, the total dose was 2.4×10^9
rads.

6.2.2 Test Procedures

Specimens received from NASA/LaRC were subjected to a general inspection to ensure that they were straight, free of rough edges, and had properly installed/aligned end-tabs. Some specimens were rejected over the
course of the Phase I test series because of flaws. Only those specimens
that passed the inspection were preconditioned. After preconditioning,
another inspection was made to ensure none of the specimens had warped.

Specimens were preconditioned prior to radiation or testing by expo
sure to a temperature of 65°F (150°F) for 72 hours in a vacuum of 10^{-5} torr.
Upon completion of the preconditioning sequence, specimens were placed in a
vacuum desiccator and evacuated with a mechanical pump for transportation
to the laboratory or for storing prior to installation on the carousel target plane or testing in the Instron machine. In most instances the specimens, once preconditioned, were immediately tested to failure (Instron
tests) or installed on the carousel target plane and placed in the vacuum/
irradiation test chamber. Thus, preconditioned specimens were tested to

38

failure or under vacuum in the test chamber within 3 hours of exposure to ambient conditions.

The specimens to be tested in the vacuum/irradiation chamber, once full vacuum was reached, were permitted to sit 48 to 72 hours before the start of irradiation or before the start of in vacuo baseline tests.

Except for one test sequence (Sequence No. 4), irradiation was applied approximately 8 hours/day in a nearly continuous manner with only minor interruptions during that 8-hour period. There was an approximate 16-hour stand-down period between daily irradiations. Irradiations were performed on consecutive days with no weekend or holiday interruptions. For Sequence 4, irradiation was applied in a nearly continuous manner 24 hours/day, with only minor interruptions during the total period ($\approx$34 hours), to obtain full term dose.

At the conclusion of full term dose or at intermediate dose levels, specimens were tensile tested to failure using the in situ loading apparatus described in Section 5.2 and in the sequences described in Section 6.2.1.

After completion of tensile testing on each batch of specimens (18 specimens for radiation test sequences), the specimens or remnants thereof were removed from the vacuum chamber and placed in a plastic container for storage. Microscopic examination of each specimen was performed and photomicrographs were taken to illustrate typical damage and failure modes.

Following completion of post-test examinations at TRW, specimens from each test sequence were returned to NASA/Langley for customer examination. Results of any customer-conducted examinations/tests were not available for inclusion in this report.

6.2.3 Tensile Properties

The Phase I Test Series results are summarized in Tables 6-2 through 6-6. These tables present the calculated values of modulus of elasticity (E), ultimate tensile strength (F_{TU}), yield strength (F_{TY}) and ultimate elongation (ε_u) for the T300/5208 [$\pm$45/$\mp$45] laminate composite material for Test Sequences 1 through 5. Refer to Appendix C for a definition of these

Table 6-2. Phase I Test Series, Sequence 1 Test Results,
T300/5208 [±45/∓45], Baseline, Instron Machine,
No Radiation

S/N	Irradiation Temperature °C (°F)	Tensile Test Temperature °C (°F)	Tensile Test Environment	E Tensile Modulus GPa	(Msi)	F$_{TU}$ Ultimate Tensile Strength MPa	(ksi)	Deflection Measurement Method
1				10.3	(1.5)	144.8	(21.0)	
2				10.3	(1.5)	153.1	(22.2)	
3	N/A	20 (68)	Ambient	11.0	(1.6)	144.8	(21.0)	Head Travel of Machine*
4				11.0	(1.6)	151.7	(22.0)	
5				9.7	(1.4)	142.7	(20.7)	
6				17.2	(2.5)	160.6	(23.3)	
7				19.6	(2.7)	148.9	(21.6)	
8				13.8	(2.0)	151.0	(21.9)	
9				13.1	(1.9)	130.3	(18.9)	Extensiometer (2.54 cm G.L.)
10	N/A	20 (68)	Ambient	18.6	(2.7)	160.0	(23.2)	
11				15.1	(2.2)	151.0	(21.9)	
12				15.1	(2.2)	140.0	(20.3)	
13				14.5	(2.1)	142.7	(20.7)	
14				13.1	(1.9)	139.3	(20.2)	

*Specimen gripped in machine with special grips and pin through specimen end tabs

$\bar{E}$ = 10.5 GPa (1.52 Msi) (Head Travel)

$\bar{E}$ = 15.5 GPa (2.24 Msi) (Extensiometer)

$\bar{F}_{TU}$ = 147.4 MPa (21.38 ksi) (Head Travel)

$\bar{F}_{TU}$ = 147.1 MPa (21.33 ksi) (Extensiometer)

Table 6-3. Phase I Test Series, Sequence 2 Test Results, T300/5208 [±45/∓45], Baseline Properties, In the Vacuum Chamber, No Radiation

S/N	Irradiation Temperature °C (°F)	Tensile Test Temperature °C (°F)	Tensile Test Environment	E Tensile Modulus GPa	(Msi)	F_{TU} Ultimate Tensile Strength MPa	(ksi)	F_{TY} Yield Tensile Strength* MPa	(ksi)	ϵ_u Ultimate Elongation (Percent)
1			In vacuo	10.9	(1.58)	138.4	(20.069)	87.8	(12.738)	1.83
2				11.2	(1.62)	139.8	(20.275)	92.0	(13.344)	1.93
3				11.4	(1.66)	146.5	(21.251)	89.0	(12.902)	2.18
4				11.8	(1.71)	150.9	(21.892)	100.4	(14.558)	2.01
5				11.1	(1.61)	140.7	(20.408)	86.6	(12.559)	2.20
6				11.2	(1.63)	147.2	(21.347)	91.7	(13.304)	2.11
7			In vacuo	12.8	(1.85)	145.9	(21.167)	95.2	(13.803)	2.00
8			In air	11.3	(1.64)	154.5	(22.409)	92.6	(13.424)	2.12
9	N/A	20 (58)		11.3	(1.64)	152.0	(22.045)	94.5	(13.714)	2.17
10				11.4	(1.66)	143.1	(20.762)	95.7	(13.876)	1.85
11				13.7	(1.98)	147.8	(21.435)	107.2	(15.547)	1.79
12				12.6	(1.83)	149.8	(21.726)	97.2	(14.101	1.90
13				12.8	(1.86)	152.6	(22.141)	91.7	(13.306)	2.22
14				12.6	(1.83)	149.1	(21.628)	105.0	(15.233)	1.85
15				12.1	(1.75)	148.7	(21.568)	99.5	(14.425)	1.91
16				12.6	(1.83)	154.1	(22.349)	92.1	(13.358)	2.11
17				12.6	(1.82)	147.0	(21.315)	95.3	(13.825)	2.01
18			In air	12.3	(1.79)	148.3	(21.504)	97.1	(14.089)	1.88

*Strength at 1 percent (0.010 in/in) elongation

$\overline{E}$ = 11.5 GPa (1.67 Msi) (In vacuo)

$\overline{E}$ = 12.3 GPa (1.78 Msi) (In air)

$\overline{F}_{TU}$ = 144.2 MPa (20.916 ksi) (In vacuo)

$\overline{F}_{TU}$ = 149.7 MPa (21.716 ksi) (In air)

$\overline{F}_{TY}$ = 91.8 MPa (13.315 ksi) (In vacuo)

$\overline{F}_{TY}$ = 98.4 MPa (14.082 ksi) (In air)

$\overline{\epsilon}_u$ = 2.04 percent (In vacuo)

$\overline{\epsilon}_u$ = 1.98 percent (In air)

41

Table 6-4. Phase I Test Series, Sequence 3 Test Results, T300/5208 [±45/∓45], 1 x 10⁹ Rads Dose (≈8 Hrs/Day, 4-1/2 Days Irradiation)

S/N	Irradiation Temperature °C (°F)	Tensile Test Temperature °C (°F)	Tensile Test Environment	E Tensile Modulus GPa	(Msi)	F_{TU} Ultimate Tensile Strength MPa	(ksi)	F_{TY} Yield Tensile Strength(a) MPa	(ksi)	ϵ_u Ultimate Elongation (Percent)
1		18.5 (65)	In vacuo	9.6	(1.39)	158.4	(23.041)	80.5	(11.673)	2.81
2		18.9 (66)		12.5	(1.81)	164.0	(23.785)	91.3	(13.237)	3.04
3		17.5 (63)	(b)	11.2	(1.62)	152.7	(22.150)	84.7	(12.283)	2.59
4		13.5 (56)		11.8	(1.71)	154.4	(22.399)	94.0	(13.639)	2.22
5		12.2 (54)		12.8	(1.85)	151.9	(22.033)	98.1	(14.223)	2.40
6		11.1 (52)	In vacuo	10.4	(1.51)	152.5	(22.116)	87.4	(12.681)	2.48
7		17.5 (63)	In air	12.1	(1.75)	154.7	(22.432)	91.0	(13.195)	2.46
8		15.0 (59)		12.1	(1.75)	152.5	(22.116)	93.0	(13.493)	2.36
9	7 (45)	15.5 (60)	(c)	12.2	(1.77)	157.8	(22.883)	94.1	(13.648)	2.53
10		15.5 (60)		12.6	(1.82)	156.2	(22.662)	96.8	(14.039)	2.47
11		15.5 (60)		12.9	(1.87)	156.7	(22.732)	99.3	(14.408)	2.24
12		15.5 (60)	In air	13.5	(1.96)	166.1	(24.092)	94.9	(13.759)	2.74
13			In air	12.9	(1.87)	155.7	(22.584)	101.0	(14.648)	2.63
14				12.6	(1.82)	160.8	(23.324)	94.6	(13.720)	2.89
15		18.5 (65)	(d)	13.3	(1.93)	150.0	(21.753)	100.0	(14.502)	2.48
16				12.6	(1.82)	168.5	(24.440)	99.0	(14.358)	3.54
17				12.4	(1.80)	169.2	(24.538)	95.6	(13.860)	3.70
18(e)			In air	10.3	(1.50)	90.0	(13.051)	90.0	(13.052)	1.04

(a) Strength at 1 percent (0.010 in/in) elongation
(b) Within 3 to 30 min. after termination of radiation
(c) Within 3 to 46 min. after exposure to air
(d) 72 hrs. after exposure to air
(e) Thermocouple covered back of specimen; results not included in averages

$\overline{E}$ = 11.4 GPa (1.65 Msi) (In vacuo)
$\overline{E}$ = 12.6 GPa (1.82 Msi) (In air, ≈25 min)
$\overline{E}$ = 12.8 GPa (1.85 Msi) (In air, 72 hrs)
$\overline{F}_{TU}$ = 155.7 MPa (22.587 ksi) (In vacuo)
$\overline{F}_{TU}$ = 157.3 MPa (22.820 ksi) (In air, ≈25 min)
$\overline{F}_{TU}$ = 160.8 MPa (23.328 ksi) (In air, 72 hrs)

$\overline{F}_{TY}$ = 89.3 MPa (12.956 ksi) (In vacuo)
$\overline{F}_{TY}$ = 94.8 MPa (13.757 ksi) (In air, ≈25 min)
$\overline{F}_{TY}$ = 98.0 MPa (14.218 ksi) (In air, 72 hrs)
$\overline{\epsilon}_u$ = 2.59 percent (In vacuo)
$\overline{\epsilon}_u$ = 2.47 percent (In air, 25 min)
$\overline{\epsilon}_u$ = 3.05 percent (In air, 72 hrs)

Table 6-5. Phase I Test Series, Sequence 4 Test Results, T300/5208 [±45/∓45], 1 x 10^9 Rads Dose (24 Hrs/Day for 1-1/2 Days Continuous)

S/N	Irradiation Temperature °C (°F)	Tensile Test Temperature °C (°F)	Tensile Test Environment	E Tensile Modulus GPa	(Msi)	F_{TU} Ultimate Tensile Strength MPa	(ksi)	F_{TY} Yield Tensile Strength(a) MPa	(ksi)	ε_u Ultimate Elongation (Percent)
1		15.5 (60)	In situ	11.2	(1.62)	149.6	(21.701)	82.9	(12.028)	2.98
2(b)		1.7 (35)	In vacuo	10.8	(1.56)	105.4	(15.292)	90.0	(13.064)	1.41
3		-1.7 (29)	In vacuo	11.0	(1.59)	155.6	(22.574)	86.4	(12.530)	2.83
4		12.2 (54)	In situ	10.9	(1.58)	163.7	(23.752)	82.6	(11.980)	3.61
5		12.8 (55)	In vacuo	11.5	(1.67)	151.3	(21.948)	82.1	(11.906)	2.83
6		12.8 (55)	In vacuo	11.1	(1.61)	153.7	(22.294)	82.9	(12.020)	2.89
7		18.5 (65)	In situ	10.5	(1.53)	142.8	(20.717)	78.1	(11.330)	2.83
8		22.8 (73)	In vacuo	11.0	(1.60)	154.9	(22.470)	85.1	(12.344)	3.08
9	7 (45)	23.9 (75)	In vacuo	11.4	(1.66)	152.8	(22.160)	88.1	(12.780)	2.97
10		30.6 (87)	In situ	11.0	(1.59)	142.8	(20.715)	80.2	(11.633)	2.81
11		34.4 (94)	In vacuo	12.8	(1.85)	159.4	(23.118)	84.9	(12.310)	2.98
12		35.0 (95)	In vacuo	11.6	(1.68)	150.2	(21.790)	86.9	(12.610)	2.76
13		35.6 (96)	In situ	11.1	(1.61)	157.6	(22.857)	85.8	(12.444)	3.54
14		34.4 (94)	In vacuo	13.0	(1.88)	168.2	(24.392)	90.4	(13.106)	3.27
15		29.4 (85)	In vacuo	11.2	(1.62)	148.0	(21.464)	80.1	(11.622)	2.99
16		35.0 (95)	In situ	10.9	(1.58)	145.0	(21.027)	80.2	(11.626)	3.08
17		35.6 (96)	In vacuo	11.0	(1.59)	149.6	(21.704)	84.3	(12.227)	2.90
18		40.0 (104)	In vacuo	11.2	(1.62)	153.0	(22.190)	84.6	(12.272)	3.27

(a) Strength at 1 percent (0.010 in/in) elongation
(b) Specimen failed in grips; results not included in averages

$\overline{E}$ = 11.0 GPa (1.59 Msi) (In situ)

$\overline{E}$ = 11.5 GPa (1.67 Msi) (In vacuo)

$\overline{F}_{TU}$ = 150.3 MPa (21.795 ksi) (In situ)

$\overline{F}_{TU}$ = 161.1 MPa (23.373 ksi) (In vacuo)

$\overline{F}_{TY}$ = 82.7 MPa (11.840 ksi) (In situ)

$\overline{F}_{TY}$ = 85.1 MPa (12.339 ksi) (In vacuo)

$\overline{\varepsilon}_u$ = 3.14 percent (In situ)

$\overline{\varepsilon}_u$ = 2.98 percent (In vacuo)

43

Table 6-6. Phase I Test Series, Sequence 5 Test Results, T300/5208 [±45/∓45], 2.4 x 10^9 Rads Dose (≈8 Hrs/Day, 9 Days Irradiation)

S/N	Irradiation Temperature °C (°F)	Tensile Test Temperature °C (°F)	Tensile Test Environment	E Tensile Modulus GPa	(Msi)	F_{TU} Ultimate Tensile Strength MPa	(ksi)	F_{TY} Yield Tensile Strength[a] MPa	(ksi)	ε_u Ultimate Elongation (Percent)
12		29.4 (85)	In vacuo	11.7	(1.69)	154.4	(22.394)	99.6	(14.441)	3.00
13				11.0	(1.59)	154.7	(22.436)	89.2	(12.938)	3.00
14			(b)	14.7	(2.13)	174.9	(25.365)	99.3	(14.402)	3.45
15				12.1	(1.76)	147.4	(21.385)	93.8	(13.604)	2.56
16				11.7	(1.70)	154.6	(22.426)	89.6	(12.994)	3.20
17		29.4 (85)	In vacuo	11.3	(1.64)	153.4	(22.256)	98.5	(14.286)	2.50
6		21.1 (70)	In air	14.3	(2.07)	162.2	(23.523)	111.1	(16.116)	2.55
7	110-118[e]			13.2	(1.92)	150.3	(21.800)	94.4	(13.693)	2.65
8	(230-245)		(c)	13.2	(1.91)	147.7	(21.421)	94.1	(13.649)	2.80
9				13.1	(1.90)	152.9	(22.177)	86.8	(12.595)	3.25
10				15.0	(2.17)	153.6	(22.277)	97.1	(14.082)	3.03
11			In air	12.3	(1.78)	151.4	(21.959)	94.2	(13.664)	2.95
1			In air	12.9	(1.87)	159.0	(23.069)	89.7	(13.005)	3.50
2				13.0	(1.89)	146.8	(21.300)	90.6	(13.137)	3.25
3			(d)	12.2	(1.77)	150.7	(21.853)	88.5	(12.837)	3.00
4				12.7	(1.84)	151.3	(21.941)	91.7	(13.301)	3.25
5				14.4	(2.09)	151.8	(22.017)	95.4	(13.832)	2.75
18		21.1 (70)	In air	15.1	(2.19)	168.7	(24.464)	101.7	(14.745)	3.50

(a) Strength at 1 percent (0.010 in/in) elongation
(b) Within 3 to 30 min after termination of radiation
(c) Within 3 to 45 min after exposure to air
(d) 72 hrs after exposure to air
(e) First 8 hours and last 12 hours were at 46°C (115°F); otherwise, the remaining 48 hours were at 110-118°C (230-245°F)

$\overline{E}$ = 12.1 GPa (1.75 Msi) (In vacuo)

$\overline{E}$ = 13.5 GPa (1.96 Msi) (In air, ≈25 min)

$\overline{E}$ = 13.4 GPa (1.94 Msi) (In air, 72 hrs)

$\overline{F}_{TU}$ = 156.6 MPa (22.710 ksi) (In vacuo)

$\overline{F}_{TU}$ = 153.0 MPa (22.193 ksi) (In air, ≈25 min)

$\overline{F}_{TU}$ = 154.7 MPa (22.441 ksi) (In air, 72 hrs)

$\overline{F}_{TY}$ = 95.0 MPa (13.778 ksi) (In vacuo)

$\overline{F}_{TY}$ = 96.3 MPa (13.967 ksi) (In air, ≈25 min)

$\overline{F}_{TY}$ = 92.9 MPa (13.476 ksi) (In air, 72 hrs)

$\overline{\varepsilon}_u$ = 2.97 percent (In vacuo)

$\overline{\varepsilon}_u$ = 2.87 percent (In air, 25 min)

$\overline{\varepsilon}_u$ = 3.21 percent (In air, 72 hrs)

properties and how they were calculated from the raw data (load-deflection curves). At the bottom of the tables are listed average values for each test condition and material property.

Almost all specimens were well behaved and failed in the center of the gage length region (see Figure 6-1). No problems were experienced with the tensile testing mechanism incorporated into the vacuum/irradiation chamber. The load-deflection curves were all of a similar nature - having a fairly linear portion over the first part of the curve, then departing from linearity and rising to a maximum load value, then experiencing a noticeable load dropoff due to initiation of failure, followed by total loss of load due to complete failure (separation) of the specimen. In most instances initiation of failure was at a strain level very close to that where maximum loading occurred.

Review of the baseline data (Tables 6-2 and 6-3) indicates that for modulus values, the data is comparable for the Instron and the test vacuum chamber when using similar deflection monitoring techniques (i.e., head travel). The Instron modulus data do indicate that the use of an exten-siometer does provide a truer measurement of modulus of elasticity because the localized deflections on the grips and specimen end tabs are not recorded. Ultimate strength values are not affected by the test equipment used, and the effects on ultimate elongation would be expected to be small. Furthermore, the load-deflection data does not appear to be affected by the presence of air or vacuum in the chamber.

As this was an exploratory program, greater emphasis was placed on the results obtained from testing in the vacuum chamber because: (1) the presence of trends was considered more important than absolute values; and (2) the "boundary conditions" assocated with the tensile testing were identical for Test Sequences 2 through 5.

Table 6-7 presents a statistical analysis summary of the Phase I Test Series data obtained from vacuum chamber testing. The data is arranged by groups of material properties and includes the average values ($\overline{X}$) from the previous tables, plus standard deviation (S) and coefficient of variation (S/$\overline{X}$). The scatter within the individual groups of data in Tables 6-3 through 6-6 is small, with a coefficient of variation being less than 10 percent in almost all instances.

Figure 6-1. Typical Failure Mode (T300/5208, Specimen No. 4, 2×10^9 Rads, Tested in Air).

Table 6-7. Phase I Test Series Data Summary, T300/5208 [±45/∓45] Laminate Composite Material

	TEST CONDITIONS										
Test Sequence	Radiation Dose Level (x10^9 rads)	Radiation Dose Application	Irradiation Temperature °C (°F)	Tensile Test Temperature °C (°F)	Tensile Test Environment	Elapsed Time After Irradiation or Exposure to Air	Material Property	No. of Specimens N	Average Value $\bar{X}$	Standard Deviation S	Coefficient of Variation S/$\bar{X}$
2	0	N/A	N/A	20 (68)	In vacuo	N/A		7	11.5 (1.666)	0.63 (0.091)	0.055
2	0	N/A	N/A	20 (68)	In air	N/A		11	12.3 (1.785)	0.72 (0.105)	0.059
3	1	8 hr/day, 4 1/2 days	7 (45)	15 (59)	In vacuo	15 min		6	11.4 (1.648)	1.22 (0.177)	0.108
3	1	8 hr/day, 4 1/2 days	7 (45)	15.6 (60)	In air	25 min	E	6	12.6 (1.820)	0.57 (0.083)	0.046
3	1	8 hr/day, 4 1/2 days	7 (45)	18.3 (65)	In air	72 hrs	Modulus of	5	12.7 (1.848)	0.37 (0.053)	0.028
4	1	24 hr/day, 1 1/2 days	7 (45)	24.4 (76)	In situ	During irradiation	Elasticity	6	10.9 (1.585)	0.21 (0.031)	0.020
4	1	24 hr/day, 1 1/2 days	7 (45)	25.6 (78)	In vacuo	5 min	GPa	11	11.5 (1.670)	0.70 (0.101)	0.061
5	2.4	8 hr/day, 9 days	116 (240)	29.4 (85)	In vacuo	15 min	(Msi)	6	12.1 (1.750)	1.34 (0.194)	0.111
5	2.4	8 hr/day, 9 days	116 (240)	29.4 (85)	In air	25 min		6	13.5 (1.960)	0.96 (0.139)	0.171
5	2.4	8 hr/day, 9 days	116 (240)	21.1 (70)	In air	72 hrs		6	13.4 (1.940)	1.12 (0.162)	0.083
2	0	N/A	N/A	20 (68)	In vacuo	N/A		7	144.2 (20.916)	4.6 (0.671)	0.032
2	0	N/A	N/A	20 (68)	In air	N/A		11	149.7 (21.717)	3.4 (0.489)	0.023
3	1	8 hr/day, 4 1/2 days	7 (45)	15 (59)	In vacuo	15 min	F_{TU}	6	155.7 (22.587)	4.8 (0.692)	0.031
3	1	8 hr/day, 4 1/2 days	7 (45)	15.6 (60)	In air	25 min	Ultimate	6	157.3 (22.820)	4.7 (0.678)	0.030
3	1	8 hr/day, 4 1/2 days	7 (45)	18.3 (65)	In air	72 hrs	Tensile	5	160.8 (23.328)	8.3 (1.197)	0.051
4	1	24 hr/day, 1 1/2 days	7 (45)	24.4 (76)	In situ	During irradiation	Strength	6	150.3 (21.795)	8.7 (1.256)	0.058
4	1	24 hr/day, 1 1/2 days	7 (45)	25.6 (78)	In vacuo	5 min	MPa	11	154.2 (22.373)	5.6 (0.810)	0.036
5	2.4	8 hr/day, 9 days	116 (240)	29.4 (85)	In vacuo	15 min	(ksi)	6	156.6 (22.710)	9.4 (1.361)	0.060
5	2.4	8 hr/day, 9 days	116 (240)	29.4 (85)	In air	25 min		6	153.0 (22.193)	5.0 (0.719)	0.032
5	2.4	8 hr/day, 9 days	116 (240)	21.1 (70)	In air	72 hrs		6	154.7 (22.441)	7.9 (1.146)	0.051
2	0	N/A	N/A	20 (68)	In vacuo	N/A		7	91.8 (13.315)	4.8 (0.690)	0.051
2	0	N/A	N/A	20 (68)	In air	N/A		11	97.1 (14.082)	5.1 (0.734)	0.052
3	1	8 hr/day, 4 1/2 days	7 (45)	15 (59)	In vacuo	15 min	F_{TY}	6	89.3 (12.956)	6.4 (0.930)	0.072
3	1	8 hr/day, 4 1/2 days	7 (45)	15.6 (60)	In air	25 min	Yield	6	94.8 (13.757)	2.9 (0.424)	0.031
3	1	8 hr/day, 4 1/2 days	7 (45)	18.3 (65)	In air	72 hrs	Tensile	5	97.9 (14.218)	2.8 (0.407)	0.029
4	1	24 hr/day, 1 1/2 days	7 (45)	24.4 (76)	In situ	During irradiation	Strength	6	81.6 (11.840)	2.7 (0.392)	0.033
4	1	24 hr/day, 1 1/2 days	7 (45)	25.6 (78)	In vacuo	5 min	MPa	11	85.1 (12.339)	2.9 (0.414)	0.034
5	2.4	8 hr/day, 9 days	116 (240)	29.4 (85)	In vacuo	15 min	(ksi)	6	95.0 (13.778)	4.8 (0.698)	0.051
5	2.4	8 hr/day, 9 days	116 (240)	29.4 (85)	In air	25 min		6	96.3 (13.967)	8.0 (1.164)	0.083
5	2.4	8 hr/day, 9 days	116 (240)	21.1 (70)	In air	72 hrs		6	92.8 (13.467)	4.9 (0.709)	0.053
2	0	N/A	N/A	20 (68)	In vacuo	N/A		7	2.04	0.135	0.066
2	0	N/A	N/A	20 (68)	In air	N/A		11	1.98	0.149	0.075
3	1	8 hr/day, 4 1/2 days	7 (45)	15 (59)	In vacuo	15 min		6	2.59	0.295	0.114
3	1	8 hr/day, 4 1/2 days	7 (45)	15.6 (60)	In air	25 min	ϵ_u	6	2.47	0.168	0.068
3	1	8 hr/day, 4 1/2 days	7 (45)	18.3 (65)	In air	72 hrs	Ultimate	5	3.05	0.545	0.179
4	1	24 hr/day, 1 1/2 days	7 (45)	24.4 (76)	In situ	During irradiation	Elongation	6	3.14	0.351	0.112
4	1	24 hr/day, 1 1/2 days	7 (45)	25.6 (78)	In vacuo	5 min	(Percent)	11	2.98	0.169	0.057
5	2.4	8 hr/day, 9 days	116 (240)	29.4 (85)	In vacuo	15 min		6	2.97	0.349	0.118
5	2.4	8 hr/day, 9 days	116 (240)	29.4 (85)	In air	25 min		6	2.87	0.258	0.089
5	2.4	8 hr/day, 9 days	116 (240)	21.1 (70)	In air	72 hrs		6	3.21	0.292	0.091

There doesn't appear to be trends in the data to indicate any appreciable change in tensile properties caused by radiation (or radiation at elevated temperature), nor any significant differences as the result of in situ, in vacuo or ex situ testing, or as the result of continuous versus intermittent irradiation procedures. Through null hypothesis statistical analysis of the average values and standard deviations, comparing various post-irradiation test environments and radiation methods, the results indicate that the differences in average values among the groups of data is statistically insignificant except in a few isolated cases.

6.2.4 Post-Test Examination

All specimens were microscopically examined at 20x for possible differences in failure mechanisms or other evidence of changes or degradation. No indication of any physical change was observed as the result of irradiation of 1 or 2 x 10^9 rads dose.

Typical specimens at each test condition were photographed at approximately 2x for record purposes. These same specimens were then examined at high magnification (typically 1000x) using a scanning electron microscope. Again, the failed surfaces appeared to be very similar and no differences in failure mechanism were discernable.

6.3 PHASE II TEST RESULTS

6.3.1 Test Plan

Results from the Phase I Test Series on T300/5208 graphite epoxy laminate material indicated that, for dose levels up to 2 x 10^9 rads and temperatures up to 120°C (248°F), the resulting changes in tensile properties were small. The data also showed that the post-irradiation test environments had negligible effect on the results. One reason postulated for the latter result was that radiation damage thresholds were not achieved with the applied dose levels. Therefore, it was concluded that the dose levels would have to be substantially increased in an attempt to obtain radiation damage thresholds. If damage thresholds were achieved, then the effects of post-irradiation test environment could be more realistically evaluated.

Table 6-8 presents the Phase II Test Series. The series consisted of six test sequences. Two composite materials were tested: T300/934 [±45/∓45] laminate graphite/expoxy and C6000/P1700 [±45/∓45] laminate graphite/polysulfone. Control specimens were tested during Sequences 1, 2, 3 and 4 to obtain baseline material properties. Tests on irradiated specimens were conducted during Sequences 5 and 6 to evaluate the differences between in vacuo and ex situ effects on tensile properties.

The objectives of Sequences 1 and 2 (3 and 4) were as follows: (1) to obtain baseline data, (2) to determine any differences in test data caused by differences between the load-deflection apparatus of the Instron and vacuum chamber equipment, and (3) to evaluate whether dry air or vacuum has any effect on the baseline results. For Sequences 1 and 3, six unirradiated control specimens of each material were tensile tested to failure under ambient conditions using a standard Instron testing machine. For Sequences 2 and 4, twelve unirradiated control specimens of each material were tensile tested to failure in the vacuum/irradiation chamber. For each material, six specimens were tested under vacuum and six specimens were tested with dry air in the chamber.

The objectives of Sequence 5 were to determine the radiation damage threshold for T300/934 material and to evaluate in vacuo and ex situ effects on tensile properties. Eighteen specimens were subjected in vacuum to a nominal dose of 1×10^{10} rads. Radiation occurred over a consecutive 33-day period (≈ 8 hours/day), with specimens at a nominal temperature of 120°C (248°F). At incremental dose levels of 3×10^9 rads and 6×10^9 rads, four specimens were tensile tested to failure immediately after cessation of irradiation (in vacuo tests). At the end of the full term dose of 1×10^{10} rads, five specimens were immediately tensile tested to failure in vacuum (in vacuo test). The chamber was then back-filled with dry air and the remaining five specimens were tensile tested to failure after 72 hours exposure in air.

The objectives of Sequence 6 tests were identical to those of Sequence 5, except for C6000/P1700 material. The radiation levels, temperatures and post-irradiation test environments were the same as those used in Sequence 5.

Table 6-8. Phase II Test Series

Test Sequence	Radiation Parameters	Radiation Time (Hours)	Specimen Temperature °C (°F)	Test Machine	Tensile Test Atmosphere	Material	Number of Specimens Tested	Remarks
1	No radiation	0	20 (68)	Instron	In air	T300/934 [+45/+45]	6	Control specimen tests.
2a	No radiation	0	20 (68)	Chamber	In vacuo	T300/934 [+45/+45]	6	Control specimen tests comparing the effects of air and vacuum on tensile properties and comparing chamber results with Instron results.
2b	No radiation	0	20 (68)	Chamber	In air		6	
3	Identical to Test Sequence 1 except using C6000/P1700 material.							
4a 4b	Identical to Test Sequences 2a, 2b except using C6000/P1700 material.							
5a	3×10^9, 6×10^9 and		120 (248) (Irradiated)		In vacuo		4	18 specimens on target plane. 4 specimens tested to failure in vacuum immediately after reaching 3×10^9 rads dose. Radiation is continued on remaining specimens up to 6×10^9 rads dose. 4 specimens tested to failure in vacuum immediately after reaching 6×10^9 rads. Radiation is continued on remaining specimens up to 1×10^{10} rads dose. 5 specimens tested to failure in vacuum immediately after reaching 1×10^{10} rads. 5 remaining specimens tested to failure in air 72 hours after chamber is backfilled with dry air.
5b	1×10^{10} rads;	250 hrs total at ≈8 hrs per day for 33 days	120 (248) (Irradiated)	Chamber	In vacuo	T300/934 [+45/+45]	4	
5c	700 keV electrons;		20 (68) (Tensile tested)		In vacuo		5	
5d	2.9×10^{11} e/cm^{2}sec; Up to 2.6×10^{17} e/cm^2; 10^{-6} torr				In air		5	
6a 6b 6c 6d	Identical to Test Sequence 5a, 5b, 5c 5d except using C6000/P1700 material.							

6.3.2 Test Procedures

Test procedures were identical to those used for the Phase I Test Series (see Section 6.2.2) with respect to: pretest inspection of specimens, specimen preconditioning and handling, daily radiation schedules (i.e., ≈8 hours/day for consecutive days until incremental or full term dose was achieved), post-irradiation testing techniques, and post-test specimen examination.

6.3.3 Tensile Properties

The Phase II Test Series results are summarized in Tables 6-9 though 6-14. These tables present the calculated values of modulus of elasticity (E), ultimate tensile strength (F_{TU}), yield strength (F_{TY}), and ultimate elongation (ϵ_u) for the T300/934 and C6000/P1700 [±45/∓45] laminate composite materials for Test Sequences 1 through 6. Refer to Appendix C for a definition of these properties and how they were calculated from the raw data (load-deflection curves). At the bottom of the tables are listed average values for each test condition and material property.

Almost all specimens were well behaved and failed in the center of the gage length region (see Figure 6-2). One irradiated T300/934 specimen and four irradiated C6000/P1700 specimens warped sufficiently as the result of radiation/elevated temperature to render them unusable. No problems were experienced with the tensile testing mechanism incorporated into the vacuum/irradiation chamber. The shape of the load-deflection curves were similar to those obtained from the Phase I Test Series.

Because of the type of end gripping used for the Instron tests it was impossible to compare baseline results between Instron and vacuum chamber testing for the T300/934 material. However, there was good correlation for the C6000/P1700 baseline tests, although consistently higher values for ultimate tensile strength were obtained in the chamber tests. For both materials, there was a greater difference between the in vacuo and in air chamber test results for modulus of elasticity (in vacuo gave lower results) than experienced in the Phase I baseline chamber tests.

Tables 6-15 and 6-16 present a statistical analysis summary of the Phase II Test Series data obtained from the vacuum chamber testing for T300/934 and C6000/P1700, respectively. The data is arranged by groups of
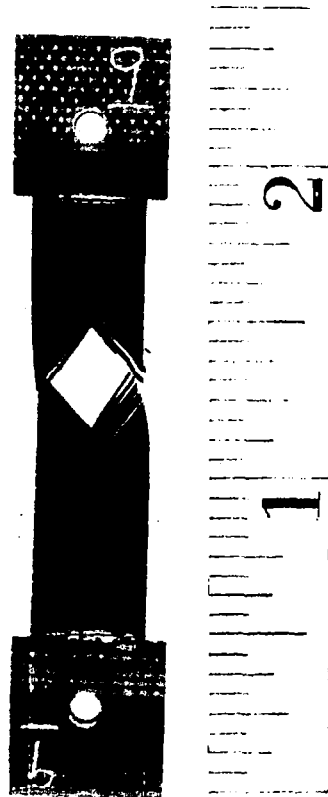
(a) T300/934, Specimen No. 9,
   1×10^{10} Rads, Tested In Vacuo
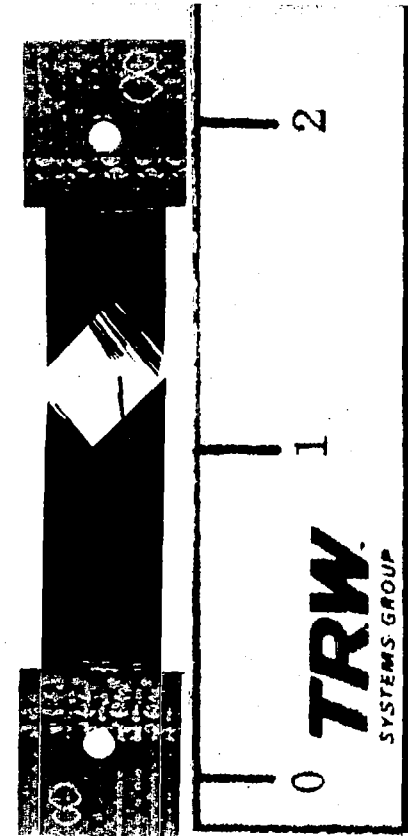
(b) C6000/P1700, Specimen No. 8,
   1×10^{10} Rads, Tested In Vacuo

Figure 6-2. Typical Failure Mode.

Table 6-9. Phase II Test Series, Sequence 1 Test Results
T300/934 [±45/∓45], Baseline, Instron Machine,
No Radiation

S/N	Irradiation Temperature °C (°F)	Tensile Test Temperature °C (°F)	Tensile Test Environment	E Tensile Modulus GPa	(Msi)	F_{TU} Ultimate Tensile Strength MPa	(ksi)	Deflection Measurement Method
1				7.6	(1.1)	153.7	(22.3)	
2				8.3	(1.2)	162.7	(23.6)	
3	N/A	20 (68)	Ambient	8.3	(1.2)	155.1	(22.5)	Head Travel*
4				6.9	(1.0)	158.6	(23.0)	of Machine
5				7.6	(1.1)	138.6	(20.1)	
6				20.0	(2.9)	159.2	(23.1)	
7				20.0	(2.9)	151.0	(21.9)	
8	N/A	20 (68)	Ambient	17.9	(2.6)	158.6	(23.0)	Extensiometer (2.54 cm G.L.)
9				20.0	(2.9)	149.6	(21.7)	
10				20.7	(3.0)	153.7	(22.3)	

*Specimen gripped in machine only by pins through end specimen tabs

$\overline{E}$ = 7.7 GPa (1.12 Msi) (Head Travel)

$\overline{E}$ = 19.7 GPa (2.86 Msi) (Extensiometer)

$\overline{F}_{TU}$ = 153.7 MPa (22.3 ksi) (Head Travel)

$\overline{F_{TU}}$ = 154.4 MPa (22.4 ksi) (Extensiometer)

Table 6-10. Phase II Test Series, Sequence 2 Test Results,
T300/934 [±45/∓45], Baseline, in the Vacuum
Chamber, No Radiation

S/N	Irradiation Temperature °C (°F)	Tensile Test Temperature °C (°F)	Tensile Test Environment	E Tensile Modulus GPa	(Msi)	F_{TU} Ultimate Tensile Strength MPa	(ksi)	F_{TY} Yield Tensile Strength(a) MPa	(ksi)	ϵ_u Ultimate Elongation (Percent)
1			In air	11.8	(1.71)	119.7	(17.358)	87.5	(12.696)	1.91
2(b)				--	--	--	--	--	--	--
3				14.2	(2.06)	151.8	(22.015)	105.2	(15.264)	2.01
4				11.0	(1.60)	121.2	(17.578)	84.4	(12.247)	2.02
5				10.1	(1.47)	121.6	(17.638)	82.2	(11.917)	2.02
6			In air	9.2	(1.34)	127.6	(18.512)	83.8	(12.154)	2.10
7	N/A	20 (68)	In vacuo	9.6	(1.39)	137.4	(19.933)	81.3	(11.797)	2.30
8				9.3	(1.35)	128.8	(18.681)	78.1	(11.322)	2.23
9(b)				--	--	--	--	--	--	--
10				9.4	(1.36)	129.1	(18.720)	75.5	(10.956)	2.00
11				9.4	(1.37)	132.5	(19.221)	83.6	(12.129)	1.96
12			In vacuo	9.7	(1.40)	131.8	(19.112)	85.8	(12.447)	2.01

(a) Strength at 1 percent (0.010 in/in) elongation

(b) Specimens were not preconditioned; test results not included

E = 11.4 GPa (1.63 Msi) (In air)

$\bar{E}$ = 9.4 GPa (1.37 Msi) (In vacuo)

F_{TU} = 128.4 MPa (18.620 ksi) (In air)

$\bar{F}_{TU}$ = 131.9 MPa (19.133 ksi) (In vacuo)

F_{TY} = 88.6 MPa (12.856 ksi) (In air)

$\bar{F}_{TY}$ = 80.9 MPa (11.730 ksi) (In vacuo)

$\bar{\epsilon}_u$ = 2.01 percent (In air)

$\bar{\epsilon}_u$ = 2.10 percent (In vacuo)

Table 6-11. Phase II Test Series, Sequence 5 Test Results, T300/934 [±45/∓45], 1 x 10^{10} Rads Dose (≈8 Hours/Day, 34 Days)

S/N	Irradiation Temperature °C (°F)	Tensile Test Temperature °C (°F)	Tensile Test Environment	Dose (x10^{10} rads)	E Tensile Modulus GPa	(Msi)	F_{TU} Ultimate Tensile Strength MPa	(ksi)	F_{TY} Yield Tensile Strength[a] MPa	(ksi)	ε_u Ultimate Elongation (Percent)
1		20.0 (68)	In air	1.0	11.0	(1.59)	156.0	(22.632)	92.1	(13.353)	3.57
2		20.0 (68)			11.7	(1.70)	164.2	(23.821)	88.0	(12.768)	4.15
3[b]		-- --	(c)		--	--	--	--	--	--	--
4		20.0 (68)			15.6	(2.26)	185.1	(26.849)	121.0	(17.546)	3.42
5		20.0 (68)	In air		11.2	(1.63)	157.7	(22.876)	91.0	(13.202)	3.23
6		23.9 (75)	In vacuo		10.3	(1.50)	140.0	(20.302)	82.0	(11.898)	2.97
7		26.1 (79)			13.0	(1.88)	151.0	(21.896)	89.6	(13.001)	2.36
8		29.4 (85)			13.9	(2.01)	157.5	(22.839)	103.7	(15.048)	2.39
9		29.4 (85)			11.8	(1.71)	161.8	(23.473)	88.3	(12.813)	2.95
10	120 (248)	37.8 (100)		1.0	11.4	(1.65)	174.2	(25.270)	84.8	(12.295)	4.82
11		32.2 (90)	(d)	0.67	8.3	(1.21)	146.2	(21.210)	76.0	(11.029)	3.08
12		29.4 (85)		0.67	10.3	(1.49)	170.0	(24.652)	86.3	(12.523)	5.50
13		30.0 (86)		0.67	11.3	(1.64)	157.7	(22.875)	89.9	(13.043)	3.44
14		32.8 (91)		0.67	9.8	(1.42)	156.5	(22.698)	84.4	(12.245)	5.47
15		33.9 (93)		0.33	11.5	(1.67)	157.9	(22.896)	86.5	(12.553)	4.12
16		36.7 (98)		0.33	11.5	(1.67)	145.4	(21.086)	95.1	(13.794)	3.19
17		38.9 (102)		0.33	12.2	(1.77)	145.4	(19.470)	95.9	(13.907)	2.13
18		43.3 (110)	In vacuo	0.33	13.5	(1.96)	173.0	(25.099)	106.6	(15.455)	3.68

(a) Strength at 1 percent (0.010 in/in) elongation
(b) Specimen warped, not tested
(c) 72 hours after exposure to dry air
(d) Within 3 to 30 minutes after termination of radiation

$\overline{E}$ = 12.2 GPa (1.77 Msi) (0.33 x 10^{10} rads, vac)
$\overline{E}$ = 9.9 GPa (1.44 Msi) (0.67 x 10^{10} rads, vac)
$\overline{E}$ = 12.0 GPa (1.75 Msi) (1 x 10^{10} rads, vac)
$\overline{E}$ = 12.4 GPa (1.80 Msi) (1 x 10^{10} rads, air)
$\overline{F}_{TU}$ = 152.6 MPa (22.138 ksi) (0.33 x 10^{10} rads, vac)
$\overline{F}_{TU}$ = 157.6 MPa (22.859 ksi) (0.67 x 10^{10} rads, vac)
$\overline{F}_{TU}$ = 156.9 MPa (22.756 ksi) (1 x 10^{10} rads, vac)
$\overline{F}_{TU}$ = 165.8 MPa (24.044 ksi) (1 x 10^{10} rads, air)

$\overline{F}_{TY}$ = 96.0 MPa (13.927 ksi) (0.33 x 10^{10} rads, vac)
$\overline{F}_{TY}$ = 84.2 MPa (12.210 ksi) (0.67 x 10^{10} rads, vac)
$\overline{F}_{TY}$ = 89.7 MPa (13.011 ksi) (1 x 10^{10} rads, vac)
$\overline{F}_{TY}$ = 98.0 MPa (14.217 ksi) (1 x 10^{10} rads, vac)
$\overline{\varepsilon}_u$ = 3.28 percent (0.33 x 10^{10} rads, vac)
$\overline{\varepsilon}_u$ = 4.37 percent (0.67 x 10^{10} rads, vac)
$\overline{\varepsilon}_u$ = 3.10 percent (1 x 10^{10} rads, vac)
$\overline{\varepsilon}_u$ = 3.59 percent (1 x 10^{10} rads, air)

Table 6-12. Phase II Test Series, Sequence 3 Test Results, C6000/P1700 [±45/∓45], Baseline, Instron Machine, No Radiation

S/N	Irradiation Temperature °C (°F)	Tensile Test Temperature °C (°F)	Tensile Test Environment	E Tensile Modulus GPa	(Msi)	F_{TU} Ultimate Tensile Strength MPa	(ksi)	Deflection Measurement Method
1				11.7	(1.7)	56.5	(8.2)	
2				8.3	(1.2)	47.6	(6.9)	
3	N/A	20 (68)	Ambient	8.3	(1.2)	57.2	(8.3)	Head Travel* of Machine
4				9.7	(1.4)	61.4	(8.9)	
5				11.0	(1.6)	73.1	(10.6)	
6				11.7	(1.7)	68.9	(10.0)	

*Specimen gripped in machine with special grips and pin through specimen end tabs

$\overline{E}$ = 10.1 GPa (1.47 Msi)

$\overline{F}_{TU}$ = 61.6 MPa (8.82 ksi)

Table 6-13. Phase II Test Series, Sequence 4 Test Results, C6000/P1700 [±45/∓45],
Baseline, In the Vacuum Chamber, No Radiation

S/N	Irradiation Temperature °C (°F)	Tensile Test Temperature °C (°F)	Tensile Test Environment	E Tensile Modulus GPa	(Msi)	F_{TU} Ultimate Tensile Strength MPa	(ksi)	F_{TY} Yield Tensile Strength* MPa	(ksi)	ϵ_u Ultimate Elongation (Percent)
1			In air	9.7	(1.40)	64.8	(9.400)	52.9	(7.673)	1.78
2				11.6	(1.68)	53.6	(7.778)	44.7	(6.481)	1.69
3				9.7	(1.41)	76.0	(11.026)	55.7	(8.076)	3.32
4				13.7	(1.99)	91.3	(13.248)	63.2	(9.172)	4.23
5				10.1	(1.47)	76.0	(11.025)	56.3	(8.162)	3.49
6	N/A	20 (68)	In air	11.3	(1.64)	61.5	(8.924)	56.1	(8.143)	1.50
7			In vacuo	10.7	(1.55)	80.2	(11.630)	56.5	(8.194)	2.37
8				8.2	(1.28)	88.1	(12.772)	47.6	(6.899)	6.15
9				11.2	(1.63)	74.7	(10.840)	60.8	(8.824)	2.02
10				7.9	(1.15)	70.1	(10.172)	49.3	(7.210)	2.26
11				8.3	(1.20)	87.5	(12.697)	57.1	(8.280)	5.44
12			In vacuo	8.4	(1.22)	82.9	(12.026)	55.1	(7.996)	5.40

*Strength at 1 percent (0.010 in/in) elongation

$\overline{E}$ = 11.0 GPa (1.60 Msi) (In air)

$\overline{E}$ = 9.2 GPa (1.34 Msi) (In vacuo)

$\overline{F}_{TU}$ = 70.6 MPa (10.234 ksi) (In air)

$\overline{F}_{TU}$ = 80.6 MPa (11.690 ksi) (In vacuo)

$\overline{F}_{TY}$ = 54.8 MPa (7.951 ksi) (In air)

$\overline{F}_{TY}$ = 54.5 MPa (7.901 ksi) (In vacuo)

$\overline{\epsilon}_u$ = 2.67 percent (In air)

$\overline{\epsilon}_u$ = 3.94 percent (In vacuo)

Table 6-14. Phase II Test Series, Sequence 6 Test Results, C6000/P1700 [±45/∓45], 1 x 10^10 Rads Dose (≈8 Hours/Day, 34 Days)

S/N	Irradiation Temperature °C (°F)	Tensile Test Temperature °C (°F)	Tensile Test Environment	Dose (x10^10 rads)	E Tensile Modulus GPa	(Msi)	F_{TU} Ultimate Tensile Strength MPa	(ksi)	F_{TY} Yield Tensile Strength(a) MPa	(ksi)	ϵ_u Ultimate Elongation (Percent)
1(b)		--	In air	1.0	--	--	--	--	--	--	--
2(b)		--			--	--	--	--	--	--	--
3		18.3 (65)	(c)		13.7	(1.99)	75.8	(10.989)	65.4	(9.490)	2.21
4		18.3 (65)			13.3	(1.93)	84.8	(12.298)	62.6	(9.073)	4.36
5		18.3 (65)			11.5	(1.67)	72.5	(10.522)	63.1	(9.151)	1.65
6(e)		--	In air		--	--	--	--	--	--	--
7		17.8 (64)	In vacuo		8.9	(1.29)	80.7	(11.703)	55.8	(8.088)	2.65
8		17.8 (64)			10.1	(1.46)	79.2	(11.491)	57.8	(8.385)	4.55
9	20 (248)	17.8 (64)			11.1	(1.61)	79.3	(11.503)	65.2	(9.451)	2.11
10(e)		--		1.0	--	--	--	--	--	--	--
11		17.8 (64)		0.67	9.8	(1.42)	70.4	(10.218)	55.4	(8.037)	2.41
12		17.8 (64)	(d)	0.67	12.6	(1.82)	75.8	(10.991)	63.6	(9.226)	1.95
13		18.3 (65)		0.67	11.4	(1.66)	77.0	(11.174)	52.3	(7.591)	2.54
14		20.0 (68)		0.67	8.7	(1.26)	69.1	(10.021)	55.2	(8.012)	1.83
15		29.4 (85)		0.33	8.8	(1.28)	64.3	(9.326)	51.4	(7.461)	1.76
16		33.3 (92)		0.33	9.4	(1.36)	83.7	(12.140)	57.0	(8.272)	6.03
17		37.2 (99)		0.33	10.7	(1.55)	55.1	(7.987)	55.1	(7.987)	0.99
18		40.0 (104)	In vacuo	0.33	9.1	(1.32)	67.7	(9.819)	55.2	(8.004)	4.01

(a) Strength at 1 percent (0.010 in/in) elongation
(b) Specimen warped, not tested
(c) 72 hours after exposure to dry air
(d) Within 3 to 30 minutes after termination of radiation
(e) Slight bend in specimen; results not included in averages

$\bar{E}$ = 9.5 GPa (1.38 Msi) (0.33 x 10^10 rads, vac)

$\bar{E}$ = 10.6 GPa (1.54 Msi) (0.67 x 10^10 rads, vac)

$\bar{E}$ = 10.0 GPa (1.45 Msi) (1 x 10^10 rads, vac)

$\bar{E}$ = 12.8 GPa (1.86 Msi) (1 x 10^10 rads, air)

$\bar{F}_{TU}$ = 67.7 MPa (9.818 ksi) (0.33 x 10^10 rads, vac)

$\bar{F}_{TU}$ = 73.2 MPa (10.611 ksi) (0.67 x 10^10 rads, vac)

$\bar{F}_{TU}$ = 79.7 MPa (11.565 ksi) (1 x 10^10 rads, vac)

$\bar{F}_{TU}$ = 77.7 MPa (11.271 ksi) (1 x 10^10 rads, air)

$\bar{F}_{TY}$ = 54.7 MPa (7.931 ksi) (0.33 x 10^10 rads, vac)

$\bar{F}_{TY}$ = 56.7 MPa (8.217 ksi) (0.67 x 10^10 rads, vac)

$\bar{F}_{TY}$ = 59.6 MPa (8.641 ksi) (1 x 10^10 rads, vac)

$\bar{F}_{TY}$ = 63.7 MPa (9.238 ksi) (1 x 10^10 rads, air)

$\bar{\epsilon}_u$ = 3.28 percent (0.33 x 10^10 rads, vac)

$\bar{\epsilon}_u$ = 2.18 percent (0.67 x 10^10 rads, vac)

$\bar{\epsilon}_u$ = 3.10 percent (1 x 10^10 rads, vac)

$\bar{\epsilon}_u$ = 2.74 percent (1 x 10^10 rads, air)

Table 6-15. Phase II Test Series Data Summary, T300/934 [±45/∓45] Laminate Composite Material

			Test Conditions											
Test Sequence	Radiation Dose Level (x10^10 Rads)	Radiation Dose Application	Irradiation Temperature °C	(°F)	Tensile Test Temperature °C	(°F)	Tensile Test Environment	Elapsed Time After Irradiation or Exposure to Air	Material Property	No. of Specimens N	Average Value X̄		Standard Deviation S		Coefficient of Variation S/X̄
2	0	N/A	N/A		20	(68)	In vacuo	N/A	E Modulus of Elasticity GPa (Msi)	6	9.4	(1.37)	0.14	(0.021)	0.015
2	0	N/A	N/A		20	(68)	In air	N/A		5	11.4	(1.63)	1.89	(0.275)	0.168
5	0.33	8 Hr/Day, 11 Days	120	(248)	38	(100)	In vacuo	•15 Min		4	12.2	(1.77)	0.94	(0.137)	0.077
5	0.67	8 Hr/Day, 22 Days	120	(248)	31	(88)	In vacuo	•15 Min		4	9.9	(1.44)	1.23	(0.179)	0.124
5	1.0	8 Hr/Day, 34 Days	120	(248)	29	(85)	In vacuo	•15 Min		5	12.0	(1.75)	1.37	(0.199)	0.114
5	1.0	8 Hr/Day, 34 Days	120	(248)	20	(68)	In air	72 Hrs		4	12.4	(1.80)	2.16	(0.313)	0.174
2	0	N/A	N/A		20	(68)	In vacuo	N/A	F_{TU} Ultimate Tensile Strength MPa (ksi)	6	131.9	(19.133)	3.48	(0.506)	0.026
2	0	N/A	N/A		20	(68)	In air	N/A		5	128.4	(18.620)	13.43	(1.948)	0.104
5	0.33	8 Hr/Day, 11 Days	120	(248)	38	(100)	In vacuo	•15 Min		4	152.6	(22.138)	16.68	(2.420)	0.109
5	0.67	8 Hr/Day, 22 Days	120	(248)	31	(88)	In vacuo	•15 Min		4	157.6	(22.859)	9.72	(1.410)	0.062
5	1.0	8 Hr/Day, 34 Days	120	(248)	29	(85)	In vacuo	•15 Min		5	156.9	(22.756)	12.71	(1.844)	0.081
5	1.0	8 Hr/Day, 34 Days	120	(248)	20	(68)	In air	72 Hrs		4	165.8	(24.044)	13.37	(1.939)	0.081
2	0	N/A	N/A		20	(68)	In vacuo	N/A	F_{TY} Yield Tensile Strength MPa (ksi)	6	80.9	(11.730)	4.14	(0.601)	0.051
2	0	N/A	N/A		20	(68)	In air	N/A		5	88.6	(12.856)	9.48	(1.376)	0.107
5	0.33	8 Hr/Day, 11 Days	120	(248)	38	(100)	In vacuo	•15 Min		4	96.0	(13.927)	8.19	(1.189)	0.085
5	0.67	8 Hr/Day, 22 Days	120	(248)	31	(88)	In vacuo	•15 Min		4	84.2	(12.210)	5.88	(0.854)	0.070
5	1.0	8 Hr/Day, 34 Days	120	(248)	29	(85)	In vacuo	•15 Min		5	89.7	(13.011)	8.40	(1.219)	0.094
5	1.0	8 Hr/Day, 34 Days	120	(248)	20	(68)	In air	72 Hrs		4	98.0	(14.217)	15.39	(2.233)	0.157
2	0	N/A	N/A		20	(68)	In vacuo	N/A	ε_u Ultimate Elongation (%)	6	2.10		0.154		0.073
2	0	N/A	N/A		20	(68)	In air	N/A		5	2.01		0.068		0.034
5	0.33	8 Hr/Day, 11 Days	120	(248)	38	(100)	In vacuo	•15 Min		4	3.28		0.856		0.260
5	0.67	8 Hr/Day, 22 Days	120	(248)	31	(88)	In vacuo	•15 Min		4	4.37		1.293		0.296
5	1.0	8 Hr/Day, 34 Days	120	(248)	29	(85)	In vacuo	•15 Min		5	3.10		1.006		0.325
5	1.0	8 Hr/Day, 34 Days	120	(248)	20	(68)	In air	72 Hrs		4	3.59		0.397		0.111

Table 6-16. Phase II Test Series Data Summary, C6000/P1700 [±45/∓45] Laminate Composite Material

	Test Conditions						Material Property	No. of Specimens N	Average Value $\bar{X}$	Standard Deviation S	Coefficient of Variation $S/\bar{X}$
Test Sequence	Radiation Dose Level (x10^10 Rads)	Radiation Dose Application	Irradiation Temperature °C (°F)	Tensile Test Temperature °C (°F)	Tensile Test Environment	Elapsed Time After Irradiation or Exposure to Air					
4	0	N/A	N/A	20 (68)	In vacuo	N/A	ε Modulus of Elasticity GPa (Msi)	6	9.2 (1.34)	1.39 (0.201)	0.150
4	0	N/A	N/A	20 (68)	In air	N/A		6	11.0 (1.60)	1.55 (0.225)	0.141
6	0.33	8 Hr/Day, 11 Days	120 (248)	35 (95)	In vacuo	=15 Min		4	9.5 (1.38)	0.83 (0.120)	0.087
6	0.67	8 Hr/Day, 22 Days	120 (248)	18.3 (65)	In vacuo	=15 Min		4	10.6 (1.54)	1.72 (0.249)	0.162
6	1.0	8 Hr/Day, 34 Days	120 (248)	17.8 (64)	In vacuo	=15 Min		3	10.0 (1.45)	1.10 (0.160)	0.110
6	1.0	8 Hr/Day, 34 Days	120 (248)	18.3 (65)	In air	72 Hrs		3	12.8 (1.86)	1.17 (0.170)	0.091
4	0	N/A	N/A	20 (68)	In vacuo	N/A	F_{TU} Ultimate Tensile Strength MPa (ksi)	6	80.6 (11.690)	7.11 (1.032)	0.088
4	0	N/A	N/A	20 (68)	In air	N/A		6	70.6 (10.234)	13.36 (1.938)	0.189
6	0.33	8 Hr/Day, 11 Days	120 (248)	35 (95)	In vacuo	=15 Min		4	67.7 (9.818)	11.91 (1.727)	0.176
6	0.67	8 Hr/Day, 22 Days	120 (248)	18.3 (65)	In vacuo	=15 Min		4	73.2 (10.611)	3.91 (0.567)	0.053
6	1.0	8 Hr/Day, 34 Days	120 (248)	17.8 (64)	In vacuo	=15 Min		3	79.7 (11.565)	0.82 (0.119)	0.010
6	1.0	8 Hr/Day, 34 Days	120 (248)	18.3 (65)	In air	72 Hrs		3	77.7 (11.271)	6.35 (0.921)	0.082
4	0	N/A	N/A	20 (68)	In vacuo	N/A	F_{TY} Yield Tensile Strength MPa (ksi)	6	54.5 (7.901)	4.94 (0.717)	0.091
4	0	N/A	N/A	20 (68)	In air	N/A		6	54.8 (7.951)	6.03 (0.875)	0.110
6	0.33	8 Hr/Day, 11 Days	120 (248)	35 (95)	In vacuo	=15 Min		4	54.7 (7.931)	2.34 (0.339)	0.043
6	0.67	8 Hr/Day, 22 Days	120 (248)	18.3 (65)	In vacuo	=15 Min		4	56.7 (8.217)	4.85 (0.703)	0.086
6	1.0	8 Hr/Day, 34 Days	120 (248)	17.8 (64)	In vacuo	=15 Min		3	59.6 (8.641)	4.94 (0.717)	0.083
6	1.0	8 Hr/Day, 34 Days	120 (248)	18.3 (65)	In air	72 Hrs		3	63.7 (9.238)	1.53 (0.222)	0.024
4	0	N/A	N/A	20 (68)	In vacuo	N/A	ε_u Ultimate Elongation (Percent)	6	3.94	1.910	0.485
4	0	N/A	N/A	20 (68)	In air	N/A		6	2.67	1.153	0.432
6	0.33	8 Hr/Day, 11 Days	120 (248)	35 (95)	In vacuo	=15 Min		4	3.28	2.198	0.670
6	0.67	8 Hr/Day, 22 Days	120 (248)	18.3 (65)	In vacuo	=15 Min		4	2.18	0.345	0.158
6	1.0	8 Hr/Day, 34 Days	120 (248)	17.8 (64)	In vacuo	=15 Min		3	3.10	1.282	0.413
6	1.0	8 Hr/Day, 34 Days	120 (248)	18.3 (65)	In air	72 Hrs		3	2.74	1.431	0.522

material properties and includes average values ($\overline{X}$) from the previous tables plus standard deviation (S) and coefficient of variation (S/$\overline{X}$). The scatter within the individual groups of data for both materials in Tables 6-10, 6-11, 6-13, and 6-14 is larger than that experienced for the Phase I tests, especially for ultimate elongation. Even so, except for a few instances in the modulus and strength data, the coefficient of variation is less than 15 percent. There appears to be more scatter in the C6000/P1700 data than in the T300/934 data. Through null hypothesis statistical analysis of the average values and standard deviations, comparing various post-irradiation test environments and dose effects, the results indicate that the differences in the average values among the groups of data is statistically insignificant, except in a few isolated cases.

Figures 6-3 through 6-6 plot the average values of the tensile properties evaluated as a function of dose level for the T300/934 and C6000/P1700 [±45/∓45] laminate composite materials. Each data point shown represents the average of 3 to 6 individual test points. Only data obtained from tensile testing in the vacuum/irradiation chamber is shown. Ex situ results (in air baseline and after full term dose) and in vacuo results are included, with lines connecting the in vacuo data. There appears to be no appreciable radiation-induced changes to the tensile properties for both materials. It is difficult to identify substantial trends in the data although some may exist. Comparing the in vacuo baseline data to the full term dose in vacuo data indicates the following:

1) Slight stiffening of the materials (10 to 20 percent increase in modulus of elasticity)

2) Slight strengthening of the materials (10 to 20 percent increase in ultimate tensile strength, with a lesser effect on yield strength)

3) Because of the large scatter in the ultimate elongation data, it is very difficult to reach any conclusion; however, there may be a slight increase in ultimate elongation for T300/934 and a slight decrease for C6000/P1700.

Since the absolute changes in the tensile properties were small, the existence of a post-irradiation test environment effect is difficult to determine. There appears to be a trend indicating that ex situ testing results in slightly higher test values for irradiated material, although
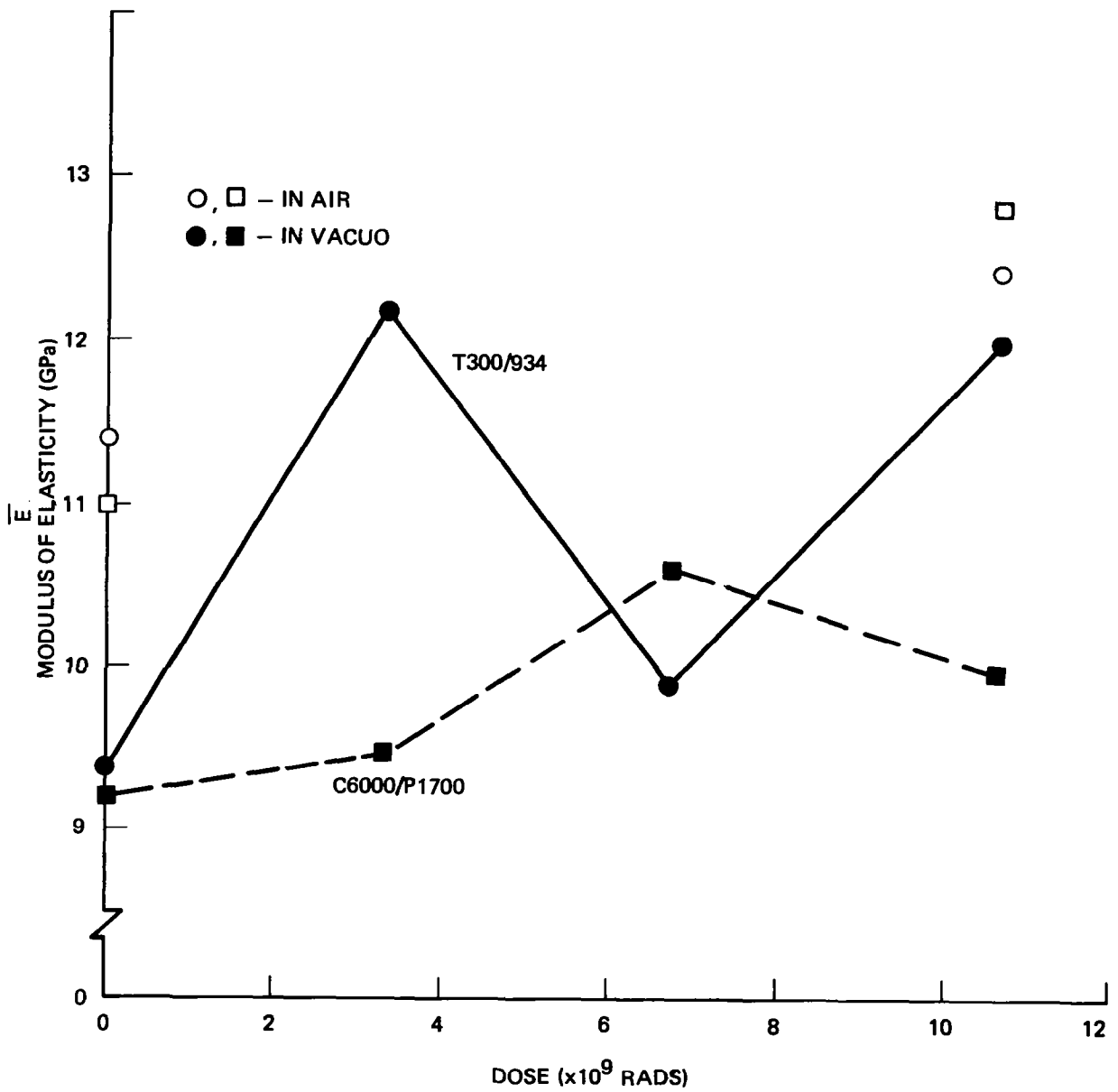
Figure 6-3. Effect of Radiation on Modulus of Elasticity,
T300/934 and C6000/P1700 [±45/∓45] Laminate
Composite Materials.

Figure 6-4. Effect of Radiation on Ultimate Tensile Strength, T300/934 and C6000/P1700 [±45/∓45] Laminate Composite Materials.
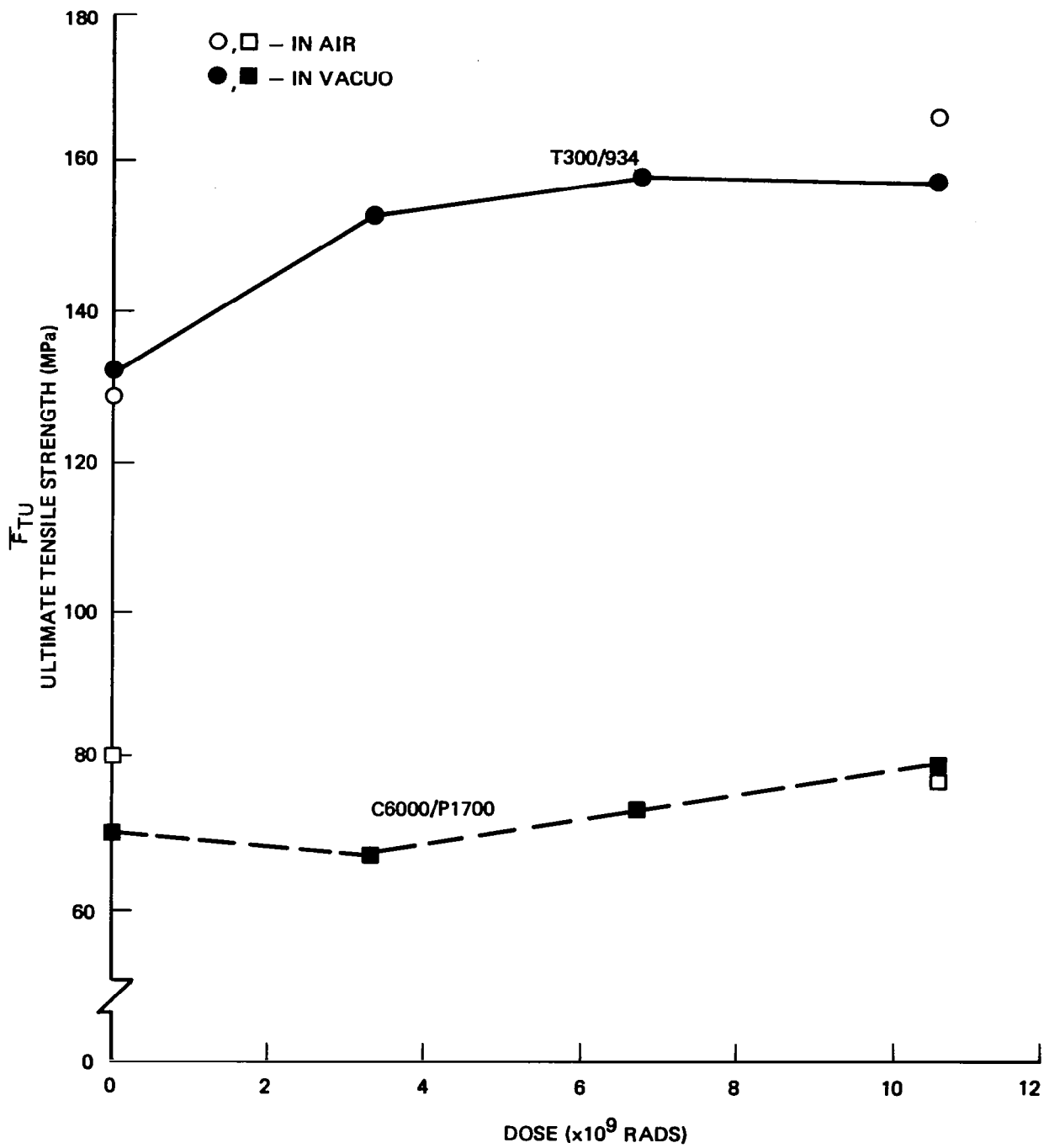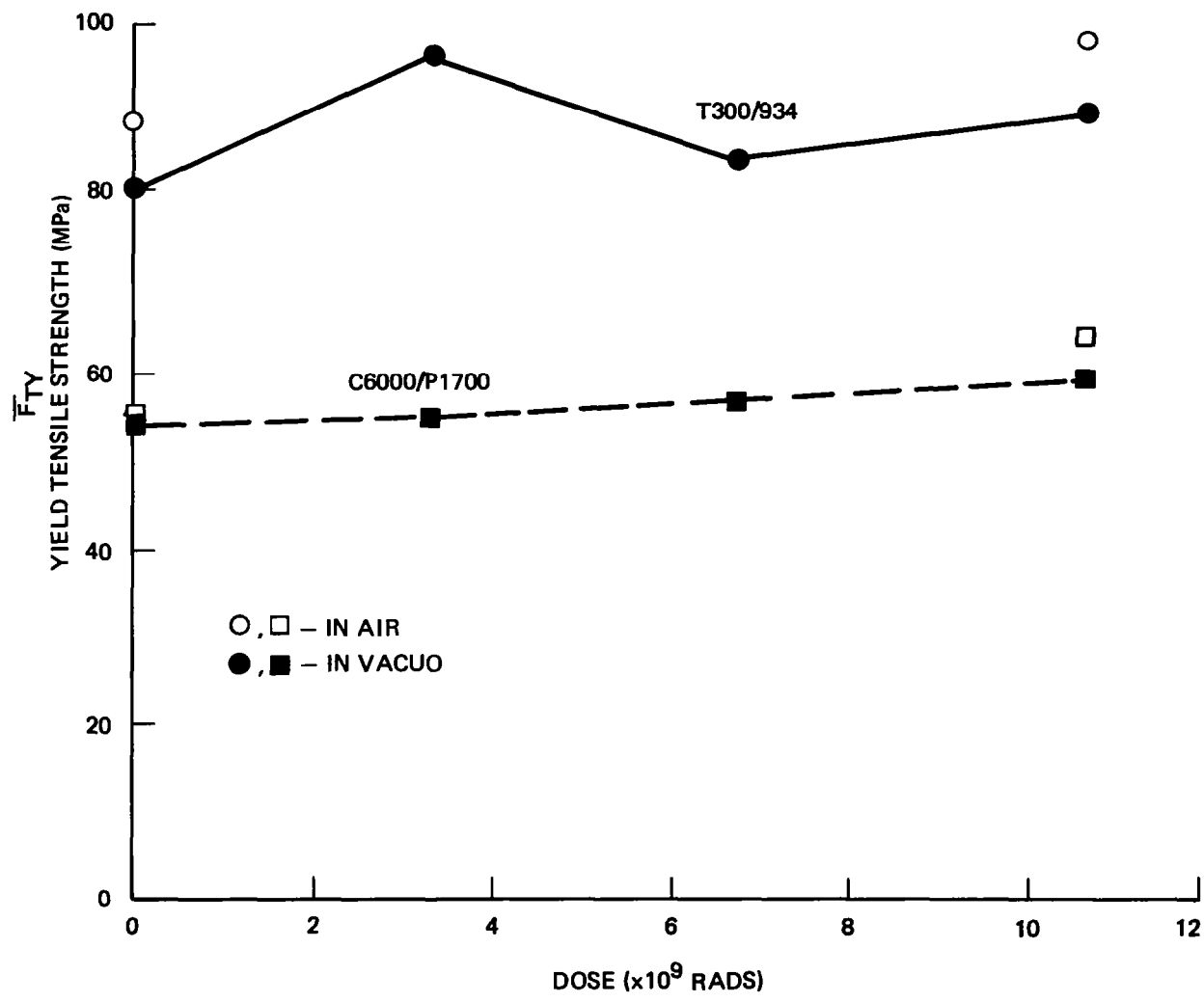
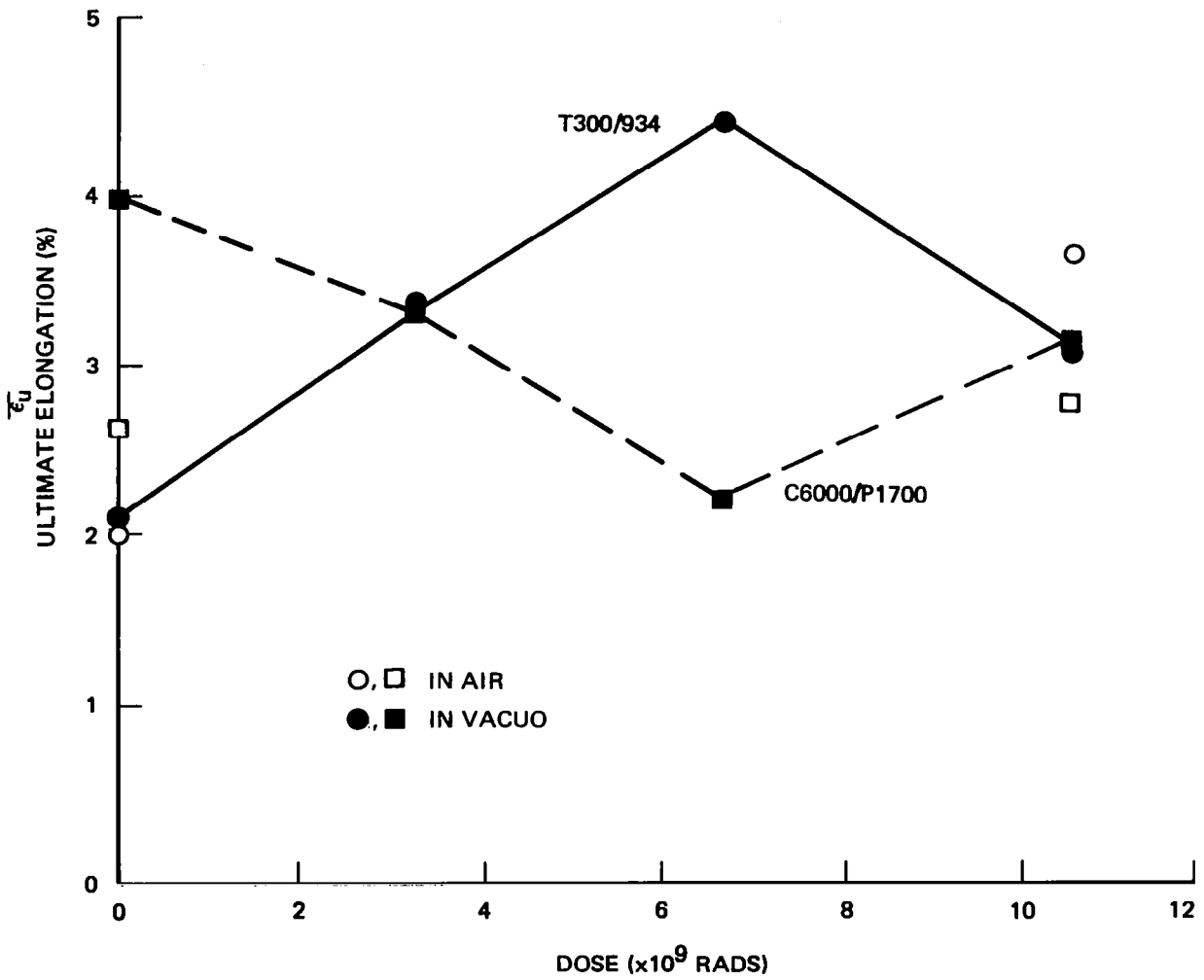Figure 6-5. Effect of Radiation on Yield Tensile Strength, T300/934 and C6000/P1700 [±45/∓45] Laminate Composite Materials.

Figure 6-6. Effect of Radiation on Ultimate Elongation, T300/934 and C6000/P1700 [±45/∓45] Laminate Composite Materials.

not in all instances. On the other hand, this apparant effect may be due to small differences in the behavior of the in situ tensile testing apparatus, since the baseline chamber tensile testing results indicated that in air data is larger than in vacuo data, in most instances.

Because of the somewhat surprising lack of radiation-induced changes at the relatively high dose level used in Phase II, a review of the test operation was made to insure that indeed the test specimens were exposed to the electron fluences generated. The data collected from the downstream annulus in the VDG beam scattering chamber, coupled with the Faraday cup calibration results, clearly indicated that the specimens were exposed to the full electron beam. As to whether the electrons penetrated the material or were somehow impeded/repulsed by the formation of an "electron cloud" at the surface of the specimens, there was no evidence to indicate this to be the case. The materials are electrically semiconductive. Any charge built up on the surface or within the material can bleed off to ground through the carousel structure. The material breakdown voltage capabilities are low relative to the 700 keV energy level. Thus, the ability to deflect the impinging beam with any surface charge buildup is small. There was no evidence of discharging marks on the surface of the specimens. Hence, it must be concluded that the specimens received and absorbed the fluences and dose levels intended.

6.3.4 Post-Test Examination

All specimens were microscopically examined at 20x for possible differences in failure mechanisms or other evidence of changes or degradation. No indication of any obvious physical change was noted as the result of the 1×10^{10} rads dose. Examination of the specimen surface revealed no discolorations or marks from any discharge phenomena.

Typical specimens were photographed at approximately 2x for record purposes. These same specimens were examined at higher magnifications (typically 1000x) using a scanning electron microscope. Figures 6-7 through 6-9 represent typical photomicrographs for control and irradiated specimens. The failed surfaces appeared very similar. No obvious differences in failure mechanisms were noticeable. Figure 6-10 shows one of the typical warped specimens. This warpage occurred more frequently on the C6000/P1700 material and was noticed after 6×10^9 rads dose.

(a) Specimen No. 2, Baseline,   (b) Specimen No. 8, 1 x 10^{10} Rads Dose
     Tested In Air   at 120°C, Tested In Vacuo

Figure 6-7. Photomicrographs (1000x) of T300/934 Specimens.

(a) Specimen No. 2, Baseline,
    Tested In Air

(b) Specimen No. 5, 1×10^{10} Rads Dose
    at 120°C, Tested In Air

Figure 6-8. Photomicrographs (1000x) of T300/934 Specimens.

(a) Specimen No. 15, 3 X 10^9 Rads Dose at 120°C, Tested In Vacuo

(b) Specimen No. 3, 1 X 10^{10} Rads Dose at 120°C, Tested In Air

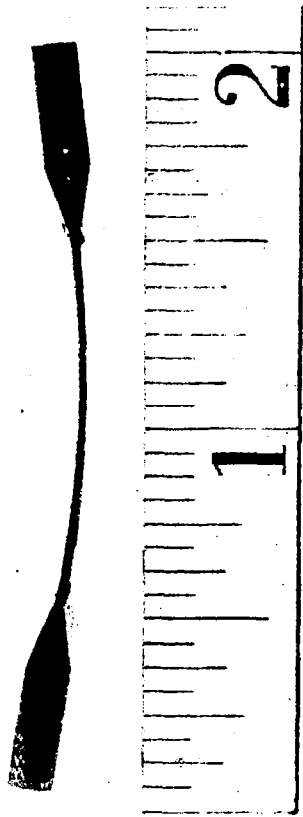Figure 6-9. Photomicrographs (1000x) of C6000/P1700 Specimens.

Figure 6-10. Photograph (2x) of Warped
C6000/P1700 Specimen No. 2,
1×10^{10} Rads Dose at 120° C.

7.0 CONCLUSIONS AND RECOMMENDATIONS

7.1 CONCLUSIONS

The ability to realistically evaluate the significance of post-irradiation test environments required: 1) there be well-established trends in the radiation-induced changes to the materials, and 2) the magnitude of the changes be large. This was not the case for the T300/5208, T300/934, and C6000/P1700 composite materials tested under this program, at least in terms of the tensile properties measured.

Using a [±45/∓45] laminate specimen provided a good opportunity to measure the radiation-induced effects on the resin matrix, as well as the resin-fiber interface, since it was assumed that the radiation damage to the reinforcement fibers would be negligible. Nevertheless, exposures up to 1×10^{10} rads dose at 120°C (248°F) caused only small changes to modulus of elasticity, ultimate tensile strength, yield strength, and ultimate elongation. The change to most properties was less than 20 percent. Differences between in vacuo test data and ex situ test data were small.

The trends obtained from the data indicated: (1) radiation slightly increased the stiffness and strength of the materials, and (2) radiation decreased the ultimate elongation of the materials.

7.2 RECOMMENDATIONS

Before concluding that the requirement for in vacuo or in situ testing of radiation-exposed composite materials is not warranted, additional studies are required to evaluate other significant material properties that were not measured. These properties include glass transition temperature, coefficient of thermal expansion, compression and shear strength. Larger sample populations are required to reduce the statistical effects and to handle the variability in properties generic to composite materials.

The simulation of the space radiation environment should be enlarged to include high energy protons, low energy charged particles and ultraviolet which can cause large absorbed doses in the surface plies. This may cause more dramatic changes in material properties not monitored under this program.

The apparent improvements in some of the tensile properties observed in this study as the result of "radiation curing" is an interesting by-product that needs further investigation.

APPENDIX A

BACKSCATTER EFFECTS ON TEST DOSE LEVELS

The dose-depth calculations shown in Figures 4-3 and 4-4 and in Table 4-1 of Section 4 assumed that there was no backing behind the test specimens that could affect the dose levels. In actuality, for some tests the only close-in backing was the rear and sides of the stainless steel vacuum chamber. For other tests, a heater unit with a stainless steel reflector plate was located in close proximity behind the specimens.

As a worst-case assumption, the previous unbacked calculations presented in Section 4.1 are repeated with a stainless steel surface being flush with the back of the test specimen. Figures A-1 and A-2 present the dose-depth profiles for the fully backed condition for 700 keV electrons, using a 2000 history case TIGER code Monte Carlo solution. Also shown is a comparison to the unbacked solutions. Table A-1 lists the average unit dose and fluence required for 1×10^9 rads dose. The results indicate that the fully backed specimen dose increases more rapidly as the thickness is traversed, such that the back-to-front dose ratio is greater than two. The average bulk dose is 33.5 percent greater than the unbacked specimen dose.

Table A-1. Average Unit Dose From a 700 keV Electron Beam Normally Incident on Specimens (Comparison of Unbacked Versus a Flush Backing of Stainless Steel)*

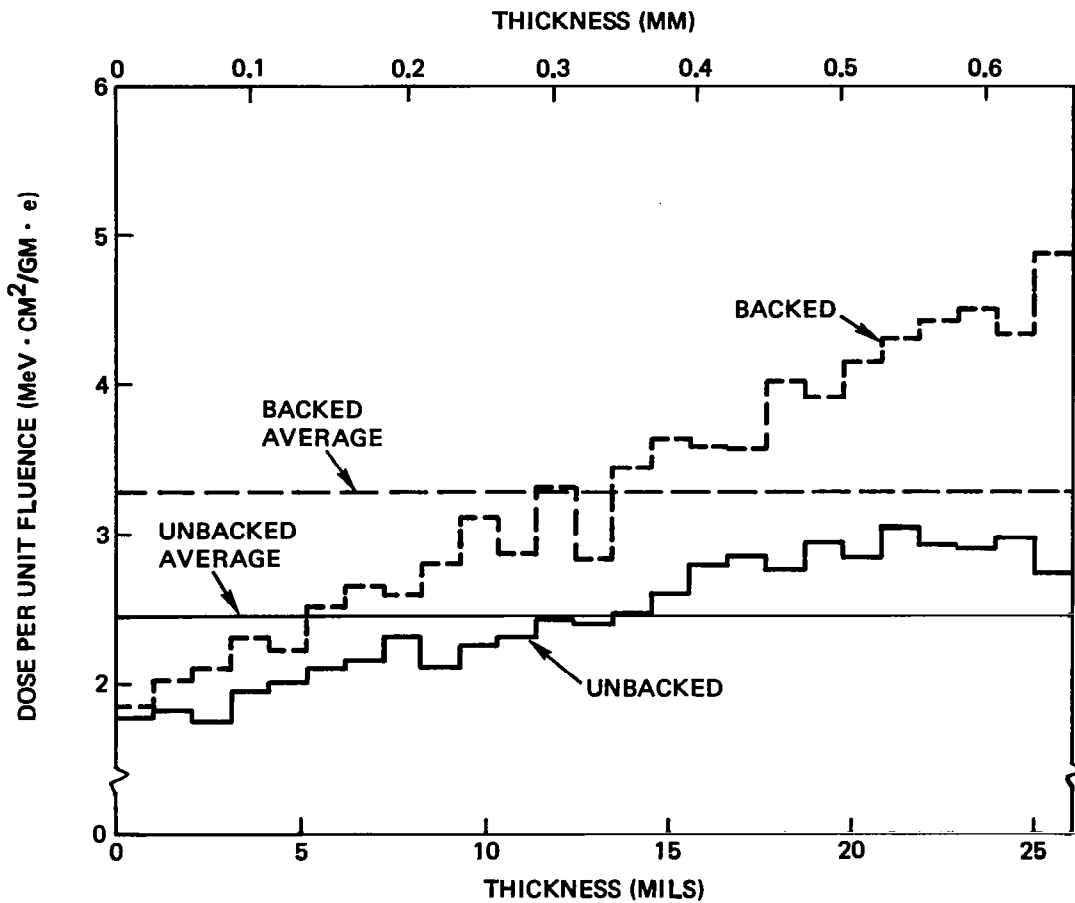| Material		Average Unit Dose		Fluence for 1×10^9 rads
		$(MeV \cdot cm^2/gm \cdot e)$	$(rad \cdot cm^2/e)$	(e/cm^2)
C6000/P1700	Unbacked	2.46	3.94×10^{-8}	2.54×10^{16}
	Backed	3.29	5.26×10^{-8}	1.90×10^{16}
T300/934	Unbacked	2.45	3.92×10^{-8}	2.55×10^{16}
	Backed	3.27	5.24×10^{-8}	1.91×10^{16}

*2000 History Monte Carlo Analysis

Figure A-1. Unit Dose as a Function of Thickness for a 700 keV
Electron Fluence Normally Incident on Material
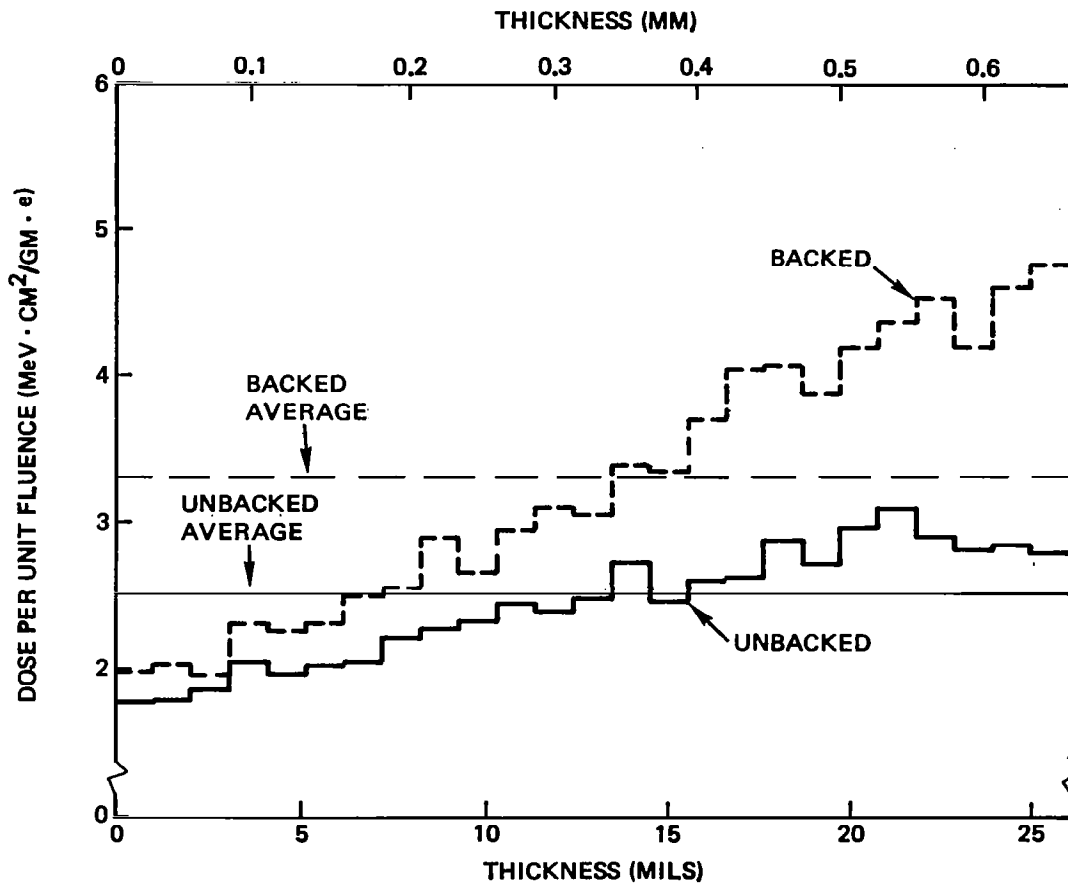C6000/P1700 Unbacked and Backed by Stainless Steel.

Figure A-2. Unit Dose as a Function of Thickness for a 700 keV Election Fluence Normally Incident on Material T300/934 Unbacked and Backed by Stainless Steel.

In reality, the actual conditions in the test chamber lie somewhere between the two extremes presented. For the condition where only the rear and side surfaces of the vacuum chamber can back-scatter the electrons, the backscattering relative to that produced by a flush mounted scatterer can be estimated assuming that: (1) the backscatter effect is isotropic in the electron direction, (2) forward scatter from the specimen is isotropic, and (3) there is little if any direct primary beam illumination of the back-scatterer. The first and second assumptions are reasonably justified by noting that the angular distributions appearing in the TIGER code calculations are roughly isotropic. The last assumption is not entirely correct. The electron beam diameter at the target plane is limited to a radius only slightly greater than the carousel radius. The target plane geometry further restricts the illuminating beam to an annulus from 10 cm to 15 cm (4 in. to 6 in.) diameter of which roughly one-half is blocked by the specimen area. The open spaces in this annular area allow the primary beam to further expand onto the chamber walls in a non-isotropic illumination. To a first approximation, it is correct to assume that the generator of forward scattering has the area of the entire annulus. Under these circumstances it can be shown that the dose, D, delivered to the specimens is approximated by:

$$\frac{D}{D_o} = 1 + \left(\frac{D_B}{D_o} - 1\right) \frac{A_s}{d^2} \cdot \frac{\Delta\Omega}{2\pi} , \tag{A1}$$

where

D_o is the bulk dose calculated for the unbacked specimen,

D_B is the bulk dose calculated for the intimately backed specimen,

A_s is the area of the forward scatterer,

d is the "average" distance of the backscatterer from the specimen,

$\Delta\Omega$ is the solid angle subtended by the backscatterer at the specimen.

As noted before, for the case of backscatter from the relatively distant chamber walls, A_s is taken as the B.3full annulus area, where:

$$A_s = \frac{\pi}{4}(15^2 - 10^2) = 98.1 \text{ cm}^2 (15.2 \text{ in.}^2) . \tag{A2}$$

The chamber rear wall is roughly (45.7 cm) (18 in.) from the target plane and the chamber diameter is (61.0 cm) (24 in.), giving an average distance of about 38.1 cm (15 in.) from the specimens to the chamber walls. The backscattering solid angle ($\Delta\Omega$) from the walls is essentially in 2π geometry. Therefore,

$$
\begin{aligned}
\frac{D}{D_o} &= 1 + \left(\frac{D_B}{D_o} - 1\right) \frac{98.1}{1451.6} \left(\frac{2\pi}{2\pi}\right) \\
&= 1 + 0.068\left(\frac{D_B}{D_o} - 1\right).
\end{aligned}
\tag{A3}
$$

Since D_B/D_o is 1.335 for the fully backed condition for the specimen materials, $D/D_o = 1.023$. Therefore, the backscattering effect from the chamber walls is negligible for Phase I testing, Sequences 3 and 4.

A heating coil/heat reflector plate was installed directly behind the specimens for the Phase I, Sequence 5 tests and all subsequent Phase II radiation tests as shown in Figure A-3. The scatterer (reflector plate) does not subtend a full 2π solid angle at the specimens. The solid angle, $\Delta\Omega$, is estimated to be approximately 1.2π steradians. The actual illumination for the heat reflector backscatterer is about 50 percent from the primary election beam normal to the reflector and about 50 percent from the forward isotropic scatter from the specimens. The first component will not produce backscatter as effectively because of the higher energy and non-isotropic impingement. Hence, the effective A_s/d^2 is reduced. The average distance (d) can be taken as that to the centerline of the reflector and equals 8.9 cm (3.5 in.). A value of 2.2 is used as a correction factor to convert from omnidirectional to isotropic reflection off the heater reflector plate.

STAINLESS STEEL HEATER REFLECTOR

SPECIMEN END FITTINGS

CAROUSEL TARGET PLANE

8.9 (3.5)

15.5φ (6.1)

5φ (2)

10.0φ (4)

15φ (6)

ELECTRON BEAM

SPECIMENS

3.8 (1.5)

6.7 (2.6)
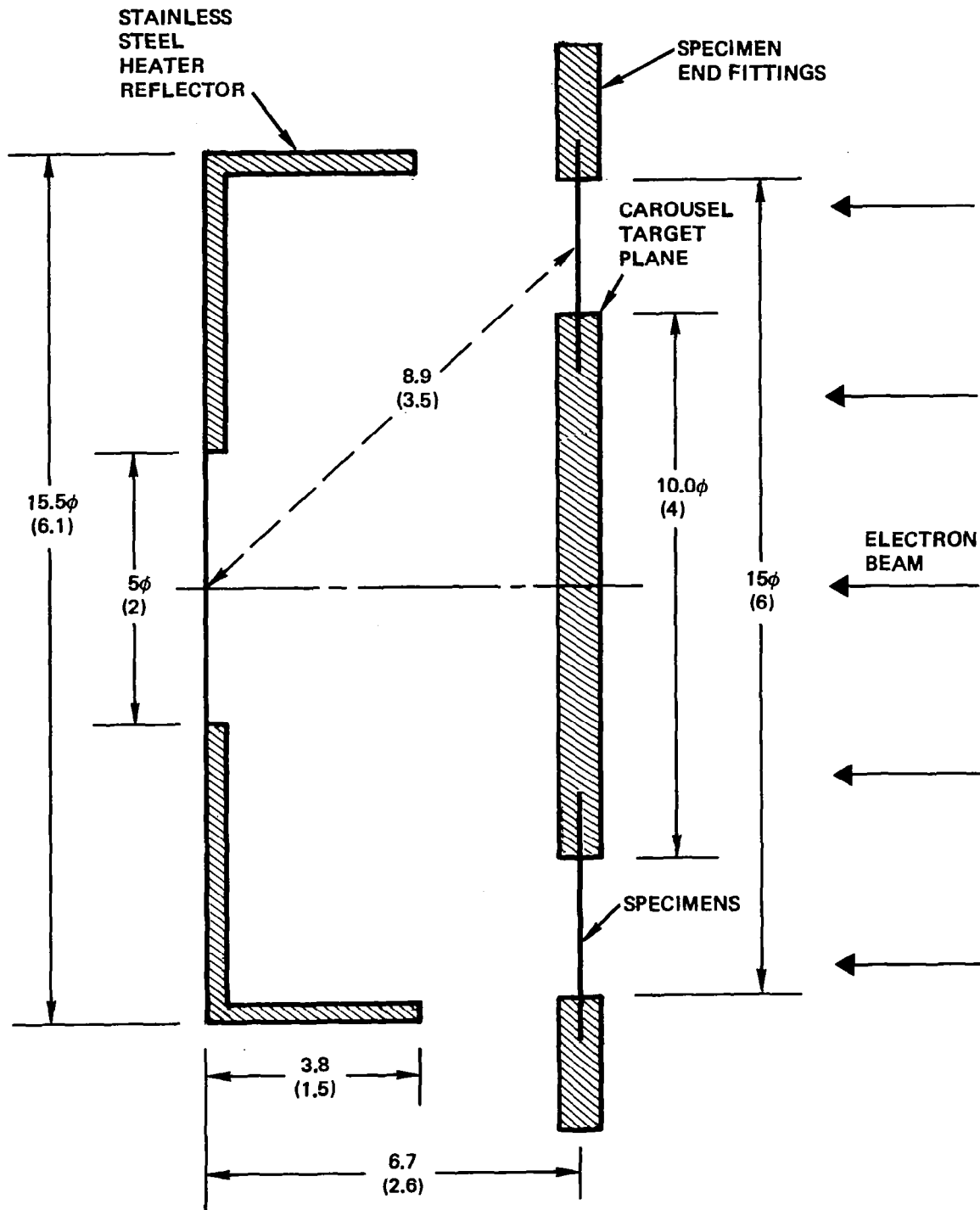
NOTE: ALL DIMENSIONS IN CM (IN.)

Figure A-3. Phase II Heater Backscattering Geometry.

Therefore,

$$\left(\frac{A_s}{d^2}\right)_{eff} = \frac{A_s/2 + A_s/(2)(2.2)}{d^2}$$

$$= \frac{0.73\ A_s}{d^2}$$

$$= 0.73\ (98.1)/(8.9)^2$$

$$= 0.90\ . \qquad\qquad (A4)$$

Thus,

$$\frac{D}{D_o} = 1 + (1.335 - 1)(0.90)\left(\frac{1.2\pi}{2\pi}\right)$$

$$= 1.18\ . \qquad\qquad (A5)$$

The effective dose is approximately 18 percent greater than the unbacked specimen dose due to the presence of the heater unit. Therefore, the 700 keV electron fluence required to produce an average dose in the specimens of 1×10^9 rads (refer to Table 4-1) for those tests having the installed heater unit is reduced to approximately

$$\frac{2.57 \times 10^{16}\ e/cm^2}{1.18} = 2.2 \times 10^{16}\ e/cm^2\ . \qquad\qquad (A6)$$

The conversion from flux to dose is increased to

$$\frac{3.89 \times 10^{-8}\ rad\ cm^2/e}{1.18} = 4.59 \times 10^{-8}\ rad\ cm^2/e. \qquad\qquad (A7)$$

APPENDIX B

CALIBRATION OF VAN DE GRAAFF HIGH-ENERGY ELECTRON SOURCE

This Appendix covers calibrations of electron beam energy, target plane flux and flux distribution, and the computations used in setting up irradiation schedules. An evaluation of the accuracies and uncertainties involved is also included.

B.1 REQUIREMENTS

The electron energy requirement was specified to be that which would allow a mono-energetic electron dose through the material to be uniform within a factor of two, within the constraints of the system energy capability and irradiation time. An energy of 700 keV was determined to be an appropriate level (see Section 4.1).

Depending on the specific test, the average absorbed dose in the test material was 1×10^9 rads, 2×10^9 rads, or 1×10^{10} rads. Section 4.1 and Appendix A summarize calculations made to arrive at a dose-to-fluence conversion factor for the case where no backing material was in the vicinity of the test specimens and for the case where a backscattering material was in the vicinity of the test specimens.

The desired goal on beam fluence variation over the specimens was to be less than ±10 percent. Since the target plane was normal to the center line of the electron beam and all specimens were at approximately the same angle with respect to this centerline, the only substantial specimen-to-specimen fluence variations could be due to the beam being off-center, to shadowing, or to localized scatterers.

Table B-1 lists the desired irradiation levels for the Phase I and Phase II tests that required electron exposure. The fluxes listed in the table were determined from machine calibrations discussed in Section B.3. In Section B.5 the actual flux, fluence and dose levels achieved during the program are listed.

Table B-1. Electron Irradiation Requirements

Test Sequence No.	Nominal Average Dose (Rads)	Nominal Fluence (e/cm^2)	Nominal Flux (e/cm^2sec)	Nominal Radiation Time
Phase I				
3	1×10^9	2.6×10^{16}	2.1×10^{11} (a)	34 hr at $\simeq$8 hr/day for 4.5 consecutive days
4	1×10^9	2.6×10^{16}	2.1×10^{11} (a)	34 hr at 24 hr/day for 1.5 days
5	2×10^9	5.2×10^{16}	2.1×10^{11} (a) (c)	68 hr at $\simeq$8 hr/day for 9 consecutive days
Phase II				
5	1×10^{10}	2.2×10^{17}	2.4×10^{11} (b)	250 hr at $\simeq$8 hr/day for 33 consecutive days
6	1×10^{10}	2.2×10^{17}	2.4×10^{11} (b)	250 hr at $\simeq$8 hr/day for 33 consecutive days

(a) No backscattering, machine operating at $\simeq$45 μA beam current

(b) 15 percent dose addition assumed due to backscattering at $\simeq$60 μA beam current

(c) Assumed rate before backscatter of heater unit was recognized

B.2 ELECTRON ENERGY

The Van de Graaff (VDG) accelerator is equipped with a generating voltmeter which samples the electrostatic field existing between the high voltage terminal and the tank wall. The instrument tracks over the voltage range of the accelerator to within one percent. Its output is coupled to a digital voltmeter (DVM) located in the VDG control console. On a previous program (Reference 4) calibrations were made against the current through the column resistors and against the attenuation of the beam in aluminum layers. It was found that 102.5 mV (±3 percent) on the digital voltmeter ≡ 100 kV terminal potential. Since the electrons are accelerated from the terminal potential to ground, a 100 kV terminal potential will accelerate electrons to 100 keV energy.

In addition to diffusing the electron beam as it passes through the scattering foils, the electron beam loses some energy. Previous programs in the SESL facility have utilized Monte Carlo calculations by Seltzer and Berger (Reference 5) in determining this energy loss; however, the published calculations do not extend above 400 keV incident energy except for one curve given for a silicon scatterer at energies up to 1 MeV. This curve plots the most probable energy after passing through the foil, which is somewhat higher than the desired average energy from which the dose distribtuion is determined. Reference 5 includes determinations within the 100-400 keV range of electron energies of both the average emergent energy and the most probable emergent energy in terms of the incident energy. These data were utilized to determine the average on-target energy for this study on the assumption that the mechanism for electron scattering is nearly the same at 700 keV as at 100-400 keV. Comparisons were made with values obtained using data from References 4 and 6.

A foil thickness was chosen for the program which would maximize the flux on the carousel. A foil that was too thin would not disperse the beam out to the proper scattering angle. If the foil were too thick, the beam would be dispersed too much. To the normal 0.0165 mm (0.65 mil) vacuum separator foil was added two thicknesses of 0.0254 mm (1 mil) aluminum foil on the rotator, giving a total thickness of 0.0673 mm (2.65 mil) of

aluminum. Using a machine setting of 746 mV on the DVM resulted in an on-target average energy level of approximately 700 keV. This was determined from the following relationships:

a) From the VDG machine calibration, 1 keV incident energy (E_o) on the foil system $\equiv$ 1.025 mV on the DVM

b) For a total foil thickness of 0.0673 mm (2.65 mil), the ratio of most probable emerging energy (E_p) to incident energy on the foil (E_o) was calculated to be 0.968

c) The ratio of on-target average energy $(\bar{E})$ to the most probable energy (E_p) was calculated to be 0.988.

Therefore,

$$E_o = \left(\frac{DVM}{1.025}\right) = \frac{746}{1.025} = 728 \text{ keV} \qquad (B1)$$

and

$$\bar{E} = E_o\left(\frac{E_p}{E_o}\right)\left(\frac{\bar{E}}{E_p}\right)$$
$$= 728(0.968)(0.988)$$
$$= 697 \text{ keV (to an uncertainty of } \pm 3 \text{ percent).}$$
$$\qquad (B2)$$

B.3 FLUX CALIBRATION

Electron Flux calibrations were made using a small three-element graphite Faraday cup with an entrance aperture area of 0.503 cm^2 (0.078 $in.^2$). The carousel was removed for the calibration to allow the Faraday cup to be positioned in the same plane as the carousel, which was oriented normal to the electron beam centerline. The Faraday cup was oriented with its centerline normal to the beam direction but displaced with respect to the axis of the carousel by 6.25 cm (2.46 in.), which is the radial distance to the center of the specimen locations. The Faraday cup centerline was positioned in azimuth in the approximate specimen position no. 5.

The electrical leads from the Faraday cup were protected from primary and secondary electron impingement by 0.20 cm (80 mil) wall thickness

copper tubing. The outer shield was grounded at the chamber. The aperture and cup bias were varied while under beam loading. No changes were noted, indicating that no secondary electron transport was taking place.

The Faraday current was monitored on a current integrator as was the current from the exit aperture. The beam energy was set a DVM reading of 746 mV (corresponding to an on-target average energy of approximately 700 keV), and three runs were made for simultaneous integration periods on each current integrator. The results are shown in Table B-2. The average current ratio is 1.69×10^{-3}. Using the Faraday cup area of 0.503 cm^2, for the charge collected on the exit aperture, this translates into a calibration constant of:

$$\frac{1.69 \times 10^{-3}}{1.602 \times 10^{-19} \times 0.503} = 2.10 \times 10^{10} \text{ e/cm}^2\text{sec}/\mu A. \tag{B3}$$

From Section 4.1 and Appendix A, for Phase I Test Sequences 3 and 4, the dose conversion factor was calculated to be 2.57×10^7 e/cm^{2}rad for the materials. For Phase I Test Sequence 5 and all Phase II Test Sequences the dose conversion factor was 2.2×10^7 e/cm^{2}rad.

Table B-2. Exit Aperture Target Plane Flux Calibration
at 746 mV DVM Electron Energy ($\equiv$ 697 keV)

Run	Beam Current (μA)	Exit Aperture (EA) Current (μA)	Exit Aperture (EA) Charge (μC)	Faraday Cup (FC) Current (μA)	Faraday Cup (FC) Charge (μC)	Q_{FC}/Q_{EA}
1	49.7	12	3000	0.020	5.08	1.69×10^{-3}
2	49.7	12	1500	0.020	2.53	1.69×10^{-3}
3	49.7	12	1500	0.020	2.52	1.68×10^{-3}

From these conversion values, the experimental values determined in Table B-2, and the requirements in Table B-1, irradiation schedules were drawn up for each sequence test run. Typical schedules for Phase I (Sequence 3) and Phase II (Sequence 5) are presented in Tables B-3 and B-4, respectively. Sequence I-4 is the same as Sequence I-3 except that the

Table B-3. Irradiation Schedule (Phase I, Test Sequence
No. 3, +30 Degree Beam Leg)

Van De Graaff Settings:

    Voltage: 746 mV on DVM

    Current: $\approx$45 μA nominal

    Shorting Bar: Not used

Scattering Foils:

    0.0165 mm (0.65 mil) alum normal and two pc at 0.0254 mm (1 mil)
each Alum on 1.27 cm (0.5 in.) aperture rotator position

Exit Aperture Current: $\approx$10 μA

Total Dose Delivered: 1×10^9 rads = 2.57×10^{16} e/cm^2 at 700 keV

Exit Aperture Conversion Factor: 2.10×10^{10} e/cm^{2}μC

Total Charge Required: $\dfrac{2.57}{2.10} \times 10^6$ μC = 1.224 C

Delivery Program: 4 1/2 days consecutive at $\approx$8 hr/day

Charge/Day: 1.224/4.5 = 0.273 C/day = 2.73×10^5 μC/day

Current Integrator Settings:

    Current Range: 30 μA

    Count Per Day: $\dfrac{2.73 \times 10^5}{30}$ = 9,100 counts

Schedule:

    First 4 days: 9,100 counts each day

    Last day: 4,550 counts

Approximate Irradiating Time:

    7.5 hr. (first 4 days)

    3.7 hr. (last day)

Table B-4. Irradiation Schedule (Phase II, Test Sequence
No. 5, +30 Degree Beam Leg)

Van de Graaff Settings:

    Voltage: 746 mV on DVM

    Current: $\approx$55 μA nominal

    Shorting Bar: Not used

Scattering Foil(s):

    0.0165 mm (0.65 mil) alum normal and two pc at 0.0254 mm (1 mil)
    each on 1.27 cm (0.5 in.) aperture rotator position

Exit Aperture Current: $\approx$12 μA

Total Dose Delivered: 1×10^{10} rads

Flux to Dose Conversion Factor: 2.23×10^{-7} e/cm^{2}rad at 700 keV

Exit Aperture Conversion Factor: 2.10×10^{10} e/cm$^2\mu$C

Total Charge Required:

    3.19 C at 3×10^9 rads
    6.39 C at 6×10^9 rads
    10.64 C at 1×10^{10} rads

Delivery Program: 34.5 days consecutive $\approx$7 hr/day

Charge/Day: $\dfrac{10.64}{34.5}$ = 0.310 C/day = 3.1×10^5 μC/day

Current Integrator Settings:

    Current Range: 30 μA

    Count Per Day: $\dfrac{3.1 \times 10^5}{30}$ = 10,333 counts

Total Count:

    103,000 counts at 3×10^9 rads
    206,660 counts at 6×10^9 rads
    354,670 counts at 1×10^{10} rads

delivery was continuous over a 34-hour period. Sequence I-5 is the same as Sequence I-3 except that the dose was increased by a factor of two to 2 x 10^9 rads; thus, the irradiation period and total count were increased proportionately (8 1/2 days and 81,900 count). Sequence II-6 was originally planned to be terminated at 6 x 10^9 rad but was replanned to continue until 1 x 10^{10} rads was reached. Hence, the schedule for Sequence II-6 was identical to Sequence II-5.

B.4 TARGET PLANE FLUX VARIATION

The target plane was mapped with small disc thermoluminescent dosimeters (TLD) to determine the variation in dose at the specimen carousel positions. The central part of the carousel, yoke and upright support bars were all in place during the calibration irradiation test. Three dosimeters were mounted at each location on a thin piece of insulating board, and carefully positioned with respect to the yoke and specimen positions every 40 degrees around the carousel. After irradiation at a DVM setting of 746 mV (700 keV), the dosimeters were removed and read out on a calibrated reader. The results are displayed in Figure B-1. The average of three readings is given in parentheses. In general, the outside TLD readings were lower than the inside TLD readings.

The average of the nine locations is 187, with high and low extremes of 209 and 153 respectively. A flux variation of +11 percent, -18 percent results. If the two upper right hand locations are not considered, the average is 197, resulting in a flux variation over three-fourths of the specimen locations of ±6 percent. The measured variation is believed due to (1) an offset of the real beam axis from the center of the carousel, and (2) the use of a foil system which maximized the flux on the specimens at the expense of having to operate in the wings of the angular scattering distribution where flux falloff is rapid with angle.

B.5 SUMMARY OF ACTUAL DOSE LEVELS

Table B-5 lists the actual doses received by the test specimen for each radiation test sequence. These have been calculated from conversion factors derived in Section B.3. The dose levels shown in Table B-5 are for specimen position no. 5 (which was closest to the Faraday cup position).

YOKE

(192)
20°

(153)
340°

(190)
60°

(155)
300°

100°
(209)

260°
(185)

140°
(208)

220°
(190)

180°
(206)

SPECIMEN LOCATIONS
FOR TEST PROGRAMS
(TYP)

TLD POSITIONING
EVERY 40°
3 DISCS EACH LOCATION
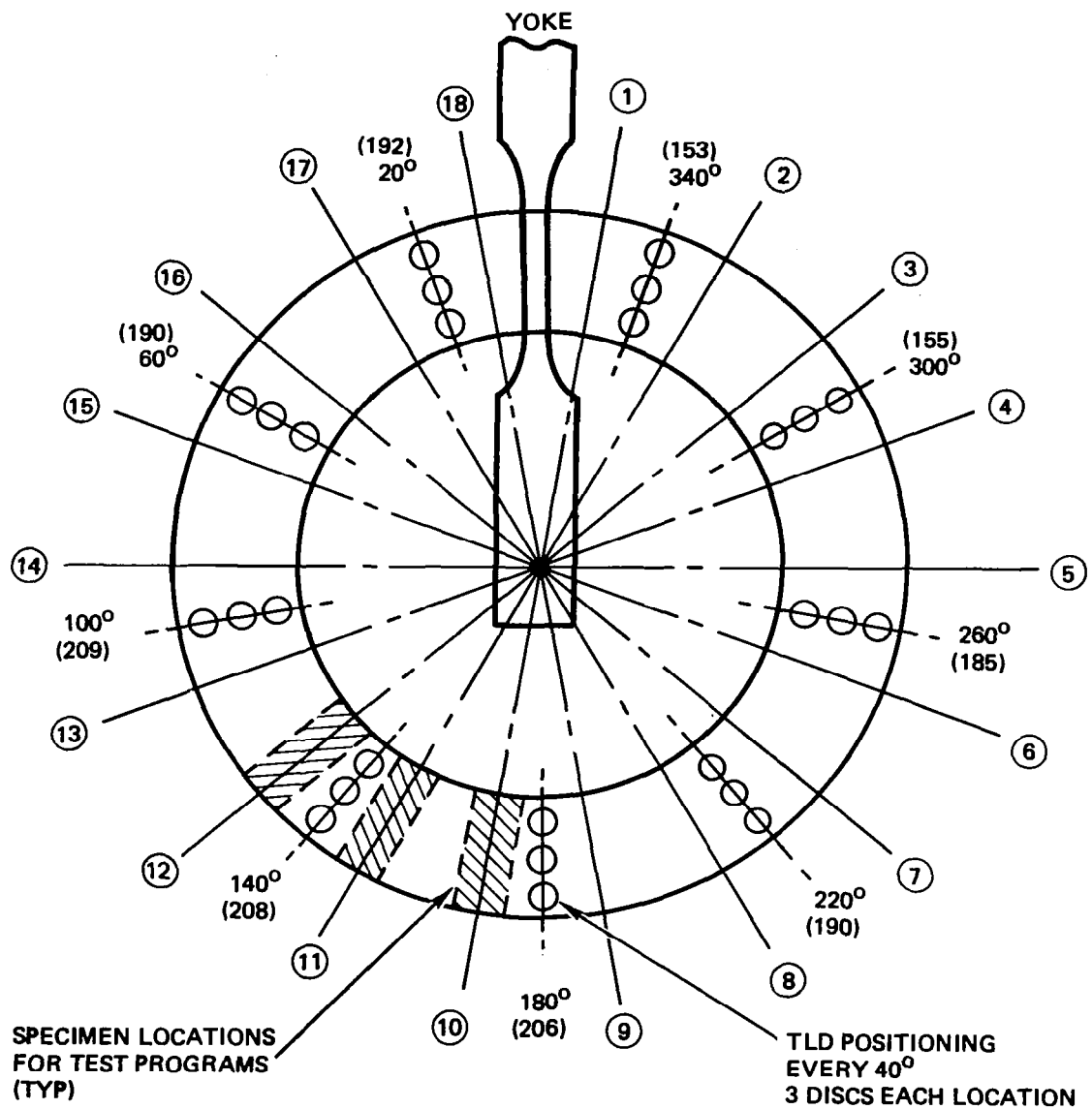
(X) SPECIMEN POSITION NUMBER
(xxx) RELATIVE TLD DOSE, AVERAGE OF 3 DOSIMETERS

Figure B-1. Relative Electron Dose Map at 700 keV Electron Energy.

Table B-5. Summary of 700 keV Electron Irradiation Run Data

Phase	Test Sequence	Planned Dose (x 10^9 rad)	Flux (x 10^{11} e/cm^{2}sec)	Charge Collected, Exit Aperture (C)	Dose Delivered (x 10^9 rads)	Delivery Schedule
	3	1.0	2.2	1.230	1.0[a]	≈8 hr/day, 4 1/2 day
I	4	1.0	2.1	1.224	1.0[a]	34 hr continuous
	5	2.0	2.4	2.457	2.4[b]	≈8 hr/day, 8 1/2 day
		3.0	2.7	3.11	3.6	≈7 hr/day, 10 days
II	5[c]	6.0	2.7	6.21	6.9	≈7 hr/day, 20 days
		10.0	2.7	10.39	10.0	≈7 hr/day, 33 1/2 days
		3.0	2.7	3.39	3.3	≈7 hr/day, 11 days
II	6[c]	6.0	2.7	6.66	6.4	≈7 hr/day, 21 1/2 days
		10.0	2.7	11.00	10.6	≈7 hr/day, 34 days

(a) Backscatter effect from vacuum chamber walls is negligible
(b) Includes backscatter effect from heater unit
(c) Electron fluence adjusted to offset backscatter effect

The doses delivered to the rest of the specimens can be obtained by using the relative dose factors shown in Figure B-1, and comparing the value at position no. 5 to the relative dose at the specimen of interest.

The high dose of 2.4×10^9 rads obtained (2×10^9 rads planned) in Phase I, Sequence 5 reflects the additional dose due to the backscatter from the heating unit installed in the chamber at that time. No allowance was made to the irradiation program at the time of the test to account for this additional dose. The Phase II testing program incorporated the backscatter effect (Appendix A) in determining the required test fluences to achieve the desired dose levels.

B.6 DOSE UNCERTAINTY/ACCURACY

The current integrators are kept in calibration by reference to N.B.S. Standards at six-month intervals and are quoted as being accurate to within ±2 percent of integrated count. The Faraday cup calibration is believed to be accurate to ±5 percent. The actual fluences experienced at each specimen position, if corrected using Figure B-1 data, would include an rms uncertainty of 3 percent for the averaged dosimeter readouts. The rms'd uncertainty in delivered electron fluence to each specimen is then about 6 percent at one sigma.

The dose calculations performed in Section 4.1 and Appendix A are subject to uncertainties caused by the statistical process of the Monte Carlo method, as well as the inaccuracies associated with the basic assumptions employed. Some estimate of the combined uncertainties can be obtained by comparison with experiment. This has been done in Reference 2 which uses most of the codes employed by TIGER. The number of histories employed in that reference is 20,000 in contrast to the 8,000 employed here. The comparison with experiment for roughly comparable electron energy and material appears to show agreement within about 5 percent. For the lowered statistics of this experiment, the uncertainty might be expected to rise to perhaps as much as 8 percent. Combined with the fluence uncertainty of 6 percent, this indicates that the average deposited dose can be assigned an uncertainty of approximately 10 percent rms.
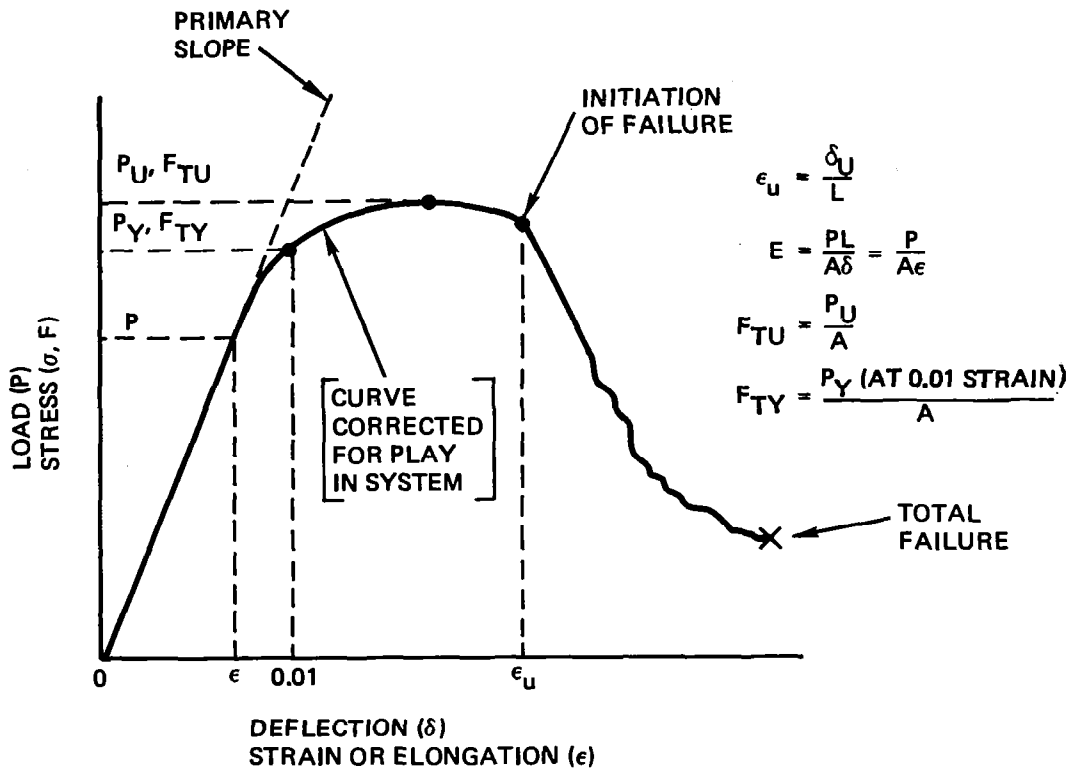
APPENDIX C

DEFINITION OF TENSILE STRESS-STRAIN PROPERTIES

The raw data consisted of load-deflection charts that were automatically plotted by the Instron test machine (for ex situ baseline measurements) or by the vacuum/irradiation chamber loading mechanism (for baseline and all irradiated measurements). All raw data was taken in the English system of units (load in pounds, deflection and length in inches, area in square inches, and strain in inches/inch). Reduction of the raw data to determine key material tensile properties was initially done in English units and then converted to appropriate SI values (gigapascal for modulus of elasticity, megapascal for strength); strain (elongation) values are identical in both system of units.

The key tensile properties determined from the raw data included: modulus of elasticity, ultimate strength, yield strength, and ultimate elongation. Figure C-1 illustrates a hypothetical load-deflection diagram and defines the key relationships. Strain (ε) is obtained by dividing the gage length (L) into the specimen change in length (δ). When the gage length is 2.54 cm (1 in.) - as was the case for most of the testing - specimen change-in-length is equivalent to strain. Elongation is merely strain expressed in percent. Stress (σ) is obtained by dividing applied load (P) by the specimen average cross-sectional area. The ultimate stress (F_{TU}) is the stress at maximum load. The yield stress (F_{TY}) is defined as the stress at 0.01 strain (1 percent elongation). The ultimate strain or elongation (ε_u) is determined at the initiation of failure, rather than at total separation of the specimen.

Modulus of elasticity (E) is the initial slope of the stress-strain curve. The initial portion of almost every test curve was fairly straight; thus it was fairly easy to draw a primary slope line. Modulus of elasticity was calculated from the primary slope line by dividing the applied load (P) at a given strain by the average cross-sectional area of the specimen (A) and the strain (ε) at that applied load level.

PRIMARY
SLOPE

INITIATION
OF FAILURE

P_U, F_{TU}

P_Y, F_{TY}

P

LOAD (P)
STRESS (σ, F)

CURVE
CORRECTED
FOR PLAY
IN SYSTEM

$\epsilon_u = \dfrac{\delta_U}{L}$

$E = \dfrac{PL}{A\delta} = \dfrac{P}{A\epsilon}$

$F_{TU} = \dfrac{P_U}{A}$

$F_{TY} = \dfrac{P_Y \text{ (AT 0.01 STRAIN)}}{A}$

TOTAL
FAILURE

0   ϵ 0.01 ϵ_u

DEFLECTION (δ)
STRAIN OR ELONGATION (ϵ)

GAGE LENGTH (L)	$\equiv$	DISTANCE BETWEEN END FITTING GRIPS IN LOADING MACHINE OR APPARATUS
DEFLECTION (δ)	$\equiv$	CHANGE IN LENGTH OF SPECIMEN OVER GAGE LENGTH REGION
STRAIN (ϵ)	$\equiv$	(SPECIMEN CHANGE IN LENGTH OR DEFLECTION)/ (GAGE LENGTH)
ELONGATION (ϵ)	$\equiv$	STRAIN x 100 IN PERCENT
STRESS (σ, F)	$\equiv$	(AXIAL LOAD)/(CROSS-SECTIONAL AREA OF SPECIMEN)
MODULUS (E)	$\equiv$	(LOAD)/(CROSS-SECTIONAL AREA)(STRAIN)

Figure C-1. Definition of Stress-Strain Parameters.

94

Calibration of the vacuum chamber load-deflection mechanism using a steel specimen indicated that the "play" in the system resulted in a 0.0254 mm (0.001 in.) deflection under a 444.8 N (100 lb) loading. Before calculating the key tensile properties, the deflection values were reduced a proportional amount (proportional to load) to correct for the "play" in the system (see Figure C-2).
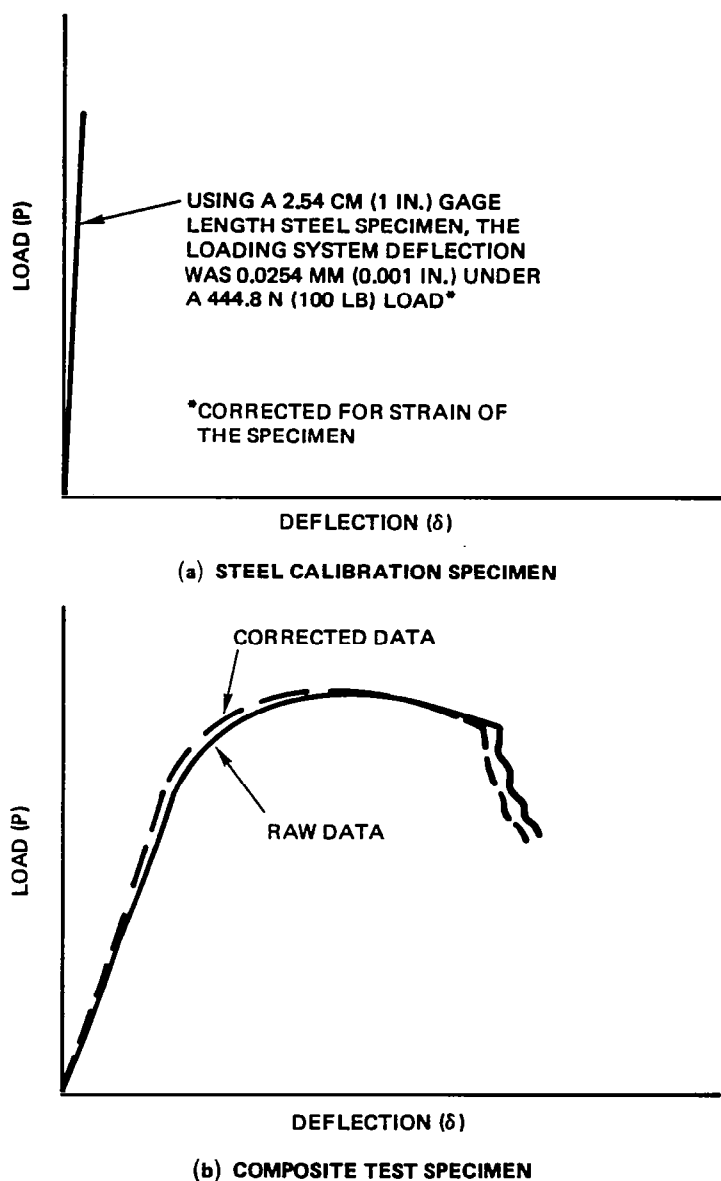
USING A 2.54 CM (1 IN.) GAGE
LENGTH STEEL SPECIMEN, THE
LOADING SYSTEM DEFLECTION
WAS 0.0254 MM (0.001 IN.) UNDER
A 444.8 N (100 LB) LOAD*

*CORRECTED FOR STRAIN OF
THE SPECIMEN

DEFLECTION (δ)

(a) STEEL CALIBRATION SPECIMEN

CORRECTED DATA

RAW DATA

DEFLECTION (δ)

(b) COMPOSITE TEST SPECIMEN

Figure C-2. Technique for Correcting Raw Data to Account
for Play in Loading System.

95

REFERENCES

1. AFML TR 79-4208 "Advanced Composites Design Data for Spacecraft Structural Applications," General Dynamics Corporation, March 1980.

2. M. J. Berger and S. M. Seltzer, "Tables of Energy Losses and Ranges of Electrons and Positrons," NASA SP-3012, 1964.

3. J. A. Halbleib and W. H. Van Devender, "TIGER: A One-Dimensional Multilayered Electron/Photon Monte Carlo Transport Code," SLA-73-1026, Sandia Laboratories, Albuquerque, New Mexico, March 1974 (achieved at the Radiation Shielding Information Center at ORNL in the RSIC computer code collection as "CCC-245/Tiger Code," updated December 1976).

4. R. M. Kurland et al., "Properties of Metallized Flexible Materials in the Space Environment," SAMSO TR 78-31, January 1978.

5. S. M. Seltzer and M. J. Berger, "Transmission and Reflection of Electrons by Foils," Nuclear Instruments and Methods, Vol. 119, No. 1, pp 157-179, July 1, 1974.

6. L. Katz and A. S. Penfold, "Range-Energy Relations for Electrons and the Determination of Beta-Ray End-Point Energies by Absorption," Review of Modern Physics, Vol. 24, No. 1, pp 28-44, 1952.

1. Report No. NASA CR-3475	2. Government Accession No.	3. Recipient's Catalog No.
4. Title and Subtitle RADIATION TESTING OF COMPOSITE MATERIALS, IN SITU VERSUS EX SITU EFFECTS		5. Report Date November 1981
		6. Performing Organization Code
7. Author(s) R.M. Kurland, J.F. Thomasson, and W.C. Beggs		8. Performing Organization Report No. 35170-6028-UT-01
		10. Work Unit No.
9. Performing Organization Name and Address TRW Defense and Space Systems Group One Space Park Redondo Beach, California 90278		11. Contract or Grant No. NAS1-15848
		13. Type of Report and Period Covered Contractor Report
12. Sponsoring Agency Name and Address National Aeronautics and Space Administration Washington DC 20546		14. Sponsoring Agency Code

15. Supplementary Notes

Langley Technical Monitor: Wayne S. Slemp
Final Report

16. Abstract

A study was conducted to investigate the effect of post-irradiation test environments on tensile properties of representative advanced composite materials (T300/5208, T300/934, C6000/P1700). Four-ply [±45/∓45] laminate tensile specimens were exposed in vacuum up to a bulk dose of 1×10^{10} rads using a mono-energetic fluence of 700 keV electrons from a Van de Graaff accelerator. Post-irradiation testing was performed while specimens were being irradiated (in situ data), in vacuum after cessation of irradiation (in vacuo data), and after exposure to air (ex situ data). Room temperature and elevated temperature effects were evaluated. The radiation-induced changes to the tensile properties were small. Since the absolute changes in tensile properties were small, the existence of a post-irradiation test environment effect was indeterminate.

17. Key Words (Suggested by Author(s)) Composite materials Mechanical properties Radiation testing techniques Space radiation effects	18. Distribution Statement Unclassified – Unlimited Subject Category 24		
19. Security Classif. (of this report) Unclassified	20. Security Classif. (of this page) Unclassified	21. No. of Pages 108	22. Price A06